Published for SISSA by Springer
Received: June 19, 2018
Revised: November 12, 2018
Accepted: November 14, 2018
Published: November 26, 2018

Simultaneous interpretation of K and B anomalies in terms of chiral-flavorful vectors

Shinya Matsuzaki,[a,b] **Kenji Nishiwaki**[c,d] **and Kei Yamamoto**[b,e,f,1]

[a] *Center for Theoretical Physics and College of Physics, Jilin University, Changchun, 130012, China*

[b] *Department of Physics, Nagoya University, Nagoya 464-8602, Japan*

[c] *School of Physics, Korea Institute for Advanced Study (KIAS), Seoul 02455, Republic of Korea*

[d] *Ruđer Bošković Institute, Division of Theoretical Physics, Bijenicka cesta 54, 10000 Zagreb, Croatia*

[e] *Graduate School of Science, Hiroshima University, Higashi-Hiroshima 739-8526, Japan*

[f] *Physik-Institut, Universität Zürich, CH-8057 Zürich, Switzerland*

E-mail: synya@hken.phys.nagoya-u.ac.jp, knishiw@irb.hr, keiy@hiroshima-u.ac.jp

Abstract: We address the presently reported significant flavor anomalies in the Kaon and B meson systems such as the CP violating Kaon decay (ϵ'/ϵ) and lepton-flavor universality violation in B meson decays ($R_{K^{(*)}}, R_{D^{(*)}}$), by proposing flavorful and chiral vector bosons as the new physics constitution at around TeV scale. The chiral-flavorful vectors (CFVs) are introduced as a 63-plet of the global SU(8) symmetry, identified as the one-family symmetry for left-handed quarks and leptons in the standard model (SM) forming the 8-dimensional vector. Thus the CFVs include massive gluons, vector leptoquarks, and W', Z'-type bosons, which are allowed to have flavorful couplings with left-handed quarks and leptons, and flavor-universal couplings to right-handed ones, where the latter arises from mixing with the SM gauge bosons. The flavor texture is assumed to possess a "minimal" structure to be consistent with the current flavor measurements on the K and B systems. Among the presently reported significant flavor anomalies in the Kaon and B meson systems (ϵ'/ϵ, $R_{K^{(*)}}, R_{D^{(*)}}$), the first two ϵ'/ϵ and $R_{K^{(*)}}$ anomalies can simultaneously be interpreted by the presence of CFVs; the $R_{D^{(*)}}$ anomaly is predicted not to survive, due to the approximate SU(8) flavor symmetry. Remarkably, we find that as long as both of the ϵ'/ϵ and $R_{K^{(*)}}$ anomalies persist beyond the SM, the CFVs predict the enhanced $K^+ \to \pi^+ \nu\bar{\nu}$ and $K_L \to \pi^0 \nu\bar{\nu}$ decay rates compared to the SM values, which will readily be explored by the NA62 and KOTO experiments, and they will also be explored in new resonance searches at the Large Hadron Collider.

Keywords: Beyond Standard Model, CP violation, Heavy Quark Physics, Kaon Physics

ArXiv ePrint: 1806.02312

[1] Corresponding author.

https://doi.org/10.1007/JHEP11(2018)164

JHEP11(2018)164

Contents

1 Introduction

Flavor physics is one of the most powerful probes for physics beyond the standard model (SM). Recently, some discrepancies with the SM are reported in several observables in Kaon and B meson decays. Among them, one of the flavor changing neutral current observables, the direct CP violation in $K \to \pi\pi$ decays, ϵ'/ϵ, has recently been paid a strong attention to because of the significant discrepancy between the SM prediction [1, 2][1] using the first lattice calculation result reported by RBC-UKQCD collaboration [6] and the experimental data. The SM prediction can be estimated as [2] $(\epsilon'/\epsilon)_{\rm SM} = (1.06 \pm 5.07) \times 10^{-4}$, which is around 2.8σ below the experimental data [7–10], $(\epsilon'/\epsilon)_{\rm exp} = (16.6 \pm 2.3) \times 10^{-4}$. In addition, the recent data on semi-leptonic B decays also report the discrepancies. Lepton-flavor universality (LFU) violating observables $R_{K^{(*)}} = {\rm Br}[\bar{B} \to K^{(*)}\mu^+\mu^-]/{\rm Br}[\bar{B} \to K^{(*)}e^+e^-]$ have been measured at around 2.1-2.6σ away from the SM prediction [11, 12]. The discrepancies have been seen also in $R_{D^{(*)}} = {\rm Br}[B \to D^{(*)}\tau\bar{\nu}]/{\rm Br}[B \to D^{(*)}\ell\bar{\nu}]$ (with ℓ standing for e or μ) [13–19]. Those flavor anomalies have nowadays made a fuss and urged theorists to make viable conjectures and interpretations for the flavor structure hidden in a possible new physics (NP).

In this paper, we propose a new conjecture to simultaneously address these flavor anomalies in the Kaon and B meson systems: it is a chiral-flavorful structure characterized by the presence of flavorful and chiral vector bosons (CFVs) as the new physics constitution at around TeV scale. The CFVs are introduced as adjoint representation of SU(8) global symmetry, which is gauged by the left-handed gauges in the SM. Hence the CFVs can be classified into a generic set of vectors; massive gluon G'-like, vector leptoquark-like, W' and Z'-like vectors.[2]

We find the characteristic feature in the present CFV scenario based on the one-family SU(8) symmetry, by which the predictions in flavor physics are derived necessarily with a significant correlation between the $2 \leftrightarrow 3$ and $1 \leftrightarrow 2$ generation-transition processes. It is shown that there are allowed parameter regions which can address both of the discrepancies in ϵ'/ϵ and in $R_{K^{(*)}}$, consistently with the several constraints on the flavor texture we adopt. New sizable enough contributions to ϵ'/ϵ are produced from G' and Z'-like CFVs via the $I = 0$ amplitude through the QCD penguin operators and the $I = 2$ one through the electroweak (EW) penguin operators (with I distinguishing isospin states), respectively, while those to the $R_{K^{(*)}}$ arise from the Z'-type and vector-leptoquark-type CFVs. Intriguingly enough as well, the CFVs do not give significant effect on the $R_{D^{(*)}}$ due to the one-family SU(8) symmetry.

The CFVs turn out to also give the nontrivial predictions to the Kaon rare decays ${\rm Br}[K_L \to \pi^0\nu\bar{\nu}]$ and ${\rm Br}[K^+ \to \pi^+\nu\bar{\nu}]$, arising from the Z'-type and vector-leptoquark-type exchanges along with the strong correlation with the presence of the $R_{K^{(*)}}$ anomaly.

[1] The results in the Dual QCD approach are supported by RBC-UKQCD lattice collaboration [3, 4]. On the other hand, the study in the chiral perturbation theory predicts a consistent value with the experimental value [5].

[2] Such CFVs can be generated as composite particles arising due to an underlying strongly coupled (a hidden QCD) dynamics as proposed in [20].

JHEP11(2018)164

These predictions will be explored by the NA62 and KOTO experiments, significantly in the correlation with the fate of B anomalies as well as new-vector resonance searches at the Large Hadron Collider (LHC), to be tested in the future high-luminosity phase.

This paper is structured as follows. In section 2 we introduce the CFV model together with the proposed flavor texture and the couplings to the SM fermions based on the SU(8) symmetry structure. Section 3 provides the CFVs contributions to the flavor physics, including the K and $B-\tau$ systems, and place the constraints on the model-parameter space, showing that the presently reported ϵ'/ϵ and $R_{K^{(*)}}$ anomalies can be simultaneously accounted for by the CFVs, while the $R_{D^{(*)}}$ anomaly is predicted not to survive, due to the approximate SU(8) flavor symmetry. With the current phenomenological bounds at hand, in section 4 we discuss the future prospect for the CFV scenario, aiming at the NA62 and KOTO experiments, in correlation with the fate of the B anomalies in the future. Expected LHC signatures specific to the presence of the CFV resonances are also addressed. Finally, section 5 is devoted to summary and several discussions including the theoretical uncertainties in the present analysis. Explicit coupling formulae for the CFVs to the SM fermions are provided in appendix A, and effective-four fermion interaction forms relevant to the flavor physics study are given in appendix B. In appendix C, we discuss a global significance of a bench mark point where the best-fit value for $b \to s\mu^+\mu^-$ is achieved and the ϵ'/ϵ anomaly can be addressed within 1σ confidence level (C.L.) consistently.

2 Chiral-flavorful vectors

In this section we introduce the CFVs (hereafter symbolically denoted as ρ) and their generic interaction properties for the SM particles.

2.1 The flavorful couplings

The CFVs (ρ) couplings to the left-handed fermions in the SM are constructed in the one-family global-SU(8) symmetric way as

$$\mathcal{L}_{\rho f_L f_L} = \sum_{i,j=1}^{3} g_{\rho L}^{ij} \overline{f}_L^i \gamma^\mu \rho_\mu f_L^j \,, \tag{2.1}$$

where $g_{\rho L}^{ij}$ denotes the (hermitian) couplings with the generation indices (i,j) in the gauge eigenbases, and f_L^i includes the left-handed SM doublet quarks ($q_L^{ic} = (u^{ic}, d^{ic})_L^T$ with the QCD color index $c = r, g, b$) and (left-handed) lepton doublets ($l_L^i = (\nu^i, e^i)_L^T$) for the ith generation, which forms the 8-dimensional vector (the fundamental representation of the SU(8)) like $f_L^i = (q^{ir}, q^{ig}, q^{ib}, l^i)_L^T$. The CFV fields are embedded in the 8×8 matrix of the SU(8) adjoint representation: $\rho_\mu = \sum_{A=1}^{63} \rho_\mu^A T^A$, where the T^A stands for the SU(8) generators, which are explicitly given in appendix A (eqs. (A.1)–(A.5)). To manifestly keep the SM gauge invariance in the coupling form of eq. (2.1), the CFVs are allowed to couple to the SM gauge fields, through the gauging of the global SU(8) symmetry. It is reflected by the covariant derivative

$$D_\mu \rho_\nu = \partial_\mu \rho_\nu - i[\mathcal{V}_\mu, \rho_\nu] \,, \tag{2.2}$$

where the SM gauge fields (G_μ, W_μ, B_μ) for the $\mathrm{SU}(3)_c \times \mathrm{SU}(2)_W \times \mathrm{U}(1)_Y$ symmetry are embedded in the 8×8 matrix form of $\mathcal{V}_\mu$ as

$$\mathcal{V}_\mu = \left(\begin{array}{c|c} \mathbf{1}_{2\times2} \otimes g_s G^a_\mu \frac{\lambda^a}{2} + \left(g_W W_\mu \tau^\alpha + \frac{1}{6} g_Y B_\mu\right) \otimes \mathbf{1}_{3\times3} & \mathbf{0}_{6\times2} \\ \hline \mathbf{0}_{2\times6} & g_W W^\alpha_\mu \tau^\alpha - \frac{1}{2} g_Y B_\mu \cdot \mathbf{1}_{2\times2} \end{array} \right), \tag{2.3}$$

where λ^a and $\tau^\alpha \equiv \sigma^\alpha/2$ $(\alpha = 1,2,3)$ are Gell-Mann and (normalized) Pauli matrices, and g_s, g_W and g_Y the corresponding gauge couplings. One can easily check that the way of embedding the SM gauges in eq. (2.3) manifestly ensures the SM gauge invariance when the CFVs couple to quarks and leptons as in eq. (2.1). It is then convenient to classify the CFVs (ρ) in the SU(8) adjoint representation by the QCD charges as

$$\rho = \begin{pmatrix} (\rho_{QQ})_{6\times6} & (\rho_{QL})_{6\times2} \\ (\rho_{LQ})_{2\times6} & (\rho_{LL})_{2\times2} \end{pmatrix}, \tag{2.4}$$

where $\rho_{QQ}, \rho_{QL} (= \rho^\dagger_{LQ})$, and ρ_{LL} include color-octet $\rho_{(8)}$ (of "massive gluon G' type"), -triplet $\rho_{(3)}$ (of "vector-leptoquark type"),[3] and -singlet $\rho_{(1)^{(\prime)}}$ (of "W' and/or Z' type"), which can further be classified by the weak isospin charges ($\pm, 3$ for triplet and 0 for singlet). Thus, decomposing the CFVs with respect to the SM charges, we find

$$\begin{aligned} \rho_{QQ} &= \left[\sqrt{2}\rho^\alpha_{(8)a} \left(\tau^\alpha \otimes \frac{\lambda^a}{2} \right) + \frac{1}{\sqrt{2}} \rho^0_{(8)a} \left(\mathbf{1}_{2\times2} \otimes \frac{\lambda^a}{2} \right) \right] \\ &\quad + \left[\frac{1}{2} \rho^\alpha_{(1)} \left(\tau^\alpha \otimes \mathbf{1}_{3\times3} \right) + \frac{1}{2\sqrt{3}} \rho^\alpha_{(1)'} \left(\tau^\alpha \otimes \mathbf{1}_{3\times3} \right) + \frac{1}{4\sqrt{3}} \rho^0_{(1)'} \left(\mathbf{1}_{2\times2} \otimes \mathbf{1}_{3\times3} \right) \right], \\ \rho_{LL} &= \frac{1}{2} \rho^\alpha_{(1)} \left(\tau^\alpha \right) - \frac{\sqrt{3}}{2} \rho^\alpha_{(1)'} \left(\tau^\alpha \right) - \frac{\sqrt{3}}{4} \rho^0_{(1)'} \left(\mathbf{1}_{2\times2} \right), \\ \rho_{QL} &= \rho^\alpha_{(3)c} \left(\tau^\alpha \otimes \mathbf{e}_c \right) + \frac{1}{2} \rho^0_{(3)c} \left(\mathbf{1}_{2\times2} \otimes \mathbf{e}_c \right), \\ \rho_{LQ} &= \left(\rho_{QL} \right)^\dagger, \end{aligned} \tag{2.5}$$

[3]Since the present CFV model includes the vector-leptoquarks on the TeV mass scale ($\rho^0_{(3)}$ and $\rho^\alpha_{(3)}$), which are flavor non-universally coupled to quarks and leptons, one might worry about the rapid proton decay. Here we therefore briefly make a comment on the proton decay via the vector leptoquarks in our scenario. The SM quantum numbers of $\rho^0_{(3)}$ and $\rho^\alpha_{(3)}$ are assigned as $(\mathrm{SU}(3), \mathrm{SU}(2), \mathrm{U}(1)) = (\mathbf{3}, \mathbf{1}, \mathbf{2/3}), (\mathbf{3}, \mathbf{3}, \mathbf{2/3})$, which respectively correspond to U_1 and U_3 in the notation of the review [21]. As mentioned in [21], leptoquarks have a well-defined quantum number $F = 3B + L$ (B/L: the baryon/lepton number of the quark/lepton) and $\rho^0_{(3)}$ and $\rho^\alpha_{(3)}$ possess $F = 0$, which means that they cannot form dimension-four diquark interactions. Up to dimension-five operators, as discussed in [22], the two gauge invariant operators under the SM gauge interactions with the Higgs doublet H, $(\overline{q^c_L} H^\dagger)\gamma^\mu d_R \rho^0_{(3)\mu}/\Lambda$ and $(\overline{q^c_L} \tau^\alpha H^\dagger)\gamma^\mu d_R \rho^\alpha_{(3)\mu}/\Lambda$, seem to provide diquark interactions. However, in the hidden local symmetry approach [23–27] on which the present CFV model is formulated based (as will be mentioned in the next subsection), those operators and the resultant rapid proton decay can be prohibited, as in the case of the literature [20] (cf., ref. [28]). Thereby, the leading effect to the proton decay would arise from dimension-six four-fermion operators, where we easily ensure a sufficiently long lifetime of the proton without fine tuning for the coefficients of four-fermion operators. Note also that the vector-leptoquarks could arise as composite particles, as in [20], hence are embedded into an ultraviolet completed and asymptotic free gauge theory. Thus, it would be possible to take $\sim 10^{16}$ GeV or higher as a cutoff scale (see ref. [20]) for the present scenario. Thus, the CFV model can safely avoid the rapid proton decay.

JHEP11(2018)164

(for more details, see appendix A (eqs. (A.1)–(A.5))), where $\mathbf{e}_c$ denotes the 3-dimensional eigenvector in the color space. The explicit expressions of the flavor-dependent CFV couplings to the SM fermions are listed in appendix A (eqs. (A.6)–(A.18)).

2.2 The flavor-universal couplings induced from vectorlike mixing with the SM gauge bosons

As seen in the above, the one-family global SU(8) symmetry is of course explicitly broken by the SM gauge interactions through the gauging in eq. (2.2), hence the CFV fields (ρ) generically mix with the SM-gauge boson fields ($\mathcal{V}$). The interaction terms can arise as the form of the kinetic term mixing like

$$\mathcal{L}_{\rho\mathcal{V}} = -\frac{1}{g_\rho}\mathrm{tr}[\mathcal{V}_{\mu\nu}\rho^{\mu\nu}]\,, \tag{2.6}$$

where $\mathcal{V}_{\mu\nu} = \partial_\mu\mathcal{V}_\nu - \partial_\nu\mathcal{V}_\mu - i[\mathcal{V}_\mu, \mathcal{V}_\nu]$ and $\rho_{\mu\nu} = D_\mu\rho_\nu - D_\nu\rho_\mu$. The g_ρ has been introduced as the mixing strength common for all the SM gauges, as if a remnant of the SU(8) symmetry were reflected, which can be justified when the CFVs are associated with gauge bosons of the spontaneously broken gauge symmetry, as in the case of the hidden-local symmetry approach [23–27]. The mixing in eq. (2.6) induces the flavor-universal couplings for the CFVs to both of the left-handed and right-handed quarks/leptons, which scale as $\sim (g^2_{s,W,Y}/g_\rho)$. Since the electroweak precision tests have severely constrained the fermion couplings to new resonances, as a safety setup we may take the mixing strength $(1/g_\rho)$ to be much smaller than $\mathcal{O}(1)$, say

$$g_\rho \sim 10\,, \tag{2.7}$$

which turns out to be a consistent size also for the flavor physics bound, as will be seen later. In that case, the mass shift among the CFVs arising from the mixing with the SM gauge bosons can be safely neglected (which is maximally about 5% correction), so that the CFVs are almost degenerated to have the SU(8) invariant mass m_ρ, which is set to be of order of TeV. Noting that at the on-shell of the CFVs, the mixing term in eq. (2.6) gives rise to the mass mixing form,

$$-\frac{2m_\rho^2}{g_\rho}\mathrm{tr}[\mathcal{V}_\mu\rho^\mu], \tag{2.8}$$

in which the $\mathcal{V}_\mu$ as in eq. (2.3) couples with the SM fermion currents, one finds the perturbatively small and flavor-universal couplings, as listed in appendix A (eq. (A.19)).

2.3 The flavor-texture ansatz

Now we introduce the flavored texture for the $g^{ij}_{\rho L}$ in eq. (2.1) so that the present flavor anomalies in K and B meson systems can be addressed. The proposed texture goes like[4]

$$g^{ij}_{\rho L} = \begin{pmatrix} 0 & g^{12}_{\rho L} & 0 \\ (g^{12}_{\rho L})^* & 0 & 0 \\ 0 & 0 & g^{33}_{\rho L} \end{pmatrix}^{ij}\,, \tag{2.9}$$

[4]In the present study, we will not specify the origin of the flavor texture, though it might be derived by assuming some discrete symmetry among fermions, and so forth.

in which the hermiticity in the Lagrangian of eq. (2.1) has been taken into account (i.e. $g_{\rho L}^{21} = (g_{\rho L}^{12})^*$ and $(g_{\rho L}^{33})^* = g_{\rho L}^{33}$). The size of the real part for $g_{\rho L}^{12}$ actually turns out to be constrained severely by the Kaon system measurements such as the indirect CP violation ϵ_K, and $K_L \to \mu^+\mu^-$, to be extremely tiny ($\lesssim \mathcal{O}(10^{-6})$) (for instance, see ref. [29]). In contrast, its imaginary part can be moderately larger, which will account for the presently reported ϵ'/ϵ anomaly (deviated by about 3 sigma [7–10]). Hence we will take it to be pure imaginary:

$$\mathrm{Re}[g_{\rho L}^{12}] = 0\,, \qquad \mathrm{Im}[g_{\rho L}^{12}] \equiv +g_{\rho L}^{12} \qquad \text{with} \quad g_{\rho L}^{12} \in \mathbf{R}\,, \tag{2.10}$$

by which the new physics contributions will be vanishing for the ϵ_K and $\mathrm{Br}[K_L \to \mu^+\mu^-]$ (for explicit formulae about those observables, e.g. see refs. [29, 30]).

The base transformation among the gauge- and flavor-eigenstates can be made by rotating fields as (under the assumption that neutrinos are massless)

$$(u_L)^i = U^{iI}(u'_L)^I, \quad (d_L)^i = D^{iI}(d'_L)^I, \quad (e_L)^i = L^{iI}(e'_L)^I, \quad (\nu_L)^i = L^{iI}(\nu'_L)^I, \tag{2.11}$$

where U, D and L stand for 3×3 unitary matrices and the spinors with the prime symbol denote the fermions in the mass basis, which are specified by the capital Latin indices I and J. The Cabibbo-Kobayashi-Maskawa (CKM) matrix is then given by $V_{\mathrm{CKM}} \equiv U^\dagger D$.[5] As in the literature [31], to address several flavor anomalies recently reported in the measurements such as $R_{K^{(*)}}$ and $R_{D^{(*)}}$ as well as to avoid severe constraints from flavor-changing neutral current processes among the first and second generations, we may take the mixing structures of D and L as

$$D = \begin{pmatrix} 1 & 0 & 0 \\ 0 & \cos\theta_D & \sin\theta_D \\ 0 & -\sin\theta_D & \cos\theta_D \end{pmatrix}, \qquad L = \begin{pmatrix} 1 & 0 & 0 \\ 0 & \cos\theta_L & \sin\theta_L \\ 0 & -\sin\theta_L & \cos\theta_L \end{pmatrix}, \tag{2.12}$$

where we recall that the up-quark mixing matrix is automatically determined through $V_{\mathrm{CKM}} = U^\dagger D$. In discussing the flavor phenomenologies, the following forms are useful to understand the flavor structure in $g_{\rho L}^{ij}$ (with $c \equiv g_{\rho L}^{12}/g_{\rho L}^{33} \in \mathbf{R}$):

$$X_{dd} \equiv D^\dagger \begin{pmatrix} 0 & i\cdot c & 0 \\ -i\cdot c & 0 & 0 \\ 0 & 0 & 1 \end{pmatrix} D = \begin{pmatrix} 0 & i\cdot c\cdot\cos\theta_D & i\cdot c\cdot\sin\theta_D \\ -i\cdot c\cdot\cos\theta_D & \sin^2\theta_D & -\cos\theta_D\sin\theta_D \\ -i\cdot c\cdot\sin\theta_D & -\cos\theta_D\sin\theta_D & \cos^2\theta_D \end{pmatrix}, \tag{2.13}$$

$$X_{ll} \equiv L^\dagger \begin{pmatrix} 0 & i\cdot c & 0 \\ -i\cdot c & 0 & 0 \\ 0 & 0 & 1 \end{pmatrix} L = \begin{pmatrix} 0 & i\cdot c\cdot\cos\theta_L & i\cdot c\cdot\sin\theta_L \\ -i\cdot c\cdot\cos\theta_L & \sin^2\theta_L & -\cos\theta_L\sin\theta_L \\ -i\cdot c\cdot\sin\theta_L & -\cos\theta_L\sin\theta_L & \cos^2\theta_L \end{pmatrix}, \tag{2.14}$$

$$X_{uu} \equiv U^\dagger \begin{pmatrix} 0 & i\cdot c & 0 \\ -i\cdot c & 0 & 0 \\ 0 & 0 & 1 \end{pmatrix} U = V_{\mathrm{CKM}} \begin{pmatrix} 0 & i\cdot c\cdot\cos\theta_D & i\cdot c\cdot\sin\theta_D \\ -i\cdot c\cdot\cos\theta_D & \sin^2\theta_D & -\cos\theta_D\sin\theta_D \\ -i\cdot c\cdot\sin\theta_D & -\cos\theta_D\sin\theta_D & \cos^2\theta_D \end{pmatrix} V_{\mathrm{CKM}}^\dagger, \tag{2.15}$$

[5] The mixing between the CFVs and SM gauge bosons through eq. (2.6) would actually generate corrections to the V_{CKM} by amount of $\mathcal{O}(m_W^2/m_\rho^2)$, which can be, however, neglected as long as the CFV mass is on the order of TeV.

$$X_{ld} \equiv L^\dagger \begin{pmatrix} 0 & i\cdot c & 0 \\ -i\cdot c & 0 & 0 \\ 0 & 0 & 1 \end{pmatrix} D = \begin{pmatrix} 0 & i\cdot c\cdot\cos\theta_D & i\cdot c\cdot\sin_D \\ -i\cdot c\cdot\cos\theta_L & \sin\theta_L\sin\theta_D & -\sin\theta_L\cos\theta_D \\ -i\cdot c\cdot\sin\theta_L & -\cos\theta_L\sin\theta_D & \cos\theta_L\cos\theta_D \end{pmatrix}, \tag{2.16}$$

$$X_{lu} \equiv L^\dagger \begin{pmatrix} 0 & i\cdot c & 0 \\ -i\cdot c & 0 & 0 \\ 0 & 0 & 1 \end{pmatrix} U = \begin{pmatrix} 0 & i\cdot c\cdot\cos\theta_D & i\cdot c\cdot\sin_D \\ -i\cdot c\cdot\cos\theta_L & \sin\theta_L\sin\theta_D & -\sin\theta_L\cos\theta_D \\ -i\cdot c\cdot\sin\theta_L & -\cos\theta_L\sin\theta_D & \cos\theta_L\cos\theta_D \end{pmatrix} V_{\rm CKM}^\dagger, \tag{2.17}$$

$$\begin{aligned} X_{ud} &\equiv U^\dagger \begin{pmatrix} 0 & i\cdot c & 0 \\ -i\cdot c & 0 & 0 \\ 0 & 0 & 1 \end{pmatrix} D = V_{\rm CKM} D^\dagger \begin{pmatrix} 0 & i\cdot c & 0 \\ -i\cdot c & 0 & 0 \\ 0 & 0 & 1 \end{pmatrix} D \\ &= V_{\rm CKM} \begin{pmatrix} 0 & i\cdot c\cdot\cos\theta_D & i\cdot c\cdot\sin\theta_D \\ -i\cdot c\cdot\cos\theta_D & \sin^2\theta_D & -\cos\theta_D\sin\theta_D \\ -i\cdot c\cdot\sin\theta_D & -\cos\theta_D\sin\theta_D & \cos^2\theta_D \end{pmatrix}. \end{aligned} \tag{2.18}$$

Note that in the limit where the mixing angles go to 0 or $\pi/2$, the $2 \leftrightarrow 3$ transitions vanish, while the $1 \leftrightarrow 2$ and $1 \leftrightarrow 3$ transitions remain accompanied by the factor c.[6]

3 Contributions to flavor physics induced from CFV exchanges

In this section we shall discuss the flavor physics constraints on the CFV-induced four-fermion contributions. The flavored-heavy CFVs exchanges generate effective four-fermion interactions at low-energy $E_{\rm ref} \ll m_\rho = \mathcal{O}(\text{TeV})$. There the left-handed current-current interactions arise from both the flavorful coupling $g_{\rho L}^{ij}$ in eq. (2.9) and flavor-universal couplings induced by mixing with the SM gauge bosons given in eq. (A.19), while the right-handed current-current interactions only from the latter ones. Since the right-handed couplings are generated by mixing with the hypercharge gauge boson, having the form like g_Y^2/g_ρ which is smaller than the left-handed coupling g_W^2/g_ρ, we may neglect the right-handed current interactions and keep only the leading order terms with respect to the gauge coupling expansion in evaluating the flavor physics contributions.

The effective four-fermion operators constructed from the left-handed current-current interactions are listed in appendix B (eqs. (B.5)–(B.17)). Hereafter we shall consider a limit where all the CFVs are degenerated to have the SU(8) invariant mass m_ρ,

$$M_{\rm CFVs} \simeq m_\rho\,, \tag{3.1}$$

namely, assuming that the possible split size by $(g_{s,W,Y}/g_\rho)\, m_\rho$ is negligibly small due to the large g_ρ as in eq. (2.7). Nevertheless, the $1/g_\rho$ mixing term will significantly contribute to the flavor physics as long as the size of g_ρ is less than a naive perturbative bound $\sim 4\pi$.[7]

[6]We note that flavor-conserving interactions appear from the mixing between $V_{\rm SM}$ and ρ, which play important roles in ϵ'/ϵ and the bound from the LHC (see appendix A for details).

[7]The present CFV model-setup is actually similar to the model proposed in ref. [20], in which the mixing strength with the SM gauge bosons, set by $g_{s,W,Y}/g_\rho$, was assumed to be ideally small (i.e. g_ρ is much larger than the perturbative value $\sim 4\pi$ because of the nonperturbative underlying dynamics). In the present model, the size of g_ρ is taken to be $< 4\pi$, so that the flavor-universal contribution will play somewhat a significant role in discussing the flavor limits, as will be seen in the later subsequent sections.

3.1 Flavor changing processes converting the third and second generations

The CFVs generate nonzero flavor-changing neutral-current contributions to the b-s transition system and the lepton flavor violation regarding the third generation charged leptons. Specifically, the relevant processes are:

- $\mathcal{O}_{2q2\ell(n)}$: $\bar{B}\to D^{(*)}\tau\bar{\nu}$ (only for $n=3$), $\bar{B}\to K^{(*)}\mu^+\mu^-$, $\bar{B}\to K^{(*)}\nu\bar{\nu}$, and $\tau\to\phi\mu$,
- $\mathcal{O}_{4q(n)}$: B_s^0–$\bar{B}_s^0$ mixing,
- $\mathcal{O}_{4\ell(n)}$: $\tau\to 3\mu$,

where n stands for types of the contraction of EW-SU(2) indices shared by fermion fields in dimension-six operators (see eq. (B.5)). These processes can be evaluated through the effective Hamiltonians for $b\to s\ell^+\ell^-$, $b\to s\nu\overline{\nu}$, $b\to c\tau^-\overline{\nu}$, $\tau\to\mu s\overline{s}$, $B_s^0\,(=s\bar{b})\leftrightarrow\overline{B_s^0}\,(=b\overline{s})$, and $\tau^-\to\mu^-\mu^+\mu^-$.

$$\mathcal{H}_{\rm eff}(b\to se_I\bar{e}_J)=-\frac{\alpha G_F}{\sqrt{2}\pi}V_{tb}V_{ts}^*\left[C_9^{IJ}(\overline{s'}_L\gamma_\mu b'_L)(\overline{e'}_I\gamma^\mu e'_J)+C_{10}^{IJ}(\overline{s'}_L\gamma_\mu b'_L)(\overline{e'}_I\gamma^\mu\gamma_5 e'_J)\right], \tag{3.2}$$

$$\mathcal{H}_{\rm eff}(b\to s\nu_I\overline{\nu}_J)=-\frac{\alpha G_F}{\sqrt{2}\pi}V_{tb}V_{ts}^*C_L^{IJ}(\overline{s'}_L\gamma_\mu b'_L)(\overline{\nu'}_I\gamma^\mu(1-\gamma_5)\nu'_J), \tag{3.3}$$

$$\mathcal{H}_{\rm eff}(b\to c\tau_I\overline{\nu}_J)=\frac{4G_F}{\sqrt{2}}V_{cb}C_V^{IJ}(\overline{c'}_L\gamma_\mu b'_L)(\overline{e'}_I\gamma^\mu\nu'_J), \tag{3.4}$$

$$\mathcal{H}_{\rm eff}(\tau\to\mu s\overline{s})=C_{\tau\mu}^{ss}(\overline{\mu'}_L\gamma_\mu\tau'_L)(\overline{s'}_L\gamma^\mu s'_L), \tag{3.5}$$

$$\mathcal{H}_{\rm eff}(bs\leftrightarrow bs)=C_{bs}^{bs}(\overline{s'}_L\gamma_\mu b'_L)(\overline{s'}_L\gamma^\mu b'_L), \tag{3.6}$$

$$\mathcal{H}_{\rm eff}(\tau^-\to\mu^-\mu^+\mu^-)=C_{\tau\mu}^{\mu\mu}(\overline{\mu'}_L\gamma_\mu\tau'_L)(\overline{\mu'}_L\gamma^\mu\mu'_L), \tag{3.7}$$

where α and G_F are the QED fine structure constant and the Fermi constant, respectively; the Wilson coefficients include both of the SM and the NP contributions like $C_X = C_X(\text{SM})+C_X(\text{NP})$; the prime symbol attached on fermion fields stands for the mass eigenstates. As noted above, the CFVs dominantly couple to the left-handed currents, so that approximately enough, we have

$$C_9^{IJ}(\text{NP}) = -C_{10}^{IJ}(\text{NP}). \tag{3.8}$$

Using eq. (2.11) and eq. (B.17) in appendix B, we find the concrete expression for the NP contributions to the Wilson coefficients:

$$C_9^{IJ}(\text{NP})=-\frac{\pi}{\sqrt{2}\alpha G_F V_{tb}V_{ts}^*}\left(C^{[1]}_{q_iq_jl_kl_l}+C^{[3]}_{q_iq_jl_kl_l}\right)\cdot D^{\dagger 2i}D^{j3}L^{\dagger Ik}L^{lJ}\left(=-C_{10}^{IJ}(\text{NP})\right), \tag{3.9}$$

$$C_L^{IJ}(\text{NP})=-\frac{\pi}{\sqrt{2}\alpha G_F V_{tb}V_{ts}^*}\left(C^{[1]}_{q_iq_jl_kl_l}-C^{[3]}_{q_iq_jl_kl_l}\right)\cdot D^{\dagger 2i}D^{j3}L^{\dagger Ik}L^{lJ}, \tag{3.10}$$

$$C_V^{IJ}(\text{NP})=\frac{1}{2\sqrt{2}G_F V_{cb}}\left(2C^{[3]}_{q_iq_jl_kl_l}\right)\cdot U^{\dagger 2i}D^{j3}L^{\dagger Ik}L^{lJ}, \tag{3.11}$$

$$C_{\tau\mu}^{ss}(\text{NP})=\left(C^{[1]}_{q_iq_jl_kl_l}+C^{[3]}_{q_iq_jl_kl_l}\right)\cdot L^{\dagger 2k}L^{l3}D^{\dagger 2i}D^{j2}, \tag{3.12}$$

$$C_{bs}^{bs}(\text{NP})=\left(C^{[1]}_{q_iq_jq_kq_l}+C^{[3]}_{q_iq_jq_kq_l}\right)\cdot D^{\dagger 2i}D^{j3}D^{\dagger 2k}D^{l3}, \tag{3.13}$$

$$C_{\tau\mu}^{\mu\mu}(\text{NP})=2\left(C^{[1]}_{l_il_jl_kl_l}+C^{[3]}_{l_il_jl_kl_l}\right)\cdot L^{\dagger 2i}L^{j3}L^{\dagger 2k}L^{l2}. \tag{3.14}$$

Here, we comment on the renormalization group effects. The chirality-conserving dimension-six semi-leptonic operators (and also fully leptonic operators) take null effects from the QCD running of the Wilson coefficients due to the current conservation (see e.g., [32]), while we need to take into account of nontrivial QCD-running effects on the fully hadronic ones in our estimation for the bound from the B_s^0-$\bar{B}_s^0$ mixing, as we will see in section 3.1.5. A short comment on the QED running effects will be provided in the summary section. In doing numerical analyses, for the SM gauge couplings we thus use the values evaluated at two-loop level, computed from the Z-boson mass scale values by running up to $m_\rho = 1\,\text{TeV}$, $g_Y^2(m_\rho) \simeq 0.129$, $g_W^2(m_\rho) \simeq 0.424$ and $g_s^2(m_\rho) \simeq 1.11$, with use of the electromagnetic couplings renormalized at the Z-boson mass scale ($m_Z \simeq 91.2\,\text{GeV}$ [10]), $\alpha(m_Z) = g_Y^2(m_Z)c_W^2/(4\pi) \simeq 1/128$ [10] and the (Z-mass shell) Weinberg angle quantity $c_W^2 = m_W^2/m_Z^2 \simeq 0.778$, and the QCD coupling $\alpha_s(m_Z) = g_s^2/(4\pi) \simeq 0.118$ [10]. In addition, the pole mass of the top quark and the Higgs mass are selected as 173.15 GeV and 125 GeV, respectively, and we refer to refs. [33–35] for the form and formalism regarding the two-loop beta functions (also to [36] for the boundary conditions).

3.1.1 $\bar{B} \to K^{(*)}\ell^+\ell^-$

Including the SM contributions, we write the effective Hamiltonian for $b \to s\ell^+\ell^-$,

$$\begin{aligned}\mathcal{H}_{\text{eff}}(b \to s\ell_I\bar{\ell}_J) = &-\frac{\alpha G_F}{\sqrt{2}\pi}V_{tb}V_{ts}^*\left(C_9^{\text{SM}}\delta^{IJ} + C_9^{IJ}(\text{NP})\right)\left(\bar{s}_L'\gamma^\mu b_L'\right)\left(\bar{\ell}_I'\gamma_\mu\ell_J'\right)\\ &-\frac{\alpha G_F}{\sqrt{2}\pi}V_{tb}V_{ts}^*\left(C_{10}^{\text{SM}}\delta^{IJ} + C_{10}^{IJ}(\text{NP})\right)\left(\bar{s}_L'\gamma^\mu b_L'\right)\left(\bar{\ell}_I'\gamma_\mu\gamma^5\ell_J'\right),\end{aligned} \tag{3.15}$$

where $V_{tb}V_{ts}^* = -0.0405 \pm 0.0012$ [10, 37], and $C_9^{\text{SM}} \simeq 0.95$ and $C_{10}^{\text{SM}} \simeq -1.00$, which are estimated at the m_b scale, (see, e.g., [38]). The favored region for $C_9^{\mu\mu}(\text{NP}) = -C_{10}^{\mu\mu}(\text{NP})$ in the left-handed scenario is given at the 2σ level as

$$-0.87 \leq C_9^{\mu\mu}(\text{NP}) = -C_{10}^{\mu\mu}(\text{NP}) \leq -0.36\,, \tag{3.16}$$

whereas the best fit point is -0.61. The quoted numbers have been taken from ref. [39] (see also [40–50]), where all available associated data from LHCb, Belle, ATLAS and CMS were combined, which are also consistent with the current measurement for the (optimized) angular observable, so-called P_5' [12, 51–57].

NP contributions to $b \to s\ell^+\ell^-$ processes have been discussed in the context of new vector-boson interactions [58–103] and/or vector-leptoquark ones [22, 104–118]. In our model, those NP contributions takes a hybrid form arising from the Z'-type and vector-leptoquark-type CFVs, as noted in Introduction.

3.1.2 $\bar{B} \to K^{(*)}\nu\bar{\nu}$

The effective Hamiltonian for $\bar{B} \to K^{(*)}\nu\bar{\nu}$ with the SM contribution included is given by

$$\mathcal{H}_{\text{eff}}(b \to s\nu_I\bar{\nu}_J) = -\frac{\alpha G_F}{\sqrt{2}\pi}V_{tb}V_{ts}^*\left(C_L^{\text{SM}}\delta^{IJ} + C_L^{IJ}(\text{NP})\right)\left(\bar{s}_L'\gamma^\mu b_L'\right)\left(\bar{\nu}_I'\gamma_\mu(1-\gamma^5)\nu_J'\right), \tag{3.17}$$

JHEP11(2018)164

where the SM contribution is $C_L^{\rm SM} \simeq -6.36$. The current upper bounds on the branching ratios of $\bar{B} \to K^{(*)}\nu\bar{\nu}$ [119, 120] place constraints on NP contributions [121], so that at 90% C.L. we find [31]

$$-13\sum_{I=1}^{3}{\rm Re}[C_L^{II}({\rm NP})] + \sum_{I,J=1}^{3}|C_L^{IJ}({\rm NP})|^2 \leq 473\,. \tag{3.18}$$

3.1.3 $\tau \to \phi\mu$

To this decay process, the SM (with three right-handed Dirac neutrinos introduced) predicts so tiny lepton flavor violation highly suppressed by the neutrino mass scale. We may adopt the constraint obtained in [31] from the 90% C.L. upper limit of $\mathcal{B}(\tau \to \mu\phi) < 8.4\times 10^{-8}$ [122], which reads

$$\left|C_{\tau\mu}^{ss}({\rm NP})\right| < 0.019 \times \left(\frac{m_\rho}{1\,{\rm TeV}}\right)^2 . \tag{3.19}$$

3.1.4 $\tau \to 3\mu$

As in the case of the $\tau \to \mu\phi$ decay, the SM prediction is negligible in this process. The branching ratio for $\tau \to 3\mu$ decay is then given by

$${\rm Br}[\tau^- \to \mu^-\mu^+\mu^-] = |C_{\tau\mu}^{\mu\mu}({\rm NP})|^2 \times \frac{0.94}{4}\frac{m_\tau^5\tau_\tau}{192\pi^3}\,, \tag{3.20}$$

where we checked the form of the branching ratio is consistent with those of refs. [123, 124]. τ_τ represents the mean lifetime of the tau lepton ($\simeq 2.9\times10^{-13}\,$s [10]). The factor 0.94 came from the phase space suppression for the decay [31]. The current upper bound at 90% C.L. is placed to be [125]:

$${\rm Br}[\tau^- \to \mu^-\mu^+\mu^-] < 2.1\times10^{-8}. \tag{3.21}$$

3.1.5 B_s^0-$\bar{B}_s^0$ mixing: ΔM_{B_s}

As noted above, the B_s^0-$\bar{B}_s^0$ mixing process would involve a bit more delicate deal than other semi-leptonic and fully leptonic decay processes, because nontrivial QCD corrections potentially come in. To this process, the effective Hamiltonian including the SM contribution is written like

$$\mathcal{H}_{\rm eff}(bs\leftrightarrow bs) = \left(\frac{G_F^2 m_W^2}{16\pi^2}(V_{tb}V_{ts}^*)^2 C_{VLL}^{\rm SM} + C_{bs}^{bs}({\rm NP, at}\ m_b^{\rm pole})\right)(\bar{s}'_L\gamma^\mu b'_L)(\bar{s}'_L\gamma_\mu b'_L)\,, \tag{3.22}$$

where $m_W = (80.379\pm0.012)\,$GeV [10], $m_b^{\rm pole}$ means the pole mass of the bottom quark and $C_{VLL}^{\rm SM}$ is given as [31, 126]

$$C_{VLL}^{\rm SM} = 4\,\eta_{2B}\,S_0(x_t), \tag{3.23}$$

with $S_0(x_t)$ being the Inami-Lim function [127]

$$S_0(x_t) = \frac{x_t}{4}\left[1 + \frac{9}{1-x_t} - \frac{6}{(1-x_t)^2} - \frac{6x_t^2\log x_t}{(1-x_t)^3}\right]. \tag{3.24}$$

In eq. (3.23) $x_t \equiv (\bar{m}_t(\bar{m}_t))^2/m_W^2$, in which $\bar{m}_t(\bar{m}_t)$ is the $\overline{\rm MS}$ mass of the top quark, and η_{2B} ($= 0.551$) dictates the next-to-leading order (NLO) QCD correction [128]. From the effective Hamiltonian in eq. (3.22), the mass difference is then evaluated as

$$\Delta M_{B_s} = \frac{2}{3} M_{B_s} f_{B_s}^2 \hat{B}_{B_s} \left| \frac{G_F^2 m_W^2}{16\pi^2} (V_{tb}V_{ts}^*)^2 C_{VLL}^{\rm SM} + C_{bs}^{bs}({\rm NP}, {\rm at}\ m_b^{\rm pole}) \right|. \tag{3.25}$$

We shall first discuss the SM prediction (the first term in eq. (3.25)). We adopt the recently reported value for the $\overline{\rm MS}$-top mass, $\bar{m}_t(\bar{m}_t) = (162.1{\pm}1.0)$ GeV, obtained in the NLO variant of the ABMP16 fit [129]. For the B_s mass we take $M_{B_s} = 5366.89(19)$ MeV [10]. As to the B_s-decay constant and the bag parameter, we adopt the FLAG17 result, $f_{B_s}\sqrt{\hat{B}_{B_s}} = (274{\pm}8)$ MeV [130, 131]. The relevant CKM factor $(V_{tb}V_{ts}^*)^2 = |V_{tb}V_{ts}^*|^2\, e^{-2i\beta_s}$ can be simplified to $|V_{tb}V_{ts}^*|^2$, because of the small complex angle ($\varphi_s^{c\bar{c}s}|_{\rm exp} = -2\beta_s = -0.030{\pm}0.033$ [132], $\varphi_s^{c\bar{c}s}|_{\rm SM} = -0.03704 \pm 0.00064$ [133, 134]). Since $C_{bs}^{bs}({\rm NP})$ turns out to be real in the CFV scenario, we can take the limit $\varphi_s^{c\bar{c}s} \to 0$ with good precision. From the particle-data group-fit results for the magnitudes of all nine CKM elements (and the Jarlskog invariant) $|V_{tb}| = 0.999105 \pm 0.000032$ and $|V_{ts}| = 0.04133 \pm 0.00074$ [10], we find $|V_{tb}| \cdot |V_{ts}| \simeq 0.0413 \pm 0.000739$. In evaluating the propagation of errors, we here simply ignored possible correlations between $|V_{tb}|$ and $|V_{ts}|$, which would be justified for estimating a conservative bound for new physics scenarios addressing the R_{K^*} anomaly.

Combining all these values, we thus estimate the SM prediction.[8]

$$\Delta M_{B_s}^{\rm SM} = (19.7 \pm 1.35)\,{\rm ps}^{-1}. \tag{3.26}$$

On the other hand, the experimental value is [132]

$$\Delta M_{B_s}^{\rm exp} = (17.757 \pm 0.021)\,{\rm ps}^{-1}. \tag{3.27}$$

Looking at the SM prediction in eq. (3.26), we should note that the theoretical uncertainty most dominantly comes from the input parameters $f_{B_s}\sqrt{\hat{B}_{B_s}}$, $V_{tb}V_{ts}^*$ and $\bar{m}_t(\bar{m}_t)$, where the errors from the first two quantities are much more dominant than the experimental uncertainty in eq. (3.27), while the error for $\bar{m}_t(\bar{m}_t)$ is subdominant compared with the other two, though being still larger than the experimental uncertainty.

We next turn to estimation for the NLO-QCD correction to the NP contribution arising by the renormalization group evolution of the $C_{bs}^{bs}({\rm NP}, {\rm at}\ m_\rho)$ with running down to the $m_b^{\rm pole}$ scale. The NLO-QCD running effect on the $C_{bs}^{bs}({\rm NP})$ can be evaluated by following the formalism given in ref. [136] (see also [137, 138]) as

$$C_{bs}^{bs}({\rm NP}, {\rm at}\ m_b^{\rm pole}) \simeq \left(b_1^{(1,1)} + \eta\,(m_\rho) c_1^{(1,1)}\right) (\eta\,(m_\rho))^{a_1} \times C_{bs}^{bs}({\rm NP}, {\rm at}\ m_\rho), \tag{3.28}$$

[8]This estimated number is close to the result reported in [135], where $\Delta M_{B_s}^{\rm SM} = (20.01 \pm 1.25)\,{\rm ps}^{-1}$, which has been estimated by using the same FLAG17 variable for $f_{B_s}\sqrt{\hat{B}_{B_s}}$ as what we have used, while the $\overline{\rm MS}$ mass of the top quark has been taken to be different from ours, $\bar{m}_t(\bar{m}_t) = 165.65(57)$ GeV. (For details in other subtleties, see [135].) Use of their $\bar{m}_t(\bar{m}_t)$ would yield $\Delta M_{B_s}^{\rm SM} = (20.2 {\pm} 1.39)\,{\rm ps}^{-1}$, in which the small enhancement in the error may originate from the increased value of $S_0(x_t)$.

JHEP11(2018)164

where $m_b^{\rm pole} = 4.6\,{\rm GeV}$, $\eta(m_\rho) \equiv \alpha_s(m_\rho)/\alpha_s(m_t)$, $a_1\,(= 0.286)$, $b_1^{(1,1)}\,(= 0.865)$ and $c_1^{(1,1)}\,(= -0.017)$ [136]. The exact form of the NLO-running QCD coupling [139, 140] together with $m_t \simeq 173\,{\rm GeV}$ (the pole mass of the top quark) and $\Lambda_{\rm QCD} \simeq 0.34\,{\rm GeV}$ (the QCD confinement scale)[9] yield $\eta\,(m_\rho = 1\,{\rm TeV}) \simeq 0.771$. We thus have

$$C_{bs}^{bs}({\rm NP}, {\rm at}\ m_b^{\rm pole}) \simeq 0.79 \times C_{bs}^{bs}({\rm NP}, {\rm at}\ m_\rho = 1\,{\rm TeV}). \tag{3.29}$$

We will take into account of this net-NLO factor $\simeq 0.79$ in the later numerical calculations.

3.1.6 $\bar{B} \to D^{(*)}\tau\bar{\nu}$

Remarkably, it turns out that the net effect of the charged CFVs on the $d \to u\ell\nu$ transition is almost vanishing, i.e.,

$$C_V^{IJ}({\rm NP}) \simeq 0\,. \tag{3.30}$$

This is because of the approximate degeneracy for CFVs (eq. (3.1)) as the consequence of the presence of the (approximate) one-family SU(8) symmetry. Possible contributions arise from the mass difference in the charged CFVs and the $V_{\rm SM}$-ρ mixing effect, both of which are suppressed (controlled) by the factor g_W^2/g_ρ^2. In fact, for $g_\rho = \mathcal{O}(10)$ as in eq. (2.7) these contributions on $R_{D^{(*)}}$ do not exceed 5% and thus it is not sufficient to account for $\mathcal{O}(10\%)$ deviations between the present data and the SM predictions in the ratios.

Generically, one could introduce extra interactions which would yield a sizable breaking effect for the SU(8) degeneracy. Nevertheless, as a minimal setup we will not consider such extra terms in the present study, so as to keep the approximate SU(8) symmetry in eq. (3.1) and hence the vanishing contribution to $R_{D^{(*)}}$.

At Belle II, we may have potential to examine $R_{D^{(*)}}$ with a few % accuracy. Thus, if the discrepancy is reduced to a few % in future observation at Belle II, it may point to the contributions from such small effects. See eq. (B.17) in appendix B for explicit expression on $C_V^{IJ}({\rm NP})$.

3.1.7 $B - \tau$ system constraint

The CFV contributions to the $2 \leftrightarrow 3$ transitions described as above are controlled by five parameters: m_ρ in eq. (3.1), g_ρ in eq. (2.7), θ_D, θ_L in eq. (2.12) and $g_{\rho L}^{33}$ in eq. (2.9). For a reference point, we take $m_\rho = 1\,{\rm TeV}$ and $g_\rho = 8$, which will turn out to be consistent with the K system bound later, and survey the allowed parameter region for the remaining couplings.

Figure 1 shows the region plot on the plane $(g_{\rho L}^{33}, \theta_L)$ constrained by the lepton flavor violating $\tau \to 3\mu$ decay. The constraint from the ΔM_{B_s} on the parameter space in the plane $(g_{\rho L}^{33}, \theta_D)$ is depicted in figure 2. We have allowed the 2σ deviation for the ΔM_{B_s} between the experimental and SM -predicted values, $\Delta M_{B_s}^{\rm exp} - \Delta M_{B_s}^{\rm SM}$. This can be thought to be conservative because of the currently present deviation $\gtrsim 1\sigma$, as captured from eqs. (3.26) and (3.27). In total, the favored parameter space in the plane $(g_{\rho L}^{33}, \theta_L)$ with $\theta_D/\pi = 2\times 10^{-3}$ fixed[10] is drawn in figure 3, where the overlapped domain (thick-blue and cyan regions)

[9] We used the approximated form for the Lambert W-function (in the '-1' branch) [141] in this estimation.

[10] The larger θ_D case will be disfavored by the presence of the $R_{K^{(*)}}$ anomaly.

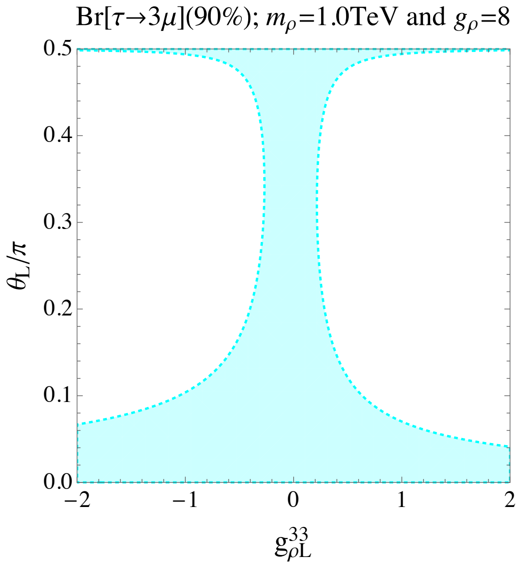

Figure 1. The $\tau \to 3\mu$ decay constraint on the plane $(g_{\rho L}^{33}, \theta_L)$ for $m_\rho = 1\,\mathrm{TeV}$ and $g_\rho = 8$. The 90% C.L. upper limit on the branching ratio has been taken from eq. (3.21). The shaded region is allowed at the 90% C.L. read off from eq. (3.21).

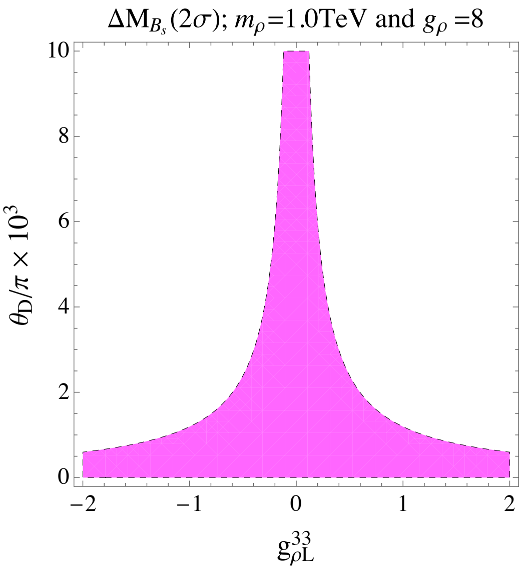

Figure 2. The ΔM_{B_s} constraint on the plane $(g_{\rho L}^{33}, \theta_D)$ for $m_\rho = 1\,\mathrm{TeV}$ and $g_\rho = 8$, where the shaded region is allowed at the 2σ level read off from eqs. (3.27) and (3.26) with taking into account the errors from the input variables $[f_{B_s}\sqrt{\hat{B}_{B_s}},\, V_{tb}V_{ts}^*$ and $\bar{m}_t(\bar{m}_t)]$ as described in the text.

satisfies the 2σ range for $C_9^{\mu\mu}$ $(= -C_{10}^{\mu\mu})$ around the best fit point in eq. (3.16), hence explains the current $R_{K^{(*)}}$ anomaly at that level consistently. The range for the $g_{\rho L}^{33}$ has been restricted to roughly $[-0.60, -0.47]$ or $[0.44, 0.60]$ (at $\theta_L \simeq \pi/2$), which is required by the ΔM_{B_s} bound for $\theta_D/\pi = 2 \times 10^{-3}$ read off from figure 2. The gray-hatched region in

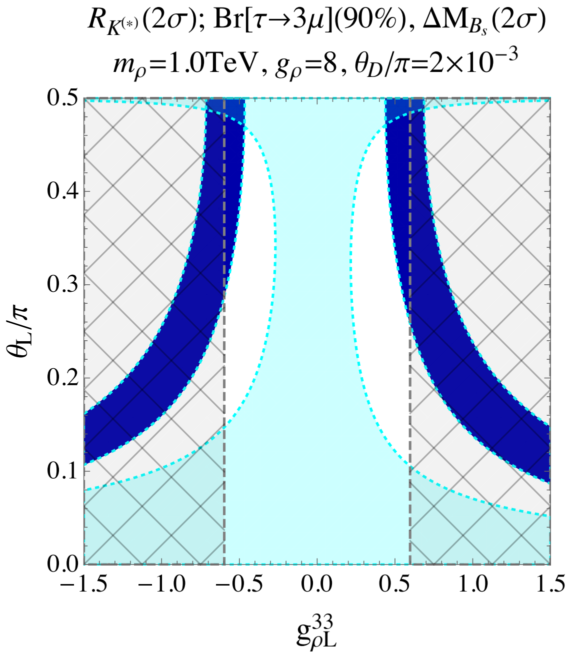

Figure 3. The region plot in the plane $(g_{\rho L}^{33}, \theta_L)$ with $\theta_D/\pi = 2 \times 10^{-3}$ fixed for $m_\rho = 1\,\text{TeV}$ and $g_\rho = 8$. The current $R_{K^{(*)}}$ anomaly can be explained in the thick-blue region at the 2σ level, while the cyan-shaded area represents the consistent region with the current 90% C.L. upper limit of Br$[\tau^- \to \mu^-\mu^+\mu^-]$ (see figure 1). The gray-hatched region is out of the 2σ-favored area for ΔM_{B_s} (see figure 2).

figure 3 is out of the 2σ-favored region for ΔM_{B_s}, which suggests that the favored region is limited to a muon-philic scenario with $\theta_L \sim \pi/2$ (in the mass-eigenstate basis).[11]

The constraints from $B \to K^{(*)}\nu\bar{\nu}$ and $\tau \to \mu\phi$ are irrelevant fully in the focused region in figure 3. We provide a comment on the constraints from other three $2 \leftrightarrow 3$ observables, namely $\bar{B} \to K^{(*)}\mu^\pm\tau^\mp$, $\Upsilon \to \mu^\pm\tau^\mp$ and $J/\psi \to \mu^\pm\tau^\mp$, where they provide no additional bound in the focused region in figure 3. Also, we have a discussion on how significant the best-fit point for $b \to s\mu^+\mu^-$ in a global sense by evaluating χ^2 variable in a benchmark point in appendix C.

3.2 Flavor changing processes converting the second and first generations

We next move on to the flavor constraints on the CFVs coming from the K system. Looking at the flavor texture introduced in section 2.3, we find that the NP contributions to the s-d

[11]The favored flavor structure is thus similar to that proposed in refs. [31, 83], where the NP is assumed to dominantly couple to the second-generation leptons and third-generation quarks in the mass-eigenstate basis. Alternatively, we can consider that (ν_μ, μ) and (t, b) are the "third generation" of the gauge eigenstates. Whichever it is called, it does not make significant difference (occurring only in ways of parametrizing mixing angles) in addressing the $R_{K^{(*)}}$ anomaly consistently. It is also interesting to note the result obtained from the present CFV scenario looks quite different from the vector boson model in ref. [31], which is essentially because of the presence of mixing with the SM gauge bosons and the (approximate) SU(8) symmetry constraining the coupling properties for Z', G' and vector leptoquarks.

JHEP11(2018)164

transition observables, ϵ'/ϵ, $K \to \pi\nu\bar{\nu}$ and K^0-$\bar{K}^0$ mixing (ΔM_K) are possibly generated. Also, we focus on the c-u transition, where observables in the D^0-$\bar{D}^0$ mixing provide us with constraints on the scenario. As discussed in the previous section, we first note that the down-sector rotation angle θ_D is severely constrained by B observables, most stringently by B_s^0-$\overline{B_s^0}$ mixing, to be almost vanishing,

$$\theta_D \sim 0\,, \tag{3.31}$$

(but should be nonzero to address B anomalies like $b \to s\mu^+\mu^-$), while the lepton angle θ_L has to be

$$\theta_L \sim \frac{\pi}{2}\,. \tag{3.32}$$

In discussing the K and D systems, we shall take these conditions to survey the allowed parameter space for the CFVs.

3.2.1 $K \to \pi\pi$

NP effects on the $K \to \pi\pi$ process have extensively been investigated in various context of scenarios beyond the SM [142–156]. To this process, in terms of effective operators, the contributions can be classified into i) $(V-A)\times(V-A)$, ii) $(V+A)\times(V+A)$, and iii) $(V-A)\times(V+A)$ current interaction types. Since in the present model, CFVs couple only to left-handed $(V-A)$ current fermions with the generation conversion allowed, only the types of i) and iii) will be relevant. As to the type i) $(V-A)\times(V-A)$ interactions, characterized by called $Q_2 = (\bar{s}'u')_{V-A}(\bar{u}'d')_{V-A}$ (charged current type), $Q_3 = (\bar{s}'d')_{V-A}\sum_{q'}(\bar{q}'q')_{V-A}$ (QCD penguin type) and $Q_9 = (\bar{s}'d')_{V-A}\sum_{q'}Q^q_{\rm em}(\bar{q}'q')_{V-A}$ (EW penguin type) operators, we see that the CFVs exchanges having only the flavored $g^{ij}_{\rho L}$ couplings do not generate any contributions, because of the third-generation-philic texture for the $g^{ij}_{\rho L}$ in eq. (2.9) and the rotation matrix D in eq. (2.12) with the constraint on θ_D in eq. (3.31) taken into account. Thus the nontrivial-leading terms to the type i) as well as the type iii) are generated necessarily along with the flavor-universal interactions suppressed by $(g_{s,W,Y}/g_\rho)$, where only the neutral CFVs $\rho^3_{(1)}, \rho^0_{(1)'}$ and $\rho^0_{(8)}$ contribute to the effective four-fermion operators (see eq. (A.19)). We thus find the relevant induced four-fermion operators like

$$\begin{aligned}
&\mathcal{H}_{\rm eff} = \sum_{j=1\text{-}10} C_j \cdot Q_j\,,\\
&Q_1 = (\bar{s}^{b\prime}u^{a\prime})_{V-A}(\bar{u}^{a\prime}d^{b\prime})_{V-A}\,, && Q_2 = (\bar{s}'u')_{V-A}(\bar{u}'d')_{V-A}\,,\\
&Q_3 = (\bar{s}'d')_{V-A}\sum_{q'}(\bar{q}'q')_{V-A}\,, && Q_4 = (\bar{s}^{b\prime}d^{a\prime})_{V-A}\sum_{q'}(\bar{q}^{a\prime}q^{b\prime})_{V-A}\,,\\
&Q_5 = (\bar{s}'d')_{V-A}\sum_{q'}(\bar{q}'q')_{V+A}\,, && Q_6 = (\bar{s}^{b\prime}d^{a\prime})_{V-A}\sum_{q'}(\bar{q}^{a\prime}q^{b\prime})_{V+A}\,,\\
&Q_7 = \frac{3}{2}(\bar{s}'d')_{V-A}\sum_{q'}Q^q_{em}(\bar{q}'q')_{V+A}\,, && Q_8 = \frac{3}{2}(\bar{s}^{b\prime}d^{a\prime})_{V-A}\sum_{q'}Q^q_{em}(\bar{q}^{a\prime}q^{b\prime})_{V+A}\,,\\
&Q_9 = \frac{3}{2}(\bar{s}'d')_{V-A}\sum_{q'}Q^q_{em}(\bar{q}'q')_{V-A}\,, && Q_{10} = \frac{3}{2}(\bar{s}^{b\prime}_L d^{a\prime}_L)_{V-A}\sum_{q'}Q^q_{em}(\bar{q}^{a\prime}q^{b\prime})_{V-A}\,,
\end{aligned} \tag{3.33}$$

where the operator notation follows refs. [1, 29] [$(\bar{q}'q')_{V\pm A}$ being defined as $(\bar{q}'\gamma^\mu(1\pm\gamma_5)q')$; γ^μ being suppressed in the above list], and a, b stand for the color indices (with repeated ones being summed). The Wilson coefficients $C_{1\text{-}10}$ are read off from eq. (B.17) in appendix B, which are interpreted as the ones evaluated at the CFV mass scale m_ρ:

$$
\begin{aligned}
&C_1(m_\rho) = 0\,, && C_2(m_\rho) = -i\cdot\frac{1}{8}\frac{g_W^2 g_{\rho L}^{12}}{m_\rho^2 g_\rho}\,,\\
&C_3(m_\rho) = i\cdot\frac{1}{24}\frac{g_s^2 g_{\rho L}^{12}}{m_\rho^2 g_\rho}+i\cdot\frac{1}{8}\frac{g_W^2 g_{\rho L}^{12}(-Y_q)}{m_\rho^2 g_\rho}-i\cdot\frac{1}{144}\frac{g_Y^2 g_{\rho L}^{12}}{m_\rho^2 g_\rho}\,, && C_4(m_\rho) = -i\cdot\frac{1}{8}\frac{g_s^2 g_{\rho L}^{12}}{m_\rho^2 g_\rho}\,,\\
&C_5(m_\rho) = i\cdot\frac{1}{24}\frac{g_s^2 g_{\rho L}^{12}}{m_\rho^2 g_\rho}\,, && C_6(m_\rho) = -i\cdot\frac{1}{8}\frac{g_s^2 g_{\rho L}^{12}}{m_\rho^2 g_\rho}\,,\\
&C_7(m_\rho) = -i\cdot\frac{1}{36}\frac{g_Y^2 g_{\rho L}^{12}}{m_\rho^2 g_\rho}\,, && C_8(m_\rho) = 0\,,\\
&C_9(m_\rho) = i\cdot\frac{1}{12}\frac{g_W^2 g_{\rho L}^{12}}{m_\rho^2 g_\rho}\,, && C_{10}(m_\rho) = 0\,,
\end{aligned}
\tag{3.34}
$$

where Y_q $(= 1/6)$ represents the weak hypercharge of the quark doublet.

The $K^0 \to \pi^0\pi^0/\pi^+\pi^-$ amplitudes, decomposed into the distinguished isospin states $(I = 0, 2)$ in the final state, are evaluated through the effective Hamiltonian as

$$
\begin{aligned}
A_I &\equiv \langle(\pi\pi)_I|\mathcal{H}_{\text{eff}}|K^0\rangle\\
&= \sum_j C_j(\mu)\langle(\pi\pi)_I|Q_j(\mu)|K^0\rangle \equiv \sum_j C_j(\mu)\langle Q_j(\mu)\rangle_I\,,
\end{aligned}
\tag{3.35}
$$

where μ represents a reference scale of the phenomenon. In later numerical calculations, we put the values of the two-loop running couplings for ϵ'/ϵ.

The CFV contributions to the direct CP violation in the $K \to \pi\pi$ processes are evaluated at the NLO perturbation in QCD and QED coupling expansions as [2]

$$
\left(\frac{\epsilon'}{\epsilon}\right)^{\text{CFVs}} = \frac{\omega_+}{\sqrt{2}\,|\epsilon_K^{\text{exp}}|\,\text{Re}A_0^{\text{exp}}}\langle\vec{Q}_{\epsilon'}(\mu)^T\rangle\hat{U}\,(\mu, m_\rho)\,\text{Im}\left[\vec{C}(m_\rho)\right],
\tag{3.36}
$$

where $\vec{C}(m_\rho) = (C_1(m_\rho), C_2(m_\rho), C_3(m_\rho), \cdots, C_{10}(m_\rho))^T$, $\text{Re}A_0^{\text{exp}} = (3.3201 \pm 0.0018) \times 10^{-7}\text{GeV}$ [157], and $\omega_+|_{\text{SM}} \equiv a\,\text{Re}A_2|_{\text{SM}}/\text{Re}A_0|_{\text{SM}} = 4.53 \times 10^{-2}$ [1, 158]. The coefficients $\langle\vec{Q}_{\epsilon'}(\mu)^T\rangle\hat{U}\,(\mu, m_\rho)$, which denote the evolution of the hadronic matrix elements from the scale μ to the NP scale m_ρ, are given in ref. [2], where $\langle\vec{Q}_{\epsilon'}(\mu)^T\rangle$ is defined as

$$
\langle\vec{Q}_{\epsilon'}(\mu)^T\rangle \equiv \frac{1}{\omega_+}\langle\vec{Q}(\mu)^T\rangle_2 - \langle\vec{Q}(\mu)^T\rangle_0(1-\hat{\Omega}_{\text{eff}}).
\tag{3.37}
$$

The vector forms $\langle\vec{Q}(\mu)^T\rangle_I$ $(I = 0, 2)$ are defined from $\langle Q_j(\mu)\rangle_I$ like $\vec{C}(m_\rho)$.[12] The factors for the isospin breaking correction are described in the matrix form,

$$
(1-\hat{\Omega}_{\text{eff}})_{ij} = \begin{cases} 0.852 & (i = j = 1-6),\\ 0.983 & (i = j = 7-10),\\ 0 & (i \neq j). \end{cases}
\tag{3.38}
$$

[12]The values of $\langle\vec{Q}(\mu)^T\rangle_I$ and the form of $\hat{U}\,(\mu, m_\rho)$ are available in [2].

Here the scale μ is set to be 1.3 GeV. In the LO analysis where $C_5(m_\rho), C_6(m_\rho)$ and $C_7(m_\rho)$ bring main effects on $C_6(m_c)$ and $C_8(m_c)$, we found that the contributions from QCD penguin Q_6 dominates in the ϵ'/ϵ, and the EW penguin Q_8 term yields about 60% contribution of them.

Actually, leptoquark-type CFVs ($\rho^{0,\alpha}_{(3)}$) would also contribute to the ϵ'/ϵ at the one-loop level as discussed in ref. [152]. However, in contrast to the literature, this kind of contributions are highly suppressed by a tiny θ_D in the present third-generation-philic scenario required by the constraint from the B meson system, specifically from the $B^0_s - \bar{B}^0_s$ mixing (eq. (3.31)). This difference manifests the characteristic feature in the present CFV scenario based on the one-family SU(8) symmetry, by which the predictions in flavor physics are derived necessarily with a significant correlation between the $2 \leftrightarrow 3$ and $1 \leftrightarrow 2$ transition processes, as will be more clearly seen later.

3.2.2 $K^+ \to \pi^+\nu\bar{\nu}$ and $K_L \to \pi^0\nu\bar{\nu}$

To these processes, the CFVs give contributions from the color-singlet Z'-like ($\rho^3_{(1)}$, $\rho^0_{(1)'}$) and the color-triplet vector leptoquark-like ($\rho^{3,0}_{(3)}$) exchanges. Those CFVs exchange contributions are read off from eq. (B.17) in appendix B as follows:

$$\begin{aligned}\mathcal{H}_{\rm eff}(s \to d\nu\bar{\nu}) \simeq & \left(-i\frac{7}{16}\frac{g^{12}_{\rho L}g^{33}_{\rho L}}{m^2_\rho}\right)(\bar{s}'_L\gamma_\mu d'_L)(\bar{\nu}_{\mu L}\gamma^\mu\nu_{\mu L}) \\ & + \left(i\frac{1}{4}\frac{g^{12}_{\rho L}}{m^2_\rho}\frac{(g^2_W + g^2_Y/3)}{g_\rho}\right)(\bar{s}'_L\gamma_\mu d'_L)\sum_{l=e,\mu,\tau}(\bar{\nu}^l_L\gamma^\mu\nu^l_L)\,,\end{aligned} \tag{3.39}$$

where we have taken into account $\theta_L \sim \pi/2$ (muon-philic condition in eq. (3.32)) in evaluating the contribution along with the flavorful coupling $g^{33}_{\rho L}$ (first line). The term in the first line comes from the Z'-type CFVs ($\rho^3_{(1)}, \rho^0_{(1)'}$) and the vector-leptoquark type ones ($\rho^{0,3}_{(3)}$) -exchanges, while the one in the second line from the Z'-type ones. The dominant term actually comes from the vector-leptoquark type exchanges: the prefactor for the flavorful coupling term in the first line of eq. (3.39) reads $7/16 = (-1/16)_{\rho^0_{(1)'}} + (1/2)_{\rho^{0,\alpha}_{(3)}}$ (see eq. (B.17)).[13]

The branching ratios $\mathrm{Br}[K^+ \to \pi^+\nu\bar{\nu}]$ and $\mathrm{Br}[K_L \to \pi^0\nu\bar{\nu}]$ are computed as [29, 160]

$$\begin{aligned}\mathrm{Br}[K^+ \to \pi^+\nu\bar{\nu}] &= \kappa_+\left[\frac{1}{3}\sum_{l=e,\mu,\tau}\left(\frac{\mathrm{Im}X^l_{\rm eff}}{\lambda^5}\right)^2 + \left(\frac{\mathrm{Re}X_{\rm eff}}{\lambda^5} + \frac{\mathrm{Re}\lambda_c}{\lambda}P_c(X)\right)^2\right], \\ \mathrm{Br}[K_L \to \pi^0\nu\bar{\nu}] &= \frac{1}{3}\kappa_L\sum_{l=e,\mu,\tau}\left(\frac{\mathrm{Im}X^l_{\rm eff}}{\lambda^5}\right)^2,\end{aligned} \tag{3.40}$$

with $\lambda = |V_{us}| = 0.225$, $P_c(X) = (9.39 \pm 0.31) \times 10^{-4}/\lambda^4 + (0.04 \pm 0.02)$, $\mathrm{Re}\lambda_c/\lambda \simeq -0.98$ being the charm contribution, $\kappa_+ = (5.157 \pm 0.025) \times 10^{-11}(\lambda/0.225)^8$ and $\kappa_L = (2.231 \pm$

[13] A similar leptoquark scenario for addressing $K \to \pi\nu\bar{\nu}$ based on the third-generation-philic texture in light of the $R_{K^{(*)}}$ anomaly has been discussed in ref. [159] where scalar leptoquarks at one-loop level play the game.

JHEP11(2018)164

$0.013) \times 10^{-10}(\lambda/0.225)^8$ [29, 160]. Here the NP effects come in $X_{\rm eff}^{(l)}$, which are in the present CFV case numerically evaluated as

$$
\begin{aligned}
{\rm Re}X_{\rm eff} &= -4.83 \times 10^{-4}\,, \\
{\rm Im}X_{\rm eff}^{l} &\simeq 2.12 \times 10^{-4} - 2.46 \left(\frac{1\,{\rm TeV}}{m_\rho}\right)^2 g_{\rho L}^{12} \left[g^l - \frac{4}{7} \frac{(g_W^2 + g_Y^2/3)}{g_\rho} \right]\,,
\end{aligned} \tag{3.41}
$$

with $g^{l=e,\tau} = 0$ and $g^{l=\mu} = g_{\rho L}^{33}$ (see eq. (3.39)), in which we have quoted the values of SM predictions from ref. [148] using the CKMFITTER result for the CKM elements.

3.2.3 K^0-$\bar{K}^0$ mixing (ΔM_K)

The CFV contributions to the ΔM_K, dominated by the flavored left-handed coupling $g_{\rho L}^{12}$, are evaluated through the effective four-fermion interaction term (see eq. (B.17) in appendix B)

$$
\begin{aligned}
\mathcal{H}_{\rm eff}(\Delta M_K) &= C_{\rm NP}^{VLL}(m_\rho) \cdot (\bar{s}_L' \gamma_\mu d_L')(\bar{s}_L' \gamma^\mu d_L')\,, \\
C_{\rm NP}^{VLL}(m_\rho) &= -\frac{7 (g_{\rho L}^{12})^2}{32 m_\rho^2}\,.
\end{aligned} \tag{3.42}
$$

This NP term contributes to $\Delta M_K^{\rm NP}$ as (e.g. see refs. [29, 161])

$$
\begin{aligned}
\Delta M_K^{\rm NP} &= 2{\rm Re}[M_{12}^K]\,, \\
(M_{12}^K)^* &= \frac{1}{3} F_K^2 \hat{B}_K\, m_K\, \eta_2\, \tilde{r} \cdot C_{\rm NP}^{VLL}(\mu)\,,
\end{aligned} \tag{3.43}
$$

with the experimental values [10] $m_K = 0.497614\,{\rm GeV}$, $F_K = 0.1561\,{\rm GeV}$, and $\hat{B}_K \simeq 0.764$, $\eta_2 \simeq 0.5765$ and $\tilde{r} \simeq 1$. We may roughly neglect the small renormalization group evolution for the Wilson coefficient $C_{\rm NP}^{VLL}$ from m_ρ scale down to $\mu\,(= 1.3\,{\rm GeV})$ in eq. (3.43), i.e., taking $C_{\rm NP}^{VLL}(m_\rho) \simeq C_{\rm NP}^{VLL}(\mu)$, because the ΔM_K inevitably involves large theoretical uncertainties coming from long-distance contributions and the coefficient $C_{\rm NP}^{VLL}$ cannot get drastic corrections such as a significant amplification for the isospin breaking effect during the running down, in contrast to the ϵ'/ϵ. More on the uncertainties for the ΔM_K will be discussed in section 5.

3.2.4 D^0-$\bar{D}^0$ mixing

In this part, we discuss the CFV effect on the D^0-$\bar{D}^0$ mixing with taking account of the CP violation term. We basically adopt the convention in [162] for the transition component of the D^0-$\bar{D}^0$ system, which is connected to the effective Hamiltonians ($\mathcal{H}^{\Delta C=2}, \mathcal{H}^{\Delta C=1}$) as

$$
2M_D \left(M_{12} - \frac{i}{2}\Gamma_{12} \right) = \langle D^0 | \mathcal{H}^{\Delta C=2} | \bar{D}^0 \rangle + \sum_n \frac{\langle D^0 | \mathcal{H}^{\Delta C=1} | n \rangle \langle n | \mathcal{H}^{\Delta C=1} | \bar{D}^0 \rangle}{M_D - E_n + i\varepsilon}, \tag{3.44}
$$

where the mass eigenstate $|D_1^0\rangle$ is almost identical with one of the CP eigenstates as $\langle D_1^0 | CP | D_1^0 \rangle \approx 1$.[14] Here, we skip to discuss the absorptive part (Γ_{12}) and put $\Gamma_{12}^{\rm NP} = 0$

[14] More concretely, $CP|D^0\rangle = -|\bar{D}^0\rangle$, $CP|\bar{D}^0\rangle = -|D^0\rangle$, $|D_1^0\rangle = p|D^0\rangle - q|\bar{D}^0\rangle$, $|D_2^0\rangle = p|D^0\rangle + q|\bar{D}^0\rangle$ with $|p|^2 + |q|^2 = 1$. If there is no CP violation, $CP|D^0_{\frac{1}{2}}\rangle = \pm|D^0_{\frac{1}{2}}\rangle$.

as an assumption, since the mass scale of CFVs is of order of TeV, greater than the EW scale [163]. M_{12} is related to $\mathcal{H}^{\Delta C=2} = \sum_i C_i \mathcal{O}_i^{\Delta C=2}$ as follows,

$$2M_D M_{12} = \sum_i C_i(\mu)\langle D^0|\mathcal{O}_i^{\Delta C=2}|\bar{D}^0\rangle, \tag{3.45}$$

where the only $\mathcal{O}_1^{\Delta C=2} = (\bar{c}'_L\gamma_\mu u'_L)(\bar{c}'_L\gamma^\mu u'_L)$ is relevant in the CFV scenario at tree level. The latest allowed intervals at 95% C.L. for three observables associated with the CP violation under the assumption of the existence of CP violation are read off from [164] to be

$$y \equiv \frac{\Delta\Gamma}{2\Gamma_D}; \qquad [0.46\%, 0.79\%], \tag{3.46}$$

$$x \equiv \frac{\Delta M}{\Gamma_D}; \qquad [0.06\%, 0.70\%], \tag{3.47}$$

$$\phi_{12} \equiv \arg\left(\frac{M_{12}}{\Gamma_{12}}\right); \quad [-2.5^\circ, 1.7^\circ]\ (\leftrightarrow [-0.044, 0.030]), \tag{3.48}$$

where $\Delta M \equiv M_1 - M_2$ and $\Delta\Gamma \equiv \Gamma_1 - \Gamma_2$. Note that the absolute values of the variables,

$$y_{12} \equiv \Gamma_{12}/\Gamma_D, \qquad\qquad x_{12} \equiv 2M_{12}/\Gamma_D, \tag{3.49}$$

are approximately the same as the values of y and x, respectively [165].[15] We also note the relationship

$$xy = |x_{12}||y_{12}|\cos\phi_{12}, \tag{3.50}$$

which tells us that x and y are the same sign since $\cos\phi_{12} > 0$ in the 95% C.L. region [165]. A constraint is put on the absolute value of the variable x_{12} (which is complex in general) at $\mu_c\,(\simeq 1.3\,\text{GeV})$ through a NP contribution to the Wilson coefficient $C_i(\mu_c)$ as

$$x_{12}^{\text{NP}} = \frac{1}{M_D\Gamma_D}\sum_i C_i(\mu_c)\langle\mathcal{O}_i^{\Delta C=2}\rangle, \tag{3.51}$$

with $M_D = 1.8648\,\text{GeV}$, $(\Gamma_D)^{-1} = \tau_D = 0.4161\,\text{ps}$ [166], $\langle\mathcal{O}_1^{\Delta C=2}\rangle\ (\equiv \langle D^0|\mathcal{O}_1^{\Delta C=2}|\bar{D}^0\rangle) \sim 0.08\,\text{GeV}^4$ [162]. Taking into account the assumption $\Gamma_{12}^{\text{NP}} = 0$, we find that in eq. (3.50), the $y_{12} = y_{12}^{\text{SM}}$ and the $\sin\phi_{12}$ can be expressed as a function of only the x_{12} up to the SM factors:

$$\sin\phi_{12} = \sin\left[\arg\left(\frac{M_{12}}{\Gamma_{12}}\right)\right] = \frac{|\Gamma_{12}^{\text{SM}}|}{\Gamma_{12}^{\text{SM}}}\frac{\text{Im}[x_{12}]}{|x_{12}|} = \frac{|\Gamma_{12}^{\text{SM}}|}{\Gamma_{12}^{\text{SM}}}\sin\left[\arg\left(x_{12}\right)\right], \tag{3.52}$$

where we used the relation in eq. (3.49).

Here, we shall make comments on the current status on estimate for the SM prediction.

- The short-distance effects of x and y in the SM are estimated in [167], which are negligible compared with the following long-distance effects.

[15] It is noted that y_{12} and x_{12} are defined as $y_{12} \equiv |\Gamma_{12}|/\Gamma_D$ and $x_{12} \equiv 2|M_{12}|/\Gamma_D$ in the original paper [162].

JHEP11(2018)164

- The ratio $x^{\rm SM}/y^{\rm SM}$ and the magnitude of $y^{\rm SM}$ have been evaluated as $-1 \lesssim x^{\rm SM}/y^{\rm SM} \lesssim -0.1$ and $|y^{\rm SM}| \sim 1\%$, respectively [168, 169]. Thereby, $|x^{\rm SM}|$ currently lies in a range $0.1\% \lesssim |x^{\rm SM}| \lesssim 1\%$. The relative sign between x and y has been reported to be minus, which seems to be a tension to the observed result (both of x and y being positive).

- In our analysis, we choose $x^{\rm SM} \sim +1\%$ or $+0.1\%$ and $y^{\rm SM} \sim +0.8\%$, which may be reasonable when we take account of possible uncertainties. Now, $y \simeq y^{\rm SM} \sim 0.8\%$ (since we assume $y^{\rm NP} = 0$), which can be within the 95% C.L. region. Thus, the sign of x is determined to be positive from the relation in eq. (3.50).

In addition to those SM terms, the CFV scenario gives the NP contribution through the operator which contributes to the D^0-$\bar{D}^0$ mixing,

$$\mathcal{H}^{D^0\text{-}\bar{D}^0} \simeq -\frac{7}{32}\frac{(g_{\rho L}^{12})^2}{m_\rho^2}(1+0.00054\, i) \times (\bar{c}_L' \gamma_\mu u_L')(\bar{c}_L' \gamma^\mu u_L'), \tag{3.53}$$

where we have taken into account the tiny imaginary part via the CKM CP phase through the relation $V_{\rm CKM} \simeq U^\dagger D$ with $\theta_D = 2\pi \times 10^{-3}$. The QCD running effect from 1 TeV (identical to the CFV mass scale m_ρ) down to $\mu_c = 1.3\,{\rm GeV}$ for the operator $\mathcal{O}_1^{\Delta C=2}$ can be extracted from [170] as

$$C_1(\mu = 1.3\,{\rm GeV}) \simeq 0.72 \times C_1(\mu = 1\,{\rm TeV}). \tag{3.54}$$

We have checked the constraints on x_{12} and ϕ_{12} in a wide range for $|g_{\rho L}^{12}|$ with the reference points at $x^{\rm SM} = +1\%$ and $x^{\rm SM} = +0.1\%$ chosen. See figure 4. Thus we see that ϕ_{12} provides us with a milder bound than that from $|x_{12}|$ for $m_\rho = 1\,{\rm TeV}$.

3.2.5 Constraints from Kaon and D systems

From eqs. (3.36), (3.41) and (3.43), we place the Kaon system limits on the CFV couplings $(g_{\rho L}^{33})$ and $(g_{\rho L}^{12})$ with g_ρ chosen to be ~ 10 and m_ρ fixed to be on the order of $\mathcal{O}({\rm TeV})$. As to the $K^+ \to \pi^+ \nu\bar{\nu}$ we allow the model parameters in the 2σ range for the experimentally observed values [171]:

$${\rm Br}[K^+ \to \pi^+ \nu\bar{\nu}] = (17.3^{+11.5}_{-10.5}) \times 10^{-11}\,, \tag{3.55}$$

for the $K_L \to \pi^0 \nu\bar{\nu}$ we adopt the 90% C.L. upper bound at present [172],[16]

$${\rm Br}[K_L \to \pi^0 \nu\bar{\nu}] < 3.0 \times 10^{-9}\,. \tag{3.56}$$

Regarding the NP contribution to ϵ'/ϵ, we take the 1σ, 1.5σ, and 2σ ranges for the difference between the experimental value and the SM prediction ($(\epsilon'/\epsilon)_{\rm NP} \equiv (\epsilon'/\epsilon)_{\rm exp} - (\epsilon'/\epsilon)_{\rm SM}$), as done in ref. [148] (for the 1σ range),

$$\begin{aligned}
1.00 \times 10^{-3} &< (\epsilon'/\epsilon)_{\rm NP}\big|_{1\sigma} < 2.11 \times 10^{-3}\,,\\
0.72 \times 10^{-3} &< (\epsilon'/\epsilon)_{\rm NP}\big|_{1.5\sigma} < 2.39 \times 10^{-3}\,,\\
0.44 \times 10^{-3} &< (\epsilon'/\epsilon)_{\rm NP}\big|_{2\sigma} < 2.67 \times 10^{-3}\,.
\end{aligned} \tag{3.57}$$

[16]This bound was updated by the KOTO experiment very recently at ICHEP 2018 (on July 7, 2018), which has been more stringent than the previous one, ${\rm Br}[K_L \to \pi^0 \nu\bar{\nu}] < 2.6 \times 10^{-8}$ [173].

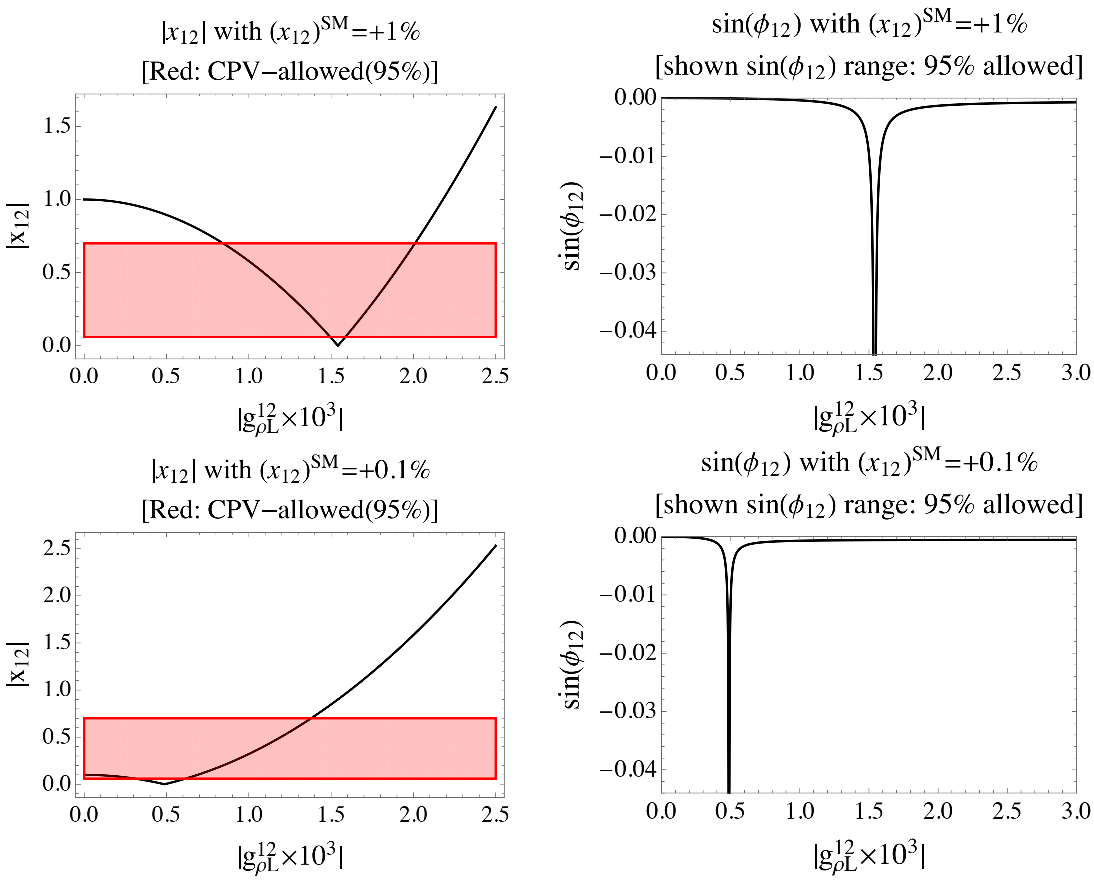

Figure 4. Curves of $|x_{12}|$ and $\sin\phi_{12}$ as functions of $|g_{\rho L}^{12}|$ with $m_\rho = 1\,\text{TeV}$ for $x^{\text{SM}} = +1\%$ (upper panels) and $x^{\text{SM}} = +0.1\%$ (lower panels). Note that the enhancements of $\sin\phi_{12}$ around $|g_{\rho L}^{12}| \sim 1.5\times 10^{-3}$ (for $x^{\text{SM}} = +1\%$) and $\sim 0.5\times 10^{-3}$ (for $x^{\text{SM}} = +0.1\%$) arises due to the vanishing $\text{Re}[x_{12}]$ by the cancellation between the CFV and the SM contributions.

For the ΔM_K in eq. (3.43), as was prescribed in ref. [148], we may derive the limit simply by allowing the NP effect to come within the 2σ uncertainty of the current measurement ($\Delta M_K^{\text{exp}} = (3.484 \pm 0.006) \times 10^{-15}\,\text{GeV}$ [10]), such as

$$|\Delta M_K^{\text{NP}}| < 3.496 \times 10^{-15}\,\text{GeV}\,. \tag{3.58}$$

First, we constrain the model parameter space by the current bound on ΔM_K in eq. (3.58) and ϵ'/ϵ in eq. (3.57), which is shown in figure 5.[17] The figure implies that as long as the g_ρ takes the value in a range such as in eq. (2.7), $g_\rho \sim 10$, the CFV mass m_ρ is severely bounded to be around $\sim 1\,\text{TeV}$, which is actually consistent with the $B-\tau$ system analysis described in the previous subsection. To address the discrepancy in ϵ'/ϵ satisfying the constraint from ΔM_K, the following conditions for $g_{\rho L}^{12}$ are required: the sign of $g_{\rho L}^{12}$

[17] Though the coefficient vector $\langle \vec{Q}_{\epsilon'}(\mu)^T \rangle \hat{U}\,(\mu, m_\rho)$ in eq. (3.36) is scale dependent, we have checked the dependence on the NP scale (m_ρ) [174] is negligibly small enough among the focused range, compared to the required accuracy for the ϵ'/ϵ of $\mathcal{O}(10^{-3})$.

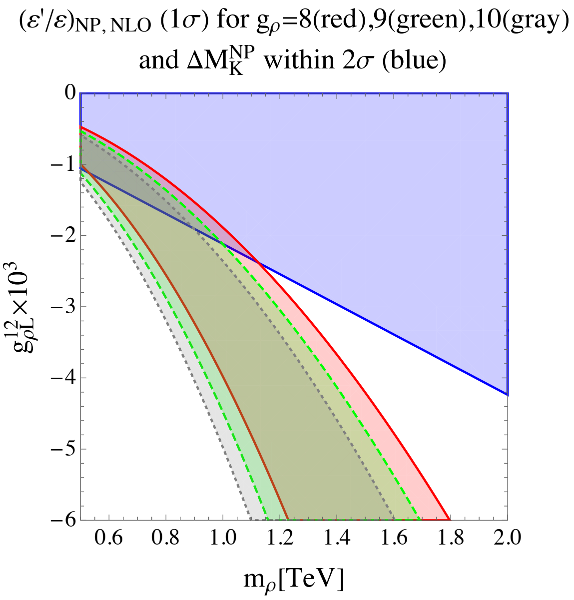

Figure 5. The ΔM_K^{NP} and $(\epsilon'/\epsilon)_{\mathrm{NP}}$ constraints on the $(m_\rho, g_{\rho L}^{12})$ plane for the three benchmark values of g_ρ.

should be negative to enhance ϵ'/ϵ, and the magnitude of $g_{\rho L}^{12}$ is constrained to be at around of $\mathcal{O}(10^{-3})$.

Second, we take account of the constraints from the D^0-$\bar{D}^0$ mixing, where large uncertainties are inevitable in contributions from the SM part as we have discussed in section 3.2.4. We exemplify the 95% C.L. intervals in the assumed values for x^{SM}, +1% and +0.1%.

Taking into account all the CFVs contributions to the K and D systems, in figure 6 we show the constraints on the coupling space $(g_{\rho L}^{12}, g_{\rho L}^{33})$ for $m_\rho = 1\,\mathrm{TeV}$, $g_\rho = 8$, $\theta_L/\pi = 1/2$ and $\theta_D/\pi = (2 \text{ or } 1.5) \times 10^{-3}$ as benchmarks. Asymmetries for the $K^+ \to \pi^+\nu\bar{\nu}$ (denoted in green) and the $K_L \to \pi^0\nu\bar{\nu}$ (in cyan) regarding the sign of the coupling $g_{\rho L}^{33}$ have been somewhat generated due to the flavor-universal coupling $(1/g_\rho)$ term in eq. (3.41). Interestingly enough, those Kaon decay rates have strong dependencies on the $g_{\rho L}^{33}$, where the pairs of neutrinos in the two processes are inclusively summed up, hence are significantly constrained by the $B - \tau$ system (horizontal lines in orange, in the figure), particularly, from the ΔM_{B_s} (placing the upper bound on the magnitude of $g_{\rho L}^{33}$ at $\theta_L \simeq \pi/2$) and the consistency with the $R_{K^{(*)}}$ (setting the lower bound). This is the characteristic consequence derived from the present CFV scenario based on the one-family SU(8) symmetry.

A part of the region where ϵ'/ϵ can be addressed seems to be excluded by the constraint from the D^0-$\bar{D}^0$ mixing. However, as shown in figure 6, the 95% C.L. interval highly depends on the choice of the uncertain input x^{SM} (refer to the discussion in section 3.2.4). Taking account of the uncertainty for x^{SM}, we can conclude that no definite bound is put on the red vertical domains (for ϵ'/ϵ) in figure 6. Overall figure 6 tells us that there exist the parameter spaces for the present CFV scenario to simultaneously account for the two anomalies in $R_{K^{(*)}}$ and ϵ'/ϵ within 2σ or 1σ C.L.

JHEP11(2018)164

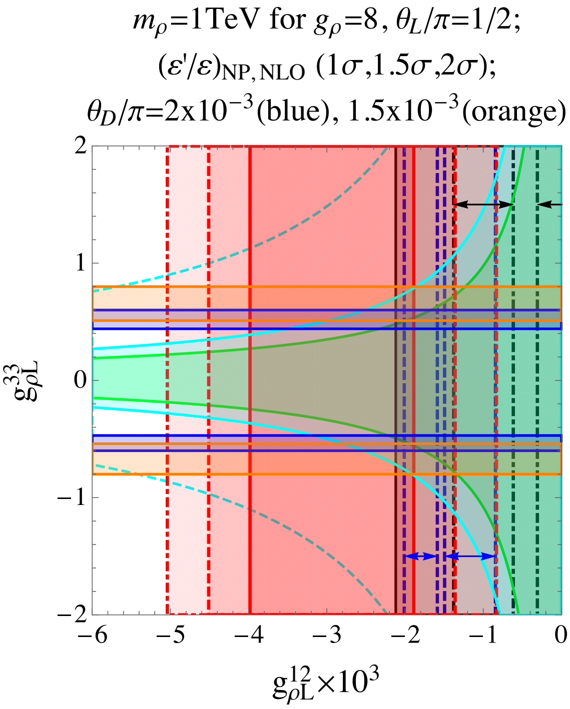

Figure 6. The combined constraint plot on $(g^{12}_{\rho L}, g^{33}_{\rho L})$ for $m_\rho = 1\,\text{TeV}$, $g_\rho = 8$, $\theta_L/\pi = 1/2$ and $\theta_D/\pi = 2 \times 10^{-3}$ (horizontal band in blue) or 1.5×10^{-3} (in orange), where the shaded regions are allowed. The red and pale-black vertical domains respectively correspond to the allowed regions set by the 1σ (surrounded by solid line boundaries), 1.5σ (by dashed ones), 2σ (by dot-dashed ones) ranges for $(\epsilon'/\epsilon)_{\rm NP}$, and the 2σ range for ΔM_K. The 2σ-allowed range for $\text{Br}[K^+ \to \pi^+ \nu\bar{\nu}]$ and the 90% C.L. upper bound for $\text{Br}[K_L \to \pi^0 \nu\bar{\nu}]$ have been reflected in domains wrapped by green and cyan regions, respectively. The upper bound on $\text{Br}[K_L \to \pi^0 \nu\bar{\nu}]$ was updated by the KOTO experiment at ICHEP in July 2018. In the figure we have also shown the previous boundary based on the previous bound by the dashed cyan curves (See also footnote 16). The regions surrounded by horizontal lines [in blue (for $\theta_D/\pi = 2 \times 10^{-3}$) or orange (for $\theta_D/\pi = 1.5 \times 10^{-3}$)] are allowed by the $B - \tau$ system constraint in figure 3, in which the lower bounds on the magnitude of $g^{33}_{\rho L}$ come from the requirement to account for the $R_{K^{(*)}}$ anomaly within the 2σ level, while the upper ones originate from circumventing the bound from ΔM_{B_s} at the 2σ level, respectively. The vertical domains identified by the blue and black horizontal arrows correspond to the 95% C.L. intervals when $x^{\rm SM} = +1\%$ and $+0.1\%$, respectively.

4 Future prospects

4.1 NA62 and KOTO experiments

The CFVs predict the deviation from the SM for the $\text{Br}[K^+ \to \pi^+ \nu\bar{\nu}]$ and $\text{Br}[K_L \to \pi^0 \nu\bar{\nu}]$, which can be tested in the upcoming data from the NA62 experiment at CERN [175] and KOTO experiment at J-PARC [176]. The SM predictions are read off, say, from ref. [148], as $\text{Br}[K^+ \to \pi^+ \nu\bar{\nu}]|_{\rm SM} = (8.5 \pm 0.5) \times 10^{-11}$ and $\text{Br}[K_L \to \pi^0 \nu\bar{\nu}]|_{\rm SM} = (3.0 \pm 0.2) \times 10^{-11}$. Remarkable to note is that as long as the $R_{K^{(*)}}$ anomaly persists beyond the SM, the CFVs necessarily give the larger values for those branching ratios than the SM predictions. In correlation with the $R_{K^{(*)}}$ anomaly, the size of the deviations for the K^+ and K_L decay rates significantly depends on the flavorful coupling $g_{\rho L}^{33}$ as seen from figure 6. Suppose that the $R_{K^{(*)}}$ anomaly will go away in the future. In that case, the lower bound on the $g_{\rho L}^{33}$ will not be placed, so we then expect from the formula in eq. (3.41) that by adjusting the couplings $g_{\rho L}^{12}$ and $g_{\rho L}^{33}$, the CFV contributions to the $K^+ \to \pi^+ \nu \bar{\nu}$ decay can be vanishing or even make the branching ratio slightly smaller than the SM prediction. According to the literature [175], by the end of 2018 the NA62 experiment will measure the $K^+ \to \pi^+ \nu \bar{\nu}$ with about 10% accuracy of the SM prediction, while the Belle II experiment is expected to measure the deviation on the $R_{K^{(*)}}$ at about 3% level with $\sim 10\,\mathrm{ab}^{-1}$ data up until 2021 [177]. (The current accuracy for the $\delta R_{K^{(*)}} \equiv R_{K^{(*)}}^{\mathrm{exp}} - R_{K^{(*)}}^{\mathrm{SM}}$ is at least about 30% – 40% [11, 12].) The KOTO experiment also plans to report new results on the data analysis on the $K_L \to \pi^0 \nu \bar{\nu}$ in the near future, to be expected to reach the level of $< 10^{-9}$ for the branching ratio, corresponding to 2015–2018 data taking [178]. The CFV scenario will therefore be very soon tested first by the NA62 and KOTO, which will constrain the size of the flavorful coupling $g_{\rho L}^{33}$ and the allowed deviation for the $R_{K^{(*)}}$, and then will be confirmed or excluded by the upcoming Belle II data.

Assuming that the $R_{K^{(*)}}$ anomaly persists in the future, in figure 7 we display the plots showing the predicted curves for the $\mathrm{Br}[K^+ \to \pi^+ \nu \bar{\nu}]$ (top- and bottom-left panels) and $\mathrm{Br}[K_L \to \pi^0 \nu \bar{\nu}]$ (top- and bottom-right panels) in the $(g_{\rho L}^{12}, g_{\rho L}^{33})$ plane with $g_\rho = 8$, $m_\rho = 1\,\mathrm{TeV}$ and $\theta_L = \pi/2$ fixed. For θ_D, we chose the two relevant values as reference points, which lead to simultaneous explanations for the anomalies in R_{K^*} (within the 2σ C.L.) and ϵ'/ϵ (within the 1σ C.L.). The parameter spaces displayed in the figure have taken into account currently available all flavor limits together with the $R_{K^{(*)}}$ anomaly (see figure 6). The figure implies that the significantly large branching ratios for the $\mathrm{Br}[K^+ \to \pi^+ \nu \bar{\nu}]$ (by about a few times larger amount) and $\mathrm{Br}[K_L \to \pi^0 \nu \bar{\nu}]$ (by about several ten times larger amount) are predicted in the presence of the $R_{K^{(*)}}$ anomaly.

4.2 LHC searches

Since the CFVs having the mass of around 1 TeV couple to the SM fermions in the flavorful form as well as in the flavor-universal form, they can potentially have a large enough sensitivity to be detected also at the LHC. As has been discussed so far, the flavor-physics analysis implies a muon-philic structure [$\theta_L \sim \pi/2$ in eq. (3.32)] and the CFVs are allowed to couple to the u and d quarks through the mixing with the SM gauge bosons [see eq. (A.19)], so the most dominant discovery channel will be a resonant dimuon process $pp \to$ CFVs $\to \mu^+\mu^-$, in which the neutral CFVs mixing with the EW gauge bosons (i.e. $\rho_{(1)}^3$ and $\rho_{(1)'}^0$) are generated by $u\bar{u}$ and $d\bar{d}$ via Drell-Yan process.[18]

[18] Actually, the bottom quark pair can also produce the neutral CFVs via the third-generation-philic coupling $g_{\rho L}^{33}$, though the contribution would be small due to the small bottom luminosity inside proton. We have checked that this $pp \to b\bar{b} \to$CFVs production is slightly subdominant to be by about a few factor smaller than the $pp \to u\bar{u}/d\bar{d} \to$ CFVs production, even for the suppressed $(g_{s,W,Y}^2/g_\rho)$ coupling. Even with inclusion of the $b\bar{b} \to$CFVs production, however, our discussion on the LHC searches would not substantially be altered, as will be manifested in figure 8.

JHEP11(2018)164

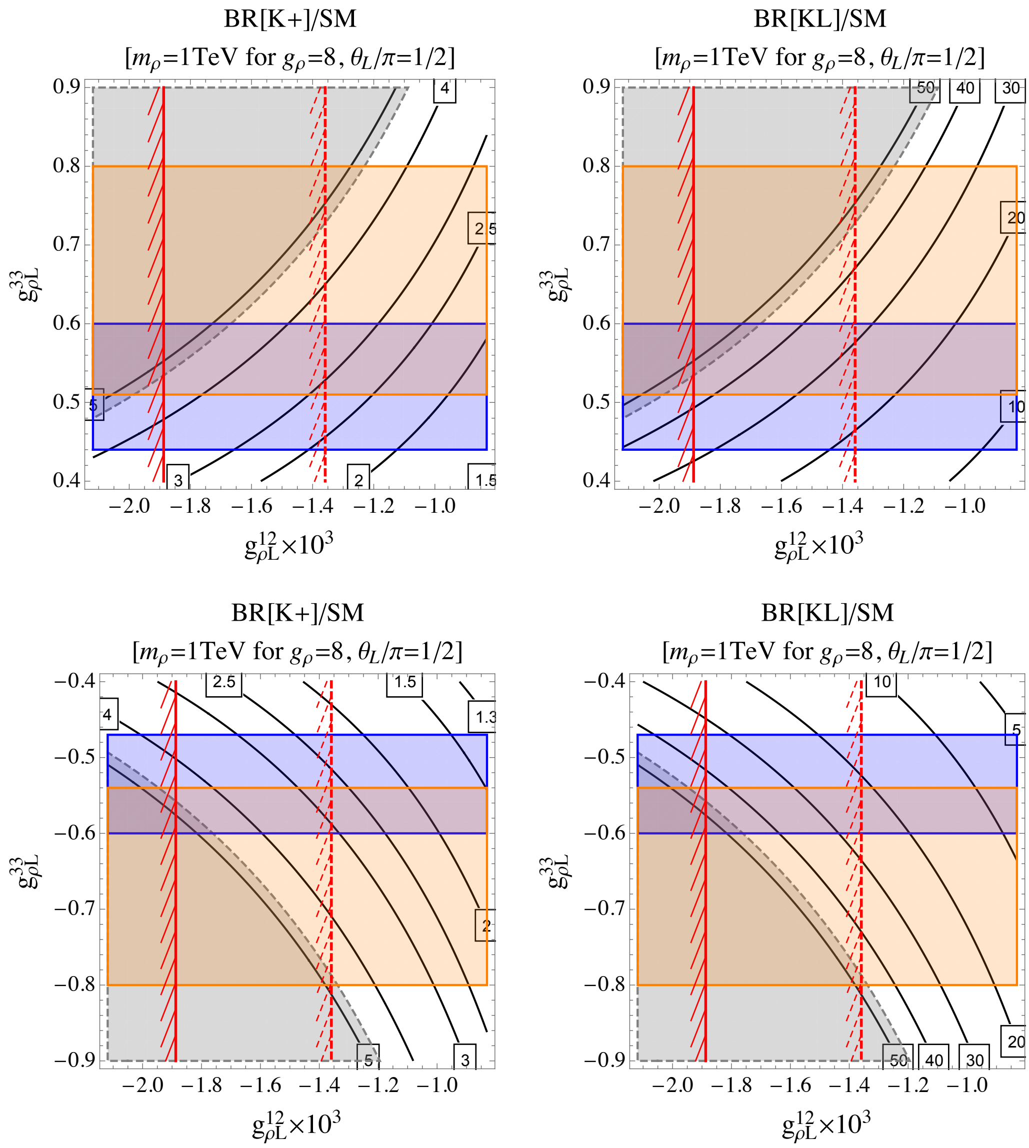

Figure 7. The plots of the predicted curves for the Br$[K^+ \to \pi^+ \nu\bar{\nu}]$ (top- and bottom-left panels) and Br$[K_L \to \pi^0 \nu\bar{\nu}]$ (top- and bottom-right panels), normalized to the SM values, in the $(g^{12}_{\rho L}, g^{33}_{\rho L})$ plane with $m_\rho = 1\,\text{TeV}$, $g_\rho = 8$ and $\theta_L = \pi/2$ fixed. The numbers attached on the curves denote the values of evaluated branching ratios over the SM predictions. The plotted ranges for $g^{12}_{\rho L}$ and $g^{33}_{\rho L}$ have been zoomed in on a viable parameter space extracted from figure 6, which fully satisfies the ΔM_K bound and are separated into two, depending on the sign of $g^{33}_{\rho L}$ (shown in top and bottom panels for positive and negative cases, respectively). The two red-vertical lines in each panel depict boundaries set by the 1σ (solid) and 1.5σ (dashed) ranges allowed by the ϵ'/ϵ constraint. The parameter spaces inside the blue and orange regions enable us to address the $R_{K^{(*)}}$ anomaly with $\theta_D/\pi = 2.0 \times 10^{-3}$ and 1.5×10^{-3}, respectively. The shaded regions colored in gray have already been excluded by the current bound on Br $[K^+ \to \pi^+ \nu\bar{\nu}]$ at the 2σ level [see eq. (3.55)]. We skipped to depict the 95% C.L. intervals drawn by $x^{\rm SM} = +1\%$ and $+0.1\%$ shown in figure 6 (where a large uncertainty exists in the choice of $x^{\rm SM}$).

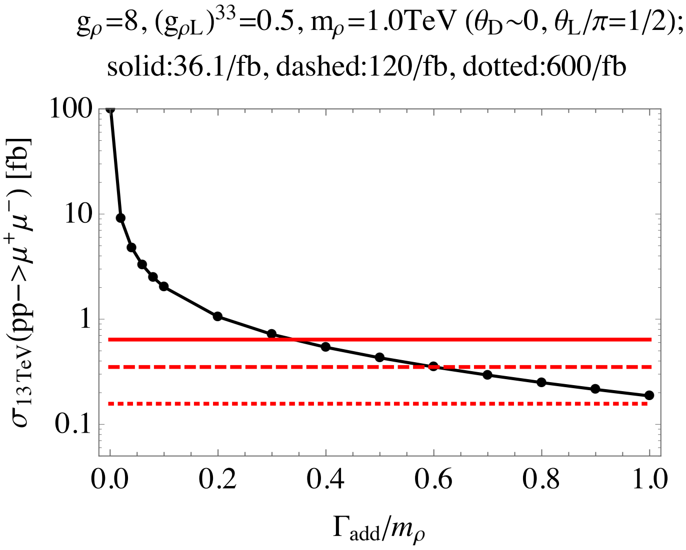

Figure 8. The dimuon resonant production cross section for the target CFVs ($\rho^3_{(1)}$ and $\rho^0_{(1)'}$) at LHC with $\sqrt{s}$ =13 TeV as a function of a possibly added width term (common for two CFVs) normalized to the mass m_ρ, for m_ρ= 1 TeV, $g_\rho = 8$, $g^{33}_{\rho L} = 0.5$ (and $\theta_D \sim 0$, $\theta_L = \pi/2$). The horizontal solid, dashed and dotted lines (in red) respectively correspond to the current 95% C.L upper limit placed by the ATLAS group with the integrated luminosity $\mathcal{L} = 36.1\,\mathrm{fb}^{-1}$ [179], and the expected upper bounds at $\mathcal{L} = 120\,\mathrm{fb}^{-1}$ and $\mathcal{L} = 600\,\mathrm{fb}^{-1}$ estimated just by simply scaling the luminosity. The LHC cross section has been computed by implementing the `CTEQ6L1` parton distribution function (PDF) [180] in `Mathematica` with the help of a PDF parser package, `ManeParse_2.0` [181], and setting $\tau_0 \equiv 4m^2_{\mathrm{threshold}}/s = 10^{-6}$ as the minimal value of the Bjorken x in the `CTEQ6L1` PDF set, where the PDF scale is set to m_ρ. The `CUBA` package [182] has been utilized for numerical integrations.

In figure 8 we show the dimuon production cross section at 13 TeV for a viable parameter space with m_ρ= 1 TeV, $g_\rho = 8$, $g^{33}_{\rho L} = 0.5$ (and $\theta_D \sim 0$, $\theta_L = \pi/2$) [see figure 6]. It is seen from the figure that the present scenario, in which the CFVs are allowed to couple only to the SM fermions, seems to have a strong tension with the current dimuon data (solid red line) provided by the ATLAS group [179] (see the black-dot point $\simeq$ 114 fb at $\Gamma_{\mathrm{add}}/m_\rho = 0$).

Assuming a possible extension from the simplest setup and incorporating an additional width (other than the widths for SM fermions decays) into the CFV propagators, we may vary the extra width term to control the dimuon cross section (see e.g., [76, 83, 102, 103]). Such an additional width would be present when the CFV can dominantly couple to a hidden dark sector including a dark matter candidate, or a pionic sector realized as in a hidden QCD with a setup similar to the present CFV content [20]. In a hidden QCD embedding, for instance, the additional width almost fully saturated by the decay channel to hidden pion pairs would be expected like $\Gamma/m_\rho \sim |g_\rho|^2/(48\pi) \simeq 0.2(0.4)$ for $g_\rho = 6(8)$, based on a simple scaling from the QCD case (up to possible group factors depending on the number of hidden-sector flavors).

The additional effect is monitored also in figure 8, where the extra width (denoted by Γ_{add}) is assumed to be in common for the target $\rho^3_{(1)}$ and $\rho^0_{(1)'}$ and is normalized to their common mass m_ρ. The figure shows that the CFVs with $\Gamma_{\rm add}/m_\rho \gtrsim 30\%$ can survive for the current dimuon bound. (The dimuon widths for $\rho^3_{(1)}$ and $\rho^0_{(1)'}$ are $\simeq 1.75\,\text{GeV}$ and $\simeq 1.39\,\text{GeV}$ for $(g^{33}_{\rho L}, g_\rho) = (0.5, 8)$, so the total widths are indeed dominated by the extra sector.) The size of the additional width can be explored up to around 60% at the LHC with $\mathcal{L} = 120\,\text{fb}^{-1}$ and will be further done in the phase of a high-luminosity LHC with $\mathcal{L} = 600\,\text{fb}^{-1}$, which would constrain modeling of a concrete CFV scenario with the CFVs coupled to a hidden sector.

5 Summary and discussion

In this paper, we have proposed flavorful and chiral vector bosons as the new physics constitution at around TeV scale, to address the presently reported significant flavor anomalies in the Kaon and B meson systems such as the CP violating Kaon decay ϵ'/ϵ and lepton-flavor violating B meson decays. We have introduced the chiral-flavorful vectors (CFVs) as a 63-plet of the global SU(8) symmetry, identified as the one-family symmetry for left-handed quarks and leptons in the standard model (SM) forming the 8-dimensional vector. Thus the CFVs include massive gluons (of G' type), vector leptoquarks, and W', Z'-type bosons, which are allowed to have flavorful couplings with left-handed quarks and leptons, and flavor-universal couplings to right-handed ones, where the latter arises from mixing with the SM gauge bosons. The characteristic feature in the present CFV scenario based on the one-family SU(8) symmetry is seen in the predictions derived necessarily with a significant correlation between the $2 \leftrightarrow 3$ and $1 \leftrightarrow 2$ transition processes, while the next-to nearest-generation transitions like $1 \leftrightarrow 3$ processes turn out to be highly suppressed in a correlation with the $1 \leftrightarrow 2$ transition constraints in the K system: based on the proposed flavor texture, the current ϵ'/ϵ (in the Kaons) and $R_{K^{(*)}}$ (in the B mesons) anomalies can simultaneously be interpreted by the presence of CFVs, where it is predicted that the $R_{D^{(*)}}$ anomaly does not survive due to the (approximate) one-family SU(8) symmetry (see section 3.1.6 for details). Remarkably, we found that as long as both the ϵ'/ϵ and the $R_{K^{(*)}}$ anomalies persist beyond the SM, the CFVs predict the enhanced $K^+ \to \pi^+ \nu\bar{\nu}$ and $K_L \to \pi^0 \nu\bar{\nu}$ decay rates compared to the SM values, which will readily be explored by the NA62 and KOTO experiments, and would also be explored in the dimuon resonant channel at the LHC with a higher luminosity.

In closing, we shall give several comments:

- Since (some of) the CFVs can mix with the SM gauge bosons at tree level, one might think that the present scenario gets severely constrained by the EW precision tests, as well as the flavor observables and direct searches at LHC, as has so far been discussed. However, it turns out not to be the case for the CFV model which is due to the vectorlike gauging and the formulation based the hidden local symmetry approach [23–27]: as was discussed in [20] where the mixing with the SM gauge boson has been determined by the hidden gauge symmetry structure in the same way as in the present CFV model, the EW precision test constraints, which mainly come from the flavor-dependent Z-mass shell observables (such as forward-backward asymmetries for charged leptons and $Z \to \bar{b}b$ decay), would place the bound for the flavorful coupling $g_{\rho L}^{33}$ at 95% C.L. [20], $-0.72 \times \left(\frac{m_\rho}{1\,\text{TeV}}\right)^2 < g_{\rho L}^{33}/g_\rho < 0.25 \times \left(\frac{m_\rho}{1\,\text{TeV}}\right)^2$, with the third-generation philic and the second-generation philic textures assumed for quarks and leptons, respectively. This bound is easily fulfilled in a typical benchmark such as $m_\rho = 1\,\text{TeV}$, $g_{\rho L}^{33} = +0.5$, and $g_\rho = 8$.

Though the tree-level contributions are somewhat insignificant, EW renormalization group effects on the semi-leptonic current operators could give non-negligible corrections to the W and Z boson currents at the NLO level (referred to as EW-NLO below, in short), hence could be severely constrained by the EW precision measurements and lepton-flavor violating observables [183, 184] (see also [110, 114, 117, 185]). Of interest is first to note the almost complete cancellation in the SU(2)-triplet(-contracted) semi-leptonic operators as the consequence of the SU(8)-one family symmetry structure, leading to null correction to the W-boson current from such EW-NLO effects. On the other hand, EW-NLO corrections to the Z-boson currents can be induced to give rise to nontrivial shifts for vector/axial-vector Z-couplings to the lepton ℓ (v_ℓ/a_ℓ) and for the number of (active) neutrinos from the invisible Z decay width (N_ν). Following the formulation in [183, 184] and taking the benchmark-parameter set in the above (with the favored mixing structure $\theta_D \sim 0$ and $\theta_L \sim \pi/2$ taken into account), we estimate the shifts for those couplings to find $\left(\frac{v_\mu}{v_e} - 1\right) \sim 5 \times 10^{-3}, \left(\frac{a_\mu}{a_e} - 1\right) \sim 4 \times 10^{-4}, (N_\nu - 3) \sim 8 \times 10^{-4}$. which are (maximally by one order of magnitude) small enough and totally safe when compared with the current bounds [10] $v_\mu/v_e|_{\text{exp}} = 0.961(61)$, $a_\mu/a_e|_{\text{exp}} = 1.0002(13)$, and $N_\nu|_{\text{exp}} = 2.9840 \pm 0.0082$. This is actually mainly due to the almost vanishing contributions from the SU(2)-triplet(-contracted) semi-leptonic operators: if they were sizable, the shifts would get as large as the current accuracies for the $v_\mu/v_e, a_\mu/a_e$ and N_ν, to have a strong tension with the B anomalies, as emphasized in [183, 184].

Besides those potentially nontrivial NLO corrections as above, similar effects on flavor-dependent Z-pole observables could arise from renomalization evolutions for fully quarkonic and leptonic operators, which is to be pursued elsewhere.

- As discussed recently in ref. [186], flavorful couplings for vector leptoquarks and W'/Z'-type vectors such as those in the present CFV model are potentially sensitive also to the LFU of $\Upsilon(nS)$ ($n = 1, 2, 3$) decays, when those couplings are large enough to account for the B anomalies. Note that in the present CFV model both semi-leptonic and fully-leptonic decay processes for b are controlled by the same Wilson coefficient of type $C_{qqll}^{[1]}$ (see eq. (B.17) and recall the consequence of the approximate SU(8) invariance leading to $C_{qqll}^{[3]} \simeq 0$), where the vector-leptoquarks ($\rho_{(3)}^{0,\alpha}$) dominantly contribute (see eq. (B.11)). Hence the bound on the CFV contribution can roughly be translated in terms of a isotriplet-vector leptoquark scenario when we talk about the correlated limit from the LFU of $\Upsilon(nS)$ decays and the B anomalies (by roughly saying that the sensitivities to the flavorful coupling are the same for the $R_{D^{(*)}}$, which was taken into account in ref. [186], and the $R_{K^{(*)}}$, which has been addressed in the present model).

JHEP11(2018)164

In fact, just following the formulae available in ref. [186], we have explicitly evaluated the CFVs contributions to the LFU of $\Upsilon(1S, 2S, 3S)$ decays, characterized by the ratio of the decay rates, $R_{\tau/\mu}^{\Upsilon(nS)} \equiv \Gamma[\Upsilon(nS) \to \tau^+\tau^-]/\Gamma[\Upsilon(nS) \to \mu^+\mu^-]$ for the viable parameter set explored by the present analysis ($\theta_L \simeq \pi/2$, $\theta_D \simeq 0$, $g_{\rho L}^{33} \simeq 0.5$, $g_\rho = 8$, $m_\rho = 1\,\text{TeV}$), to find that $R_{\tau/\mu}^{\Upsilon(1S,2S,3S)} \simeq (0.992, 0.994, 0.994)$, in accord with the numbers estimated in the reference. With the SM predictions subtracted, the numbers actually turn out to be smaller than the current 1σ uncertainties in experiments [187, 188]. Thus, the CFVs are at present fairly insensitive to the LFU of $\Upsilon(nS)$ decays, which would possibly be explored in Belle II experiment.

- For the ΔM_K in eq. (3.43), we could quantify the NP effect for the deviation from the SM by adopting the recent lattice result on the SM prediction [189], $\Delta M_K^{\text{SM}}|_{\text{lattice}} = (3.19 \pm 1.04) \times 10^{-15}\,\text{GeV}$, which includes significant long distance contributions, $\Delta M_K^{\text{NP}} \equiv \Delta M_K^{\text{exp}} - \Delta M_K^{\text{SM}}|_{\text{lattice}} = (0.29 \pm 1.04) \times 10^{-15}\,\text{GeV}$, by which the 2σ allowed range is found to be $-1.79 \times 10^{-15}\,\text{GeV} \leq \Delta M_K^{\text{NP}}|_{2\sigma} \leq 2.37 \times 10^{-15}\,\text{GeV}$. With this bound used, which gets to be more shrunk than that we have adopted in the present analysis, the NP contribution of $(\epsilon'/\epsilon)_{\text{NP}}$ would be necessary to be allowed up to $\gtrsim 1.5\sigma$ range, to be consistent with the ΔM_K, while the predicted values for the rare K-semi-leptonic decays would not be substantially affected in magnitude. Improvement on the accuracy for lattice estimates on the form factors $B_6^{1/2}$ and $B_8^{3/2}$, crucial for the SM prediction to ϵ'/ϵ, would give a more definite constraint on the present CFV scenario, in correlation with the fate of B anomalies.

- In addition to the single-neutral CFV ($\rho_{(1)}^3$ and $\rho_{(1)'}^0$) production at LHC as has been discussed so far, one might think that the vector-leptoquark pair ($\rho_{(3)}^{\alpha,0}$) production would also severely be constrained by the LHC searches. However, it would not be the case: when the CFV model is formulated based on the hidden local symmetry approach [23–27], the gluon-gluon fusion coupling to the vector leptoquark pair, which has been severely constrained by the null-results at the LHC, can be set to be suppressed as discussed in [20] with a similar model-setup for the vector bosons. Instead of such a direct coupling, the color-octet CFV ($\rho_{(8)}^0$) exchange would then dominate to couple the gluon to the vector-leptoquarks (so-called "vector meson dominance"), so that the effective vertex goes like a form factor $\sim m_\rho^2/(m_\rho^2 - \hat{s})$, where $\hat{s}$ denotes the square of the transfer momentum. Because of the almost degenerate mass structure for CFVs supported by the SU(8) symmetry, the on-shell production for the leptoquark pair through the $\rho_{(8)}^0$ exchange is kinematically forbidden, hence only the off-shell production is allowed to be highly suppressed by the form factor structure for a high energy event at LHC, like $\sim m_\rho^2/\hat{s}$. A similar argument is also applicable to the Drell-Yan process ($q\bar{q} \to \rho_{(3)}\bar{\rho}_{(3)}$ along with the similar form factor structure). Thus, the presently placed bound on the vector leptoquark pair production is not directly applicable to the CFVs detection (even if the vector-leptoquarks sub-dominantly decay to quarks and leptons due to a presence of some hidden sector). It would need other event topologies to detect the CFV-leptoquarks with the characteristic final state reflecting the second-generation- and third-generion-philic properties for leptons and quarks, respectively,[19] which would be accessible in a high-luminosity LHC through a single production process [191] with tagging muons, instead of tau leptons.

- Other flavor-changing processes like $\bar{B} \to K^{(*)}\mu^\pm\tau^\mp$, $\Upsilon \to \mu^\pm\tau^\mp$ and $J/\psi \to \mu^\pm\tau^\mp$, have been discussed to place limits on the scenarios for addressing the $R_{K^{(*)}}$ anomaly, e.g. in [192]. It turns out that no additional bound from them emerges within our focused parameter space in figure 3, where $g_{\rho L}^{33}$ and θ_L/π vary in a range $[-1.5, 1.5]$ and $[0, 0.5]$, while the other relevant parameters are fixed as $m_\rho = 1\,\text{TeV}$, $g_\rho = 8$, $\theta_D/\pi = 2 \times 10^{-3}$. In the following part, we briefly look at this parameter space as a reference point for discussing the above flavor-changing processes in terms of our scenario.

  - $\bar{B} \to K^{(*)}\mu^\pm\tau^\mp$:

    By referring to [104, 192], the following branching ratios are formulated in terms of our notation as $\text{Br}[\bar{B} \to K^{(*)}\mu^-\tau^+] \sim \left(|C_9^{\mu\tau}(\text{NP})|^2 + |C_{10}^{\mu\tau}(\text{NP})|^2\right) \times 10^{-8}$, and the conjugated processes $\bar{B} \to K^{(*)}\mu^+\tau^-$ are obtained by the replacement of $C_{9,10}^{\mu\tau}(\text{NP}) \to C_{9,10}^{\tau\mu}(\text{NP})$. The current experimental results for $B^+ \to K^+\mu\tau$ are available: $\text{Br}[B^+ \to K^+\mu^+\tau^-] = 0.8^{+1.9}_{-1.4} \times 10^{-5}$ or $< 4.5 \times 10^{-5}$ (90% C.L.); $\text{Br}[B^+ \to K^+\mu^-\tau^+] = (-0.4)^{+1.4}_{-0.9} \times 10^{-5}$ or $< 2.8 \times 10^{-5}$ (90% C.L.) [193]. Our scenario is thus apparently insignificant for those processes because $|C_{9,10}^{\mu\tau}(\text{NP})| \sim |C_{9,10}^{\mu\mu}(\text{NP})| \to \lesssim 1$ ($\sim 2\sigma$ upper bound) with fixing $m_\rho = 1\,\text{TeV}$, $\theta_D/\pi = 2.0 \times 10^{-3}$ and varying $g_{\rho L}^{33}$ in the range $[-1.5, 1.5]$.

  - $\Upsilon(nS) \to \mu^\pm\tau^\mp$:

    The formulae of the branching ratios are available in [192], and from the reference we can read off a consistent condition for $m_\rho = 1\,\text{TeV}$ as $7/16\,(g_{\rho L}^{33})^2(\sin\theta_L \cos\theta_L) \lesssim 4$.[20] Within the focused range of $g_{\rho L}^{33}$ as $[-1.5, 1.5]$, this condition is satisfied and hence the focused spot remains viable in the range.

  - $J/\psi \to \mu^\pm\tau^\mp$:

    The formulae for these decay processes take the form similar to that for $\Upsilon(nS) \to \mu^\pm\tau^\mp$ and available in [192]. We find that the bound coming from this process (and its conjugate one) is much weaker than that from $\Upsilon(nS) \to \mu^\pm\tau^\mp$ (and the focused range is completely safe) since (i) much more sizable $g_{\rho L}^{33}$ is required for putting a constraint on the focused range compared with $\Upsilon(nS) \to \mu^\pm\tau^\mp$; (ii) $c\bar{c}$ coupling is suppressed when $\theta_D \ll 1$.

[19] For the case of a scalar leptoquark candidate (S_1) for explaining the $R_{D^{(*)}}$ anomaly, e.g., see [190] for details on flavor tagging.

[20] We used experimental data for $\text{Br}[\Upsilon(2S, 3S) \to \mu^\pm\tau^\mp]$ as $\text{Br}[\Upsilon(2S) \to \mu^\pm\tau^\mp] = 0.2^{+1.5+1.0}_{-1.3-1.2} \times 10^{-6}$ or $< 3.3 \times 10^{-6}$ (90% C.L.), and $\text{Br}[\Upsilon(3S) \to \mu^\pm\tau^\mp] = (-0.8)^{+1.5+1.4}_{-1.5-1.3} \times 10^{-6}$ or $< 3.1 \times 10^{-6}$ (90% C.L.) [194]. Here the associated parameters used as inputs are $f_{\Upsilon(2S)} = (496 \pm 21)\,\text{MeV}$, $f_{\Upsilon(3S)} = (430 \pm 21)\,\text{MeV}$, $m_{\Upsilon(2S)} = 10.02326\,\text{GeV}$, $m_{\Upsilon(3S)} = 10.35526\,\text{GeV}$, $\Gamma_{\Upsilon(2S)} = (31.98 \pm 2.63)\,\text{KeV}$, and $\Gamma_{\Upsilon(3S)} = (20.32 \pm 1.85)\,\text{KeV}$, respectively [166, 192].

JHEP11(2018)164

- We make comments on other potentially-sensitive flavor-changing processes in the presence of the W', Z', G' and vector leptoquark candidates under our flavor texture. Here, we focus on typical digits on the benchmark point: $m_\rho = 1\,\text{TeV}$, $g_\rho = 8$, $\theta_D/\pi = 2 \times 10^{-3}$, $\theta_L/\pi \sim 1/2$, $g_{\rho L}^{33} \sim +0.6$ or -0.6, and $|g_{\rho L}^{12}| \sim 2 \times 10^{-3}$, where the best-fit value for $b \to s\mu^+\mu^-$ is achieved and the ϵ'/ϵ anomaly can be addressed within 1σ C.L. consistently (see figures 3 and 6).

  - $\mu \to e\gamma$:

    This process is not produced at the tree level due to the gauge invariance of the QED, but the dipole operator $\Delta_{\mu\to e\gamma}\,(\bar{e}'_R \sigma_{\mu\nu} \mu'_L) F^{\mu\nu}$ ($F_{\mu\nu}$ being the field strength tensor of the photon) is induced by the vector leptoquark exchange even when $\theta_L \sim \pi/2$ at the one loop level. The coefficient $\Delta_{\mu\to e\gamma}$ is roughly estimated as $\sim e\, m_\mu (g_{\rho L}^{12})\, (g_{\rho L}^{33}) \sin\theta_D/((4\pi)^2 m_\rho^2)$. At the focused point, we have $\mathrm{Br}[\mu \to e\gamma] \sim 7 \times 10^{-16}$ with $\tau_\mu = 2.197 \times 10^{-6}\,\text{s}$, $m_\mu = 0.1057\,\text{GeV}$ [166] used as inputs, while the latest bound is $< 4.2 \times 10^{-13}$ (90% C.L.) [195]. No competitive bound may come in the near future (where the targeting sensitivity of the MEG-II experiment is expected to reach the level of 6×10^{-14} [196]).

  - $\mu \to 3e$:

    This process is induced at the tree level, but the branching ratio is proportional to $\cos^2\theta_L$, which is vanishing at our benchmark point including $\theta_L \sim \pi/2$. At the one loop level, even in the case of $\theta_L \sim \pi/2$, the operator $\Delta_{\mu\to 3e}\,(\bar{e}'_L \gamma_\mu \mu'_L)(\bar{e}'_L \gamma^\mu e'_L)$ is induced through box diagrams with vector leptoquark exchanges, the coefficient of which ($\Delta_{\mu\to 3e}$) is roughly estimated as $\sim (m_c^2/m_\rho^2) \times (g_{\rho L}^{12})^3\, (g_{\rho L}^{33}) \sin\theta_D/((4\pi)^2 m_\rho^2)$. At the focused point, we thus have $\mathrm{Br}[\mu \to 3e] \sim 1 \times 10^{-34}$, where the latest bound is fairly above from the above estimated magnitude as $< 1.0 \times 10^{-12}$ (90% C.L.) [197].

  - $K_L \to \mu^\mp e^\pm$:

    Similar to $\mu \to 3e$, our scenario does not yield any contribution when $\theta_L \sim \pi/2$ at the tree level. A crude estimation on a typical size of the coefficients for the relevant operators, $\Delta_{K_0\to e^-\mu^+}\,(\bar{e}'_L \gamma_\mu \mu'_L)(\bar{s}'_L \gamma^\mu s'_L)$ and other three at the one loop level, gives $\sim (m_c^2/m_\rho^2) \times g_W^2 V_{cs} V_{cd}^* (g_{\rho L}^{12})\, (g_{\rho L}^{33}) \sin\theta_D/((4\pi)^2 m_\rho^2)$ (see e.g. [198]). We then find $\mathrm{Br}[K_L \to \mu^\mp e^\pm] \sim 1 \times 10^{-23}$ at the focused point with the inputs, $V_{cs} = 0.974$, $V_{cd} = 0.224$, $f_K = 155.0(1.9)\,\text{MeV}$ [199], $m_{K^0} = 497.6\,\text{MeV}$, $\tau_{K_L} = 5.18 \times 10^{-8}\,\text{s}$ [166]. Thus this is totally safe [cf. the latest bound $< 4.7 \times 10^{-12}$ (90% C.L.) [200]].

  - $\mathrm{Br}[J/\psi \to \mu^+\mu^-]/\mathrm{Br}[J/\psi \to e^+e^-]$ ($\equiv R_{J/\psi\to 2\ell}$):

    The general formula of the decay width for $J/\psi \to 2\ell$ is read off from [186] and our estimation at the focused point goes like $R_{J/\psi\to 2\ell} \simeq R_{J/\psi\to 2\ell}|_{\mathrm{SM}} \simeq 1$. From the experimental results for the branching ratios, $\mathrm{Br}[J/\psi(1S) \to e^+e^-] = 0.05971 \pm 0.00032$ and $\mathrm{Br}[J/\psi(1S) \to \mu^+\mu^-] = 0.05961 \pm 0.00033$ [166], we may estimate $R_{J/\psi\to 2\ell}|_{\mathrm{exp}} = 0.9983 \pm 0.0078$. Thus we see that no significant tension occurs from this observable.

JHEP11(2018)164

- $\tau \to \mu\nu\bar{\nu}$ and $\mu \to e\nu\bar{\nu}$:

  The SM can contribute to the process $\tau \to \mu\nu\bar{\nu}$ via the W-boson exchange at the tree level. Also in our scenario, non-vanishing contribution shows up at the tree level even for $\theta_L \sim \pi/2$. The additional contribution to the branching ratio for $\tau \to \mu\nu\bar{\nu}$ at the focused point is evaluated as $\sim 2 \times 10^{-9}$, while no tree-level correction to $\mu \to e\nu\bar{\nu}$ remains when $\theta_L \sim \pi/2$.

  According to [192, 201], a tighter bound comes from the measurement of the following ratio:

$$R_{\nu\bar{\nu}}^{(\tau\to\mu)/(\mu\to e)} \equiv \frac{\mathrm{Br}[\tau \to \mu\nu\bar{\nu}]/\mathrm{Br}[\tau \to \mu\nu\bar{\nu}]_{\mathrm{SM}}}{\mathrm{Br}[\mu \to e\nu\bar{\nu}]/\mathrm{Br}[\mu \to e\nu\bar{\nu}]_{\mathrm{SM}}},$$

  where the 2σ deviation from the SM was observed as 1.0060 ± 0.0030 with apparently $R_{\nu\bar{\nu}}^{(\tau\to\mu)/(\mu\to e)}|_{\mathrm{SM}}$ being unity. By use of $\mathrm{Br}[\tau \to \mu\nu\bar{\nu}]_{\mathrm{SM}} \simeq \mathrm{Br}[\tau \to \mu\nu\bar{\nu}]_{\mathrm{obs}} = 0.1739$ [166], we reach

$$\frac{\mathrm{Br}[\tau \to \mu\nu\bar{\nu}]}{\mathrm{Br}[\tau \to \mu\nu\bar{\nu}]_{\mathrm{SM}}} = 1 + \frac{\delta\mathrm{Br}[\tau \to \mu\nu\bar{\nu}]}{\mathrm{Br}[\tau \to \mu\nu\bar{\nu}]_{\mathrm{SM}}} \sim 1 + 1 \times 10^{-8},$$
$$\Rightarrow \; R_{\nu\bar{\nu}}^{(\tau\to\mu)/(\mu\to e)} \sim 1 + 1 \times 10^{-8},$$

  which implies an extremely tiny effect, not to reach a tractable range in the future.

- Other lepton-flavor violating τ decays:

  For example, the rare decays $\tau \to eee$ and $\tau \to e\mu\mu$ can be produced at the tree level in a way similar to $\tau \to 3\mu$ which were discussed in section 3.1.4. The magnitude of these two decay modes is much less than that for $\tau \to 3\mu$ due to the smallness of the coupling $g_{\rho L}^{12}$ of $\mathcal{O}(10^{-3})$. Thus, the CFV scenario is insensitive also to these rare decay processes.

Acknowledgments

We are grateful to Teppei Kitahara for providing us with a numeric code for the NLO calculations, and Satoshi Mishima for giving us several useful comments. K.N. thanks Chao-Qiang Geng, Hiroyuki Ishida and Ryoutaro Watanabe for fruitful discussions. This work was supported in part by the JSPS Grant-in-Aid for Young Scientists (B) #15K17645 (S.M.), the JSPS KAKENHI 16H06492 and 18J01459 (K.Y.). K.N. has been supported by the European Union through the European Regional Development Fund — the Competitiveness and Cohesion Operational Programme (KK.01.1.1.06), the European Union's Horizon 2020 research and innovation program under the Twinning grant agreement No. 692194, RBI-T-WINNING, and the grant funded from the European Structural and Investment Funds, RBI-TWINN-SIN. The authors thank the Yukawa Institute for Theoretical Physics at Kyoto University, where this work was initiated during the YITP-W-17-07 on "Progress in Particle Physics 2017".

A Explicit expressions for CFV couplings to quarks and leptons

In this appendix we present the way of embedding CFVs into the SU(8) multiplet and the CFV couplings to SM fermions.

The CFVs are embedded in the adjoint representation of the SU(8) flavor symmetry, which are defined as

$$\begin{aligned}\sum_{A=1}^{63}\rho^A\cdot T^A =& \sum_{\alpha=1}^{3}\sum_{a=1}^{8}\rho^\alpha_{(8)a}\cdot T^\alpha_{(8)a}+\sum_{a=1}^{8}\rho^0_{(8)a}\cdot T_{(8)a}\\ &+\sum_{c=r,g,b}\sum_{\alpha=1}^{3}\left[\rho^{[1]\alpha}_{(3)c}\cdot T^{[1]\alpha}_{(3)c}+\rho^{[2]\alpha}_{(3)c}\cdot T^{[2]\alpha}_{(3)c}\right]+\sum_{c=r,g,b}\left[\rho^{[1]0}_{(3)c}\cdot T^{[1]}_{(3)c}+\rho^{[2]0}_{(3)c}\cdot T^{[2]}_{(3)c}\right]\\ &+\sum_{\alpha=1}^{3}\rho^\alpha_{(1)}\cdot T^\alpha_{(1)}+\sum_{\alpha=1}^{3}\rho^\alpha_{(1)'}\cdot T^\alpha_{(1)'}+\rho^0_{(1)'}\cdot T_{(1)'}\,,\end{aligned}\tag{A.1}$$

with the SU(8) generators,

$$\begin{aligned}
T^\alpha_{(8)a}&=\frac{1}{\sqrt2}\left(\begin{array}{c|c}\tau^\alpha\otimes\lambda^a & \\ \hline & \mathbf{0_{2\times2}}\end{array}\right), & T_{(8)a}&=\frac{1}{2\sqrt2}\left(\begin{array}{c|c}\mathbf{1}_{2\times2}\otimes\lambda^a & \\ \hline & \mathbf{0_{2\times2}}\end{array}\right),\\
T^{[1]\alpha}_{(3)c}&=\frac{1}{\sqrt2}\left(\begin{array}{c|c} & \tau^\alpha\otimes\mathbf{e}_c\\ \hline \tau^\alpha\otimes\mathbf{e}_c^\dagger & \end{array}\right), & T^{[2]\alpha}_{(3)c}&=\frac{1}{\sqrt2}\left(\begin{array}{c|c} & -i\tau^\alpha\otimes\mathbf{e}_c\\ \hline i\tau^\alpha\otimes\mathbf{e}_c^\dagger & \end{array}\right),\\
T^{[1]}_{(3)c}&=\frac{1}{2\sqrt2}\left(\begin{array}{c|c} & \mathbf{1}_{2\times2}\otimes\mathbf{e}_c\\ \hline \mathbf{1}_{2\times2}\otimes\mathbf{e}_c^\dagger & \end{array}\right), & T^{[2]}_{(3)c}&=\frac{1}{2\sqrt2}\left(\begin{array}{c|c} & -i\mathbf{1}_{2\times2}\otimes\mathbf{e}_c\\ \hline i\mathbf{1}_{2\times2}\otimes\mathbf{e}_c^\dagger & \end{array}\right),\\
T^\alpha_{(1)}&=\frac{1}{2}\left(\begin{array}{c|c}\tau^\alpha\otimes\mathbf{1}_{3\times3} & \\ \hline & \tau^\alpha\end{array}\right), & T^\alpha_{(1)'}&=\frac{1}{2\sqrt3}\left(\begin{array}{c|c}\tau^\alpha\otimes\mathbf{1}_{3\times3} & \\ \hline & -3\cdot\tau^\alpha\end{array}\right),\\
T_{(1)'}&=\frac{1}{4\sqrt3}\left(\begin{array}{c|c}\mathbf{1}_{6\times6} & \\ \hline & -3\cdot\mathbf{1}_{2\times2}\end{array}\right),
\end{aligned}\tag{A.2}$$

where $\tau^\alpha=\sigma^\alpha/2$ (σ^α: Pauli matrices), λ^a and $\mathbf{e}_c$ represent the Gell-Mann matrices and three-dimensional unit vectors in color space, respectively, and the generator T^A is normalized as $\mathrm{tr}[T^AT^B]=\delta^{AB}/2$. For color-triplet components (leptoquarks), we define the following eigenforms which discriminate $\mathbf{3}$ and $\bar{\mathbf{3}}$ states of the $SU(3)_c$ gauge group,

$$\begin{aligned}
T^\alpha_{(3)c}&\equiv\frac{1}{\sqrt2}\left(T^{[1]\alpha}_{(3)c}+iT^{[2]\alpha}_{(3)c}\right)=\left(\begin{array}{c|c} & \tau^\alpha\otimes\mathbf{e}_c\\ \hline \mathbf{0_{2\times6}} & \end{array}\right), \qquad T^\alpha_{(\bar3)c}\equiv\left(T^\alpha_{(3)c}\right)^\dagger,\\
T_{(3)c}&\equiv\frac{1}{\sqrt2}\left(T^{[1]}_{(3)c}+iT^{[2]}_{(3)c}\right)=\frac12\left(\begin{array}{c|c} & \mathbf{1_{2\times2}}\otimes\mathbf{e}_c\\ \hline \mathbf{0_{2\times6}} & \end{array}\right), \qquad T_{(\bar3)c}\equiv\left(T_{(3)c}\right)^\dagger,\\
\rho^\alpha_{(3)c}&\equiv\frac{1}{\sqrt2}\left(\rho^{[1]\alpha}_{(3)c}-i\rho^{[2]\alpha}_{(3)c}\right),\quad \rho^0_{(3)c}\equiv\frac{1}{\sqrt2}\left(\rho^{[1]0}_{(3)c}-i\rho^{[2]0}_{(3)c}\right),\quad \bar\rho^\alpha_{(3)c}\equiv\left(\rho^\alpha_{(3)c}\right)^\dagger,\quad \bar\rho^0_{(3)c}\equiv\left(\rho^0_{(3)c}\right)^\dagger.
\end{aligned}\tag{A.3}$$

As in the text, the CFV fields (ρ) can be expressed by a couple of sub-block matrices as

$$\rho = \begin{pmatrix} (\rho_{QQ})_{6\times 6} & (\rho_{QL})_{6\times 2} \\ (\rho_{LQ})_{2\times 6} & (\rho_{LL})_{2\times 2} \end{pmatrix}, \tag{A.4}$$

where the entries are read off from the above decomposition form as

$$\begin{aligned}
\rho_{QQ} &= \left[\sqrt{2}\rho^{\alpha}_{(8)a}\left(\tau^{\alpha}\otimes\frac{\lambda^a}{2}\right) + \frac{1}{\sqrt{2}}\rho^{0}_{(8)a}\left(\mathbf{1}_{2\times 2}\otimes\frac{\lambda^a}{2}\right)\right] \\
&\quad + \left[\frac{1}{2}\rho^{\alpha}_{(1)}\left(\tau^{\alpha}\otimes\mathbf{1}_{3\times 3}\right) + \frac{1}{2\sqrt{3}}\rho^{\alpha}_{(1)'}\left(\tau^{\alpha}\otimes\mathbf{1}_{3\times 3}\right) + \frac{1}{4\sqrt{3}}\rho^{0}_{(1)'}\left(\mathbf{1}_{2\times 2}\otimes\mathbf{1}_{3\times 3}\right)\right], \\
\rho_{LL} &= \frac{1}{2}\rho^{\alpha}_{(1)}\left(\tau^{\alpha}\right) - \frac{\sqrt{3}}{2}\rho^{\alpha}_{(1)'}\left(\tau^{\alpha}\right) - \frac{\sqrt{3}}{4}\rho^{0}_{(1)'}\left(\mathbf{1}_{2\times 2}\right), \\
\rho_{QL} &= \rho^{\alpha}_{(3)c}\left(\tau^{\alpha}\otimes\mathbf{e}_c\right) + \frac{1}{2}\rho^{0}_{(3)c}\left(\mathbf{1}_{2\times 2}\otimes\mathbf{e}_c\right), \\
\rho_{LQ} &= \left(\rho_{QL}\right)^{\dagger}.
\end{aligned} \tag{A.5}$$

We reintroduce the above form for convenience, which appeared as eq. (2.5) in the main body of this manuscript.

Thus, by expanding coupling terms in eq. (2.1) and eq. (2.6) with the SM gauge fields in eq. (2.3) in terms of the $\rho_{(8)}$s, $\rho_{(3)}$s and $\rho_{(1),(1)'}$s, the CFV couplings are found as listed below:

- flavorful (direct) couplings:
  - for color-singlet neutral (Z' type) CFVs ($\rho^{3,0}_{(1)}, \rho^{3,0}_{(1)'}$):

$$\mathcal{L}_{\rho_1 uu} = -g^{ij}_{\rho L}\bar{u}^i_L\gamma_\mu u^j_L\left[+\frac{1}{4}\,\rho^{\mu}_{(1)3} + \frac{1}{4\sqrt{3}}\,\rho^{\mu}_{(1)'3} + \frac{1}{4\sqrt{3}}\,\rho^{\mu}_{(1)'0}\right], \tag{A.6}$$

$$\mathcal{L}_{\rho_1 dd} = -g^{ij}_{\rho L}\bar{d}^i_L\gamma_\mu d^j_L\left[-\frac{1}{4}\,\rho^{\mu}_{(1)3} - \frac{1}{4\sqrt{3}}\,\rho^{\mu}_{(1)'3} + \frac{1}{4\sqrt{3}}\,\rho^{\mu}_{(1)'0}\right], \tag{A.7}$$

$$\mathcal{L}_{\rho_1 \ell\ell} = -g^{ij}_{\rho L}\bar{e}^i_L\gamma_\mu e^j_L\left[-\frac{1}{4}\,\rho^{\mu}_{(1)3} + \frac{\sqrt{3}}{4}\,\rho^{\mu}_{(1)'3} - \frac{\sqrt{3}}{4}\,\rho^{\mu}_{(1)'0}\right], \tag{A.8}$$

$$\mathcal{L}_{\rho_1 \nu\nu} = -g^{ij}_{\rho L}\bar{\nu}^i_L\gamma_\mu \nu^j_L\left[+\frac{1}{4}\,\rho^{\mu}_{(1)3} - \frac{\sqrt{3}}{4}\,\rho^{\mu}_{(1)'3} - \frac{\sqrt{3}}{4}\,\rho^{\mu}_{(1)'0}\right]; \tag{A.9}$$

  - for color-singlet charged (W' type) CFVs ($\rho^{\pm}_{(1)}, \rho^{\pm}_{(1)'}$):

$$\mathcal{L}_{\rho_1 ud} = -g^{ij}_{\rho L}\bar{u}^i_L\gamma_\mu d^j_L\left[\frac{1}{2\sqrt{2}}\rho^{\mu}_{(1)+} + \frac{1}{2\sqrt{6}}\rho^{\mu}_{(1)'+}\right] + \text{h.c.}, \tag{A.10}$$

$$\mathcal{L}_{\rho_1 \nu\ell} = -g^{ij}_{\rho L}\bar{\nu}^i_L\gamma_\mu e^j_L\left[\frac{1}{2\sqrt{2}}\rho^{\mu}_{(1)+} - \frac{\sqrt{3}}{2\sqrt{2}}\rho^{\mu}_{(1)'+}\right] + \text{h.c.}; \tag{A.11}$$

– for color-triplet (vector-leptoquark type) CFVs ($\rho_{(3)}^{\pm,3,0}$):

$$\mathcal{L}_{\rho_3 d\ell} = -g_{\rho L}^{ij} \bar{d}_L^i \gamma_\mu e_L^j \left[-\frac{1}{2}\, \rho_{(3)3}^\mu + \frac{1}{2}\, \rho_{(3)0}^\mu \right] + \text{h.c.}\,, \tag{A.12}$$

$$\mathcal{L}_{\rho_3 u\ell} = -g_{\rho L}^{ij} \bar{u}_L^i \gamma_\mu e_L^j \left[+\frac{1}{\sqrt{2}}\, \rho_{(3)+}^\mu \right] + \text{h.c.}\,, \tag{A.13}$$

$$\mathcal{L}_{\rho_3 d\nu} = -g_{\rho L}^{ij} \bar{d}_L^i \gamma_\mu \nu_L^j \left[+\frac{1}{\sqrt{2}}\, \rho_{(3)-}^\mu \right] + \text{h.c.}\,, \tag{A.14}$$

$$\mathcal{L}_{\rho_3 u\nu} = -g_{\rho L}^{ij} \bar{u}_L^i \gamma_\mu \nu_L^j \left[+\frac{1}{2}\, \rho_{(3)3}^\mu + \frac{1}{2}\, \rho_{(3)0}^\mu \right] + \text{h.c.}\,, \tag{A.15}$$

where $\rho_{(3)0}$ and $\rho_{(3)3}$ have $+\frac{2}{3}$ electric charges whereas $\rho_{(3)\pm} = (\rho_{(3)1} \mp i\rho_{(3)2})/\sqrt{2}$ have $+\frac{5}{3}$ and $-\frac{1}{3}$, respectively;

– for color-octet (G'-type) CFVs ($\rho_{(8)}^{\pm,3,0}$):

$$\mathcal{L}_{\rho_8 uu} = -g_{\rho L}^{ij} \bar{u}_L^i \gamma_\mu \left(\frac{\lambda^a}{2} \right) u_L^j \left[+\frac{1}{\sqrt{2}} \rho_{(8)3}^{a\mu} + \frac{1}{\sqrt{2}} \rho_{(8)0}^{a\mu} \right], \tag{A.16}$$

$$\mathcal{L}_{\rho_8 dd} = -g_{\rho L}^{ij} \bar{d}_L^i \gamma_\mu \left(\frac{\lambda^a}{2} \right) d_L^j \left[-\frac{1}{\sqrt{2}} \rho_{(8)3}^{a\mu} + \frac{1}{\sqrt{2}} \rho_{(8)0}^{a\mu} \right], \tag{A.17}$$

$$\mathcal{L}_{\rho_8 ud} = -g_{\rho L}^{ij} \bar{u}_L^i \gamma_\mu \left(\frac{\lambda^a}{2} \right) d_L^j \left[+\rho_{(8)+}^{a\mu} \right]. \tag{A.18}$$

- Indirect couplings induced from mixing with the SM gauge bosons:

  Coupling eq. (2.8) to the SM fermions via the SM gauge boson exchanges with the square of the transfer momentum $q^2 = m_\rho^2$ taken, we may evaluate the CFV-on-shell couplings to the SM fermions:

$$\begin{aligned}
\mathcal{L}^{\text{indirect}} \approx -\frac{1}{g_\rho} \Bigg[& \sqrt{2} g_s^2 \left(\bar{q} \gamma_\mu \rho_{(8)}^{\mu 0} q \right) + 2 g_W^2 \left(\bar{q}_L \gamma_\mu \rho_{(1)}^\mu q_L \right) \\
& + \frac{g_Y^2}{3\sqrt{3}} \left(\bar{q}_L \gamma_\mu \rho_{(1)'}^{\mu 0} q_L \right) + \frac{2 g_Y^2}{\sqrt{3}} \left(\bar{q}_R \gamma_\mu Q_{\text{em}}^q \rho_{(1)'}^{\mu 0} q_R \right) \\
& + 2 g_W^2 \left(\bar{l}_L \gamma_\mu \rho_{(1)}^\mu l_L \right) - \frac{g_Y^2}{\sqrt{3}} \left(\bar{l}_L \gamma_\mu \rho_{(1)'}^{\mu 0} l_L \right) + \frac{2 g_Y^2}{\sqrt{3}} \left(\bar{l}_R \gamma_\mu Q_{\text{em}}^l \rho_{(1)'}^{\mu 0} l_R \right) \Bigg],
\end{aligned} \tag{A.19}$$

  where we have neglected terms suppressed by a factor of $\mathcal{O}(m_{W/Z}/m_\rho)^2$. Here we suppress the generation indices (in the gauge eigenbases) for simplicity since they are manifestly generation independent. Also, the doublet-like notations are introduced for clarity; $q_R \equiv (u_R, d_R)^T$ and $l_R \equiv (\nu_R, e_R)^T$.

JHEP11(2018)164

B Effective four-fermion operators induced from CFV exchanges

In this appendix we derive effective four-fermion operators induced from the CFVs exchanges, relevant to discussing the flavor physics contributions.

Integrating out the CFVs coupled to the SM fermions with the $g_{\rho L}^{ij}$ in eq.(2.1) together with eq. (2.5) (or eq. (A.5)) generate the following four-fermion operators at the mass scales of CFVs

$$\begin{aligned}
-\mathcal{L}_{\rm eff}^{(8)} &= \left(\sqrt{2}\right)^2 \frac{g_{\rho L}^{ij} g_{\rho L}^{kl}}{(M_{\rho^\alpha_{(8)}})^2} \Delta^{ik;jl} \left[(\bar{q}_L^i \gamma_\mu \tau^\alpha T^a q_L^j)(\bar{q}_L^k \gamma^\mu \tau^\alpha T^a q_L^l)\right] \\
&\quad + \left(\frac{1}{\sqrt{2}}\right)^2 \frac{g_{\rho L}^{ij} g_{\rho L}^{kl}}{(M_{\rho^0_{(8)}})^2} \Delta^{ik;jl} \left[(\bar{q}_L^i \gamma_\mu T^a q_L^j)(\bar{q}_L^k \gamma^\mu T^a q_L^l)\right],
\end{aligned} \tag{B.1}$$

$$\begin{aligned}
-\mathcal{L}_{\rm eff}^{(1)} &= \left(\frac{1}{2}\right)^2 \frac{g_{\rho L}^{ij} g_{\rho L}^{kl}}{(M_{\rho^\alpha_{(1)}})^2} \Delta^{ik;jl} \left[(\bar{q}_L^i \gamma_\mu \tau^\alpha q_L^j)(\bar{q}_L^k \gamma^\mu \tau^\alpha q_L^l)\right] \\
&\quad + \left(\frac{1}{2}\right)^2 \frac{g_{\rho L}^{ij} g_{\rho L}^{kl}}{(M_{\rho^\alpha_{(1)}})^2} \Delta^{ik;jl} \left[(\bar{l}_L^i \gamma_\mu \tau^\alpha l_L^j)(\bar{l}_L^k \gamma^\mu \tau^\alpha l_L^l)\right] \\
&\quad + \left(\frac{1}{2}\right)^2 \frac{g_{\rho L}^{ij} g_{\rho L}^{kl}}{(M_{\rho^\alpha_{(1)}})^2} \left[(\bar{q}_L^i \gamma_\mu \tau^\alpha q_L^j)(\bar{l}_L^k \gamma^\mu \tau^\alpha l_L^l)\right] \\
&\quad + \left(\frac{1}{2\sqrt{3}}\right)^2 \frac{g_{\rho L}^{ij} g_{\rho L}^{kl}}{(M_{\rho^\alpha_{(1)'}})^2} \Delta^{ik;jl} \left[(\bar{q}_L^i \gamma_\mu \tau^\alpha q_L^j)(\bar{q}_L^k \gamma^\mu \tau^\alpha q_L^l)\right] \\
&\quad + \left(\frac{-\sqrt{3}}{2}\right)^2 \frac{g_{\rho L}^{ij} g_{\rho L}^{kl}}{(M_{\rho^\alpha_{(1)'}})^2} \Delta^{ik;jl} \left[(\bar{l}_L^i \gamma_\mu \tau^\alpha l_L^j)(\bar{l}_L^k \gamma^\mu \tau^\alpha l_L^l)\right] \\
&\quad + \left(\frac{1}{2\sqrt{3}}\right)\left(\frac{-\sqrt{3}}{2}\right) \frac{g_{\rho L}^{ij} g_{\rho L}^{kl}}{(M_{\rho^\alpha_{(1)'}})^2} \left[(\bar{q}_L^i \gamma_\mu \tau^\alpha q_L^j)(\bar{l}_L^k \gamma^\mu \tau^\alpha l_L^l)\right] \\
&\quad + \left(\frac{1}{4\sqrt{3}}\right)^2 \frac{g_{\rho L}^{ij} g_{\rho L}^{kl}}{(M_{\rho^0_{(1)'}})^2} \Delta^{ik;jl} \left[(\bar{q}_L^i \gamma_\mu q_L^j)(\bar{q}_L^k \gamma^\mu q_L^l)\right] \\
&\quad + \left(\frac{-\sqrt{3}}{4}\right)^2 \frac{g_{\rho L}^{ij} g_{\rho L}^{kl}}{(M_{\rho^0_{(1)'}})^2} \Delta^{ik;jl} \left[(\bar{l}_L^i \gamma_\mu l_L^j)(\bar{l}_L^k \gamma^\mu l_L^l)\right] \\
&\quad + \left(\frac{1}{4\sqrt{3}}\right)\left(\frac{-\sqrt{3}}{4}\right) \frac{g_{\rho L}^{ij} g_{\rho L}^{kl}}{(M_{\rho^0_{(1)'}})^2} \left[(\bar{q}_L^i \gamma_\mu q_L^j)(\bar{l}_L^k \gamma^\mu l_L^l)\right],
\end{aligned} \tag{B.2}$$

$$-\mathcal{L}_{\rm eff}^{(3)} = \frac{g_{\rho L}^{ij} g_{\rho L}^{kl}}{(M_{\rho^\alpha_{(3)}})^2} \left[(\bar{q}_L^i \gamma_\mu \tau^\alpha l_L^j)(\bar{l}_L^k \gamma^\mu \tau^\alpha q_L^l)\right] + \left(\frac{1}{2}\right)^2 \frac{g_{\rho L}^{ij} g_{\rho L}^{kl}}{(M_{\rho^0_{(3)}})^2} \left[(\bar{q}_L^i \gamma_\mu l_L^j)(\bar{l}_L^k \gamma^\mu q_L^l)\right], \tag{B.3}$$

with $T^a \equiv \lambda^a/2$. Here, $\Delta^{ik;jl}$ is a combinatorics factor, which satisfies

$$\Delta^{ik;jl} \left(= \Delta^{ki;jl} = \Delta^{ik;lj} = \Delta^{ki;lj}\right) = \begin{cases} 1/2 & \text{for } i = k \text{ and } j = l, \\ 1 & \text{for others.} \end{cases} \tag{B.4}$$

After Fiertz transformations, we have

$$-\mathcal{L}_{\text{eff}}^{(8)+(3)+(1)}\Big|_{\text{Fiertz}} = C^{[3]}_{q_iq_jq_kq_l}(\bar{q}^i_L\gamma_\mu\sigma^\alpha q^j_L)(\bar{q}^k_L\gamma^\mu\sigma^\alpha q^l_L) + C^{[3]}_{l_il_jl_kl_l}(\bar{l}^i_L\gamma_\mu\sigma^\alpha l^j_L)(\bar{l}^k_L\gamma^\mu\sigma^\alpha l^l_L)$$
$$+ C^{[3]}_{q_iq_jl_kl_l}(\bar{q}^i_L\gamma_\mu\sigma^\alpha q^j_L)(\bar{l}^k_L\gamma^\mu\sigma^\alpha l^l_L) + C^{[1]}_{q_iq_jq_kq_l}(\bar{q}^i_L\gamma_\mu q^j_L)(\bar{q}^k_L\gamma^\mu q^l_L)$$
$$+ C^{[1]}_{l_il_jl_kl_l}(\bar{l}^i_L\gamma_\mu l^j_L)(\bar{l}^k_L\gamma^\mu l^l_L) + C^{[1]}_{q_iq_jl_kl_l}(\bar{q}^i_L\gamma_\mu q^j_L)(\bar{l}^k_L\gamma^\mu l^l_L). \tag{B.5}$$

Including the indirect coupling contributions arising from eq. (A.19) (excluding the relatively small right-handed fermion couplings), the Wilson coefficients are evaluated as

$$C^{[3]}_{q_iq_jq_kq_l} = \Delta^{ik;jl}\left\{\frac{1}{2}\left[\frac{1}{2}\alpha^{il;kj} - \frac{1}{6}\alpha^{ij;kl}\right]\frac{1}{(M_{\rho^\alpha_{(8)}})^2} + \frac{1}{16}\frac{[\alpha^{ij;kl}]_{\rho^\alpha_{(1)}}}{(M_{\rho^\alpha_{(1)}})^2} + \frac{1}{48}\frac{\alpha^{ij;kl}}{(M_{\rho^\alpha_{(1)'}})^2}\right\}, \tag{B.6}$$

$$C^{[3]}_{l_il_jl_kl_l} = \Delta^{ik;jl}\left\{\frac{1}{16}\frac{[\alpha^{ij;kl}]_{\rho^\alpha_{(1)}}}{(M_{\rho^\alpha_{(1)}})^2} + \frac{3}{16}\frac{\alpha^{ij;kl}}{(M_{\rho^\alpha_{(1)'}})^2}\right\}, \tag{B.7}$$

$$C^{[3]}_{q_iq_jl_kl_l} = \frac{1}{16}\frac{[\alpha^{ij;kl}]_{\rho^\alpha_{(1)}}}{(M_{\rho^\alpha_{(1)}})^2} - \frac{1}{16}\frac{\alpha^{ij;kl}}{(M_{\rho^\alpha_{(1)'}})^2} - \frac{1}{8}\frac{\beta^{il;kj}}{(M_{\rho^\alpha_{(3)}})^2} + \frac{1}{8}\frac{\beta^{il;kj}}{(M_{\rho^0_{(3)}})^2}, \tag{B.8}$$

$$C^{[1]}_{q_iq_jq_kq_l} = \Delta^{ik;jl}\left\{\frac{1}{2}\left[\frac{1}{2}[\alpha^{il;kj}]_{\rho^0_{(8)}} - \frac{1}{6}[\alpha^{ij;kl}]_{\rho^0_{(8)}}\right]\frac{1}{(M_{\rho^0_{(8)}})^2} + \frac{1}{48}\frac{[\alpha^{ij;kl}]_{\rho^0_{(1)'}}}{(M_{\rho^0_{(1)'}})^2}\right\}, \tag{B.9}$$

$$C^{[1]}_{l_il_jl_kl_l} = \Delta^{ik;jl}\left\{\frac{3}{16}\frac{[\alpha^{ij;kl}]_{\rho^0_{(1)'}}}{(M_{\rho^0_{(1)'}})^2}\right\}, \tag{B.10}$$

$$C^{[1]}_{q_iq_jl_kl_l} = -\frac{1}{16}\frac{[\alpha^{ij;kl}]_{\rho^0_{(1)'}}}{(M_{\rho^0_{(1)'}})^2} + \frac{3}{8}\frac{\beta^{il;kj}}{(M_{\rho^\alpha_{(3)}})^2} + \frac{1}{8}\frac{\beta^{il;kj}}{(M_{\rho^0_{(3)}})^2}, \tag{B.11}$$

where

$$\alpha^{ij;kl} \equiv g^{ij}_{\rho L}g^{kl}_{\rho L}, \tag{B.12}$$

$$\beta^{ij;kl} \equiv g^{ij}_{\rho L}(g^\dagger_{\rho L})^{kl}, \tag{B.13}$$

$$[\alpha^{ij;kl}]_{\rho^\alpha_{(1)}} \equiv \left(g^{ij}_{\rho L} + \frac{4g_W^2}{g_\rho}\delta^{ij}\right)\left(g^{kl}_{\rho L} + \frac{4g_W^2}{g_\rho}\delta^{kl}\right), \tag{B.14}$$

$$[\alpha^{ij;kl}]_{\rho^0_{(1)'}} \equiv \left(g^{ij}_{\rho L} + \frac{4g_Y^2}{3g_\rho}\delta^{ij}\right)\left(g^{kl}_{\rho L} + \frac{4g_Y^2}{3g_\rho}\delta^{kl}\right), \tag{B.15}$$

$$[\alpha^{ij;kl}]_{\rho^\alpha_{(8)}} \equiv \left(g^{ij}_{\rho L} + \frac{2g_s^2}{g_\rho}\delta^{ij}\right)\left(g^{kl}_{\rho L} + \frac{2g_s^2}{g_\rho}\delta^{kl}\right). \tag{B.16}$$

In terms of the $(u,d)^i_L$ and $(\nu,e)^i_L$ fields, we thus find

$$\begin{aligned}
-\mathcal{L}_{\rm eff}^{(8)+(3)+(1)}\Big|_{\rm Fiertz} \supset\; & \left(C^{[1]}_{q_iq_jl_kl_l} + C^{[3]}_{q_iq_jl_kl_l}\right)(\bar{d}^i_L\gamma_\mu d^j_L)(\bar{e}^k_L\gamma^\mu e^l_L) \\
& + \left(C^{[1]}_{q_iq_jl_kl_l} - C^{[3]}_{q_iq_jl_kl_l}\right)(\bar{d}^i_L\gamma_\mu d^j_L)(\bar{\nu}^k_L\gamma^\mu \nu^l_L) \\
& + 2C^{[3]}_{q_iq_jl_kl_l}\left((\bar{u}^i_L\gamma_\mu d^j_L)(\bar{e}^k_L\gamma^\mu \nu^l_L) + (\bar{d}^i_L\gamma_\mu u^j_L)(\bar{\nu}^k_L\gamma^\mu e^l_L)\right) \\
& + \left(C^{[1]}_{q_iq_jq_kq_l} + C^{[3]}_{q_iq_jq_kq_l}\right)(\bar{d}^i_L\gamma_\mu d^j_L)(\bar{d}^k_L\gamma^\mu d^l_L) \\
& + \left(C^{[1]}_{l_il_jl_kl_l} + C^{[3]}_{l_il_jl_kl_l}\right)(\bar{e}^i_L\gamma_\mu e^j_L)(\bar{e}^k_L\gamma^\mu e^l_L). \qquad (B.17)
\end{aligned}$$

C Global significance of a benchmark point

We estimate the global significance of our benchmark point where $m_\rho = 1\,\text{TeV}$, $g_\rho = 8$, $\theta_D/\pi = 2\times10^{-3}$, $\theta_L/\pi \sim 1/2$, $g^{33}_{\rho L} \sim +0.6$ or -0.6, and $|g^{12}_{\rho L}| \sim 2\times10^{-3}$, at which the best-fit value for $b\to s\mu^+\mu^-$ is achieved and the ϵ'/ϵ anomaly can be addressed within 1σ C.L. consistently (see figures 3 and 6). Note also that at this benchmark point, the CFV effect on violation of LFU is minimized, while the CFV couplings to dimuon for addressing the $b\to s\mu^+\mu^-$ anomaly are maximized.

To facilitate the analysis, it is convenient to introduce the following quantities:

$$R_X^{l_1/l_2} \equiv \frac{\text{Br}[\bar{B}\to X l_1\bar{\nu}_{l_1}]}{\text{Br}[\bar{B}\to X l_2\bar{\nu}_{l_2}]} \quad (X = D,\ D^*,\ \text{or}\ J/\psi), \qquad (C.1)$$

$$R_{\nu\bar{\nu}}^{(\tau\to\mu)/(\mu\to e)} \equiv \frac{\text{Br}[\tau\to\mu\nu\bar{\nu}]/\text{Br}[\tau\to\mu\nu\bar{\nu}]_{\rm SM}}{\text{Br}[\mu\to e\nu\bar{\nu}]/\text{Br}[\mu\to e\nu\bar{\nu}]_{\rm SM}}. \qquad (C.2)$$

We calculate the χ^2 values for the 20 observables listed in table 1, where a part of them is related to e-flavor violation and their details are provided in section 5. Several comments on our χ^2 test are in order:

- We choose the leptonic angle θ_L, the down-quark angle θ_D and $g^{33}_{\rho L}$ as relevant fit parameters and the others are treated to be fixed. Thereby, the number of the degrees of freedom (d.o.f.) is 17.
- As adopted in [192], for the variables to which only the 90% C.L. bounds are available, we assume those central values to be zero and define the 1σ error from the 90% C.L. upper bounds by simply assuming the Gaussian form.
- The quadrature form is used in combining errors of variables. When the error is asymmetric, we simply adopt the average of the (combined) errors to estimate χ^2.
- Actually, the present CFV scenario yields somewhat large partial χ^2 values, 9.0, 5.8, 0.64 and 2.9, with respect to the $R_{D^{(*)}}$-associate experimental results, $(R^{\tau/\ell}_{D^*})/(R^{\tau/\ell}_{D^*})_{\rm SM}$ (1.18 ± 0.06 [14–16, 202]), $(R^{\tau/\ell}_{D})/(R^{\tau/\ell}_{D})_{\rm SM}$ (1.36 ± 0.15 [14–16, 202]), $(R^{e/\mu}_{D^*})/(R^{e/\mu}_{D^*})_{\rm SM}$ (1.04 ± 0.05 [203]) and $(R^{\tau/\mu}_{J/\psi})/(R^{\tau/\mu}_{J/\psi})_{\rm SM}$ (2.51 ± 0.97 [204]), respectively. Such large numbers have been obtained due to the approximate SU(8) flavor symmetry which prohibits significantly exceeding from the SM predictions (see section 3.1.6 for details). Therefore, we have removed those observables from our global fit.

Observable	Experimental result	χ^2 at the BP
B anomaly		
$b\to s\mu^+\mu^-$ (combined)	$C_9^{\mu\mu}(\mathrm{NP})=-C_{10}^{\mu\mu}(\mathrm{NP})=-0.615\pm0.13$ [39]	~ 0
$2\leftrightarrow 3$ flavor transitions (see sections 3.1 and 5)		
$\mathrm{Br}[\bar{B}\to K^{(*)}\nu\bar{\nu}]/\mathrm{Br}[\bar{B}\to K^{(*)}\nu\bar{\nu}]_{\mathrm{SM}}$	$-13\sum_{I=1}^{3}\mathrm{Re}[C_L^{II}(\mathrm{NP})]+\sum_{I,J=1}^{3}\lvert C_L^{IJ}(\mathrm{NP})\rvert^2$ ≤ 473 (90% C.L.) [31]	$\lesssim 10^{-4}$
$\mathrm{Br}[\tau\to\phi\mu]$	$<8.4\times10^{-8}$ (90% C.L.) [122]	~ 0
$\mathrm{Br}[\tau\to 3\mu]$	$<2.1\times10^{-8}$ (90% C.L.) [125]	~ 0
ΔM_{B_s}	$\Delta M_{B_s}^{\mathrm{exp}}=(17.757\pm0.021)\,\mathrm{ps}^{-1}$ [132]	~ 4
$\mathrm{Br}[B^+\to K^+\tau^-\mu^+]$	$0.8^{+1.9}_{-1.4}\times10^{-5}$; $<4.5\times10^{-5}$ (90% C.L.) [193]	0.22
$\mathrm{Br}[B^+\to K^+\tau^+\mu^-]$	$(-0.4)^{+1.4}_{-0.9}\times10^{-5}$; $<2.8\times10^{-5}$ (90% C.L.) [193]	0.11
$\mathrm{Br}[\Upsilon(2S)\to\mu^\pm\tau^\mp]$	$0.2^{+1.5+1.0}_{-1.3-1.2}\times10^{-6}$; $<3.3\times10^{-6}$ (90% C.L.) [194]	0.012
$\mathrm{Br}[\Upsilon(3S)\to\mu^\pm\tau^\mp]$	$(-0.8)^{+1.5+1.4}_{-1.5-1.3}\times10^{-6}$; $<3.1\times10^{-6}$ (90% C.L.) [194]	0.16
$\mathrm{Br}[J/\psi\to\mu^\pm\tau^\mp]$	$<2.0\times10^{-6}$ (90% C.L.) [205]	~ 0
LFV associated with e flavor (see section 5)		
v_μ/v_e	0.961(61) [166]	~ 0.5
a_μ/a_e	1.0002(13) [166]	~ 0.02
N_ν	2.9840 ± 0.0082 [166]	~ 4
$\Gamma(\Upsilon(1S)\to\tau^+\tau^-)/\Gamma(\Upsilon(1S)\to\ell^+\ell^-)$	$1.005\pm0.013\pm0.022$ [187, 188]	~ 0.3
$\Gamma(\Upsilon(2S)\to\tau^+\tau^-)/\Gamma(\Upsilon(2S)\to\ell^+\ell^-)$	$1.04\pm0.04\pm0.05$ [187, 188]	~ 0.6
$\Gamma(\Upsilon(3S)\to\tau^+\tau^-)/\Gamma(\Upsilon(3S)\to\ell^+\ell^-)$	$1.05\pm0.08\pm0.05$ [187, 188]	~ 0.4
$R_{\nu\bar{\nu}}^{(\tau\to\mu)/(\mu\to e)}$	1.0060 ± 0.0030 [201]	~ 4
$\mathrm{Br}[\mu\to 3e]$ (at 1 loop)	$<1.0\times10^{-12}$ (90% C.L.) [197]	~ 0
$\mathrm{Br}[\mu\to e\gamma]$ (at 1 loop)	$<4.2\times10^{-13}$ (90% C.L.) [195]	~ 0
$\mathrm{Br}[J/\psi\to\mu^+\mu^-]/\mathrm{Br}[J/\psi\to e^+e^-]$	0.9983 ± 0.0078 (evaluated for $J/\Psi(1S)$ from the data in [166])	~ 0.05

Table 1. List of observables used for our χ^2 calculation and individual χ^2 values at the benchmark point (BP): $m_\rho = 1\,\mathrm{TeV}$, $g_\rho = 8$, $\theta_D/\pi = 2\times10^{-3}$, $\theta_L/\pi \sim 1/2$, $g_{\rho L}^{33} \sim +0.6$ or -0.6, and $|g_{\rho L}^{12}| \sim 2\times10^{-3}$, where the best-fit value for $b\to s\mu^+\mu^-$ is achieved and the ϵ'/ϵ anomaly can be addressed within 1σ C.L. consistently (see figures 3 and 6).

- Unavoidable theoretical uncertainties remain in many of observables in the K and D meson physics. We simply ignore them in the estimate on the global significance.

Thus, we can easily get

$$\left.\frac{\chi^2_{\mathrm{total}}}{(\mathrm{d.o.f.})}\right|_{\text{at the benchmark}} \simeq \frac{14.4}{17} \simeq 0.85, \tag{C.3}$$

which is less than unity and a completely acceptable goodness-of-fit at the benchmark point (p-value $\simeq 0.64$) is realized, even though sizable worse fitness comes from N_ν and $R_{\nu\bar{\nu}}^{(\tau\to\mu)/(\mu\to e)}$, where this kind of worse fitness can be seen also in the SM case.

References

[1] A.J. Buras, M. Gorbahn, S. Jäger and M. Jamin, *Improved anatomy of $\varepsilon'\varepsilon$ in the Standard Model*, JHEP **11** (2015) 202 [arXiv:1507.06345] [INSPIRE].

[2] T. Kitahara, U. Nierste and P. Tremper, *Singularity-free next-to-leading order $\Delta S = 1$ renormalization group evolution and ϵ'_K/ϵ_K in the Standard Model and beyond*, JHEP **12** (2016) 078 [arXiv:1607.06727] [INSPIRE].

[3] A.J. Buras and J.-M. Gérard, *Upper bounds on $\varepsilon'\varepsilon$ parameters $B_6^{(1/2)}$ and $B_8^{(3/2)}$ from large N QCD and other news*, JHEP **12** (2015) 008 [arXiv:1507.06326] [INSPIRE].

[4] A.J. Buras and J.-M. Gerard, *Final state interactions in $K \to \pi\pi$ decays: $\Delta I = 1/2$ rule vs. ε'/ε*, Eur. Phys. J. **C 77** (2017) 10 [arXiv:1603.05686] [INSPIRE].

[5] H. Gisbert and A. Pich, *Direct CP-violation in $K^0 \to \pi\pi$: Standard Model Status*, Rept. Prog. Phys. **81** (2018) 076201 [arXiv:1712.06147] [INSPIRE].

[6] RBC and UKQCD collaborations, Z. Bai et al., *Standard Model Prediction for Direct CP-violation in $K \to \pi\pi$ Decay*, Phys. Rev. Lett. **115** (2015) 212001 [arXiv:1505.07863] [INSPIRE].

[7] NA48 collaboration, J.R. Batley et al., *A Precision measurement of direct CP-violation in the decay of neutral kaons into two pions*, Phys. Lett. **B 544** (2002) 97 [hep-ex/0208009] [INSPIRE].

[8] KTeV collaboration, A. Alavi-Harati et al., *Measurements of direct CP-violation, CPT symmetry and other parameters in the neutral kaon system*, Phys. Rev. **D 67** (2003) 012005 [*Erratum ibid.* **D 70** (2004) 079904] [hep-ex/0208007] [INSPIRE].

[9] KTeV collaboration, E. Abouzaid et al., *Precise Measurements of Direct CP-violation, CPT Symmetry and Other Parameters in the Neutral Kaon System*, Phys. Rev. **D 83** (2011) 092001 [arXiv:1011.0127] [INSPIRE].

[10] Particle Data Group collaboration, C. Patrignani et al., *Review of Particle Physics*, Chin. Phys. **C 40** (2016) 100001 [INSPIRE].

[11] LHCb collaboration, *Test of lepton universality using $B^+ \to K^+\ell^+\ell^-$ decays*, Phys. Rev. Lett. **113** (2014) 151601 [arXiv:1406.6482] [INSPIRE].

[12] LHCb collaboration, *Test of lepton universality with $B^0 \to K^{*0}\ell^+\ell^-$ decays*, JHEP **08** (2017) 055 [arXiv:1705.05802] [INSPIRE].

[13] BaBar collaboration, J.P. Lees et al., *Evidence for an excess of $\bar{B} \to D^{(*)}\tau^-\bar{\nu}_\tau$ decays*, Phys. Rev. Lett. **109** (2012) 101802 [arXiv:1205.5442] [INSPIRE].

[14] BaBar collaboration, J.P. Lees et al., *Measurement of an Excess of $\bar{B} \to D^{(*)}\tau^-\bar{\nu}_\tau$ Decays and Implications for Charged Higgs Bosons*, Phys. Rev. **D 88** (2013) 072012 [arXiv:1303.0571] [INSPIRE].

[15] LHCb collaboration, *Measurement of the ratio of branching fractions $\mathcal{B}(\bar{B}^0 \to D^{*+}\tau^-\bar{\nu}_\tau)/\mathcal{B}(\bar{B}^0 \to D^{*+}\mu^-\bar{\nu}_\mu)$*, Phys. Rev. Lett. **115** (2015) 111803 [*Erratum ibid.* **115** (2015) 159901] [arXiv:1506.08614] [INSPIRE].

[16] BELLE collaboration, M. Huschle et al., *Measurement of the branching ratio of $\bar{B} \to D^{(*)}\tau^-\bar{\nu}_\tau$ relative to $\bar{B} \to D^{(*)}\ell^-\bar{\nu}_\ell$ decays with hadronic tagging at Belle*, Phys. Rev. **D 92** (2015) 072014 [arXiv:1507.03233] [INSPIRE].

[17] BELLE collaboration, Y. Sato et al., *Measurement of the branching ratio of $\bar{B}^0 \to D^{*+}\tau^-\bar{\nu}_\tau$ relative to $\bar{B}^0 \to D^{*+}\ell^-\bar{\nu}_\ell$ decays with a semileptonic tagging method*, Phys. Rev. **D 94** (2016) 072007 [arXiv:1607.07923] [INSPIRE].

[18] BELLE collaboration, S. Hirose et al., *Measurement of the τ lepton polarization and $R(D^*)$ in the decay $\bar{B} \to D^*\tau^-\bar{\nu}_\tau$*, Phys. Rev. Lett. **118** (2017) 211801 [arXiv:1612.00529] [INSPIRE].

[19] LHCb collaboration, *Measurement of the ratio of the $B^0 \to D^{*-}\tau^+\nu_\tau$ and $B^0 \to D^{*-}\mu^+\nu_\mu$ branching fractions using three-prong τ-lepton decays*, Phys. Rev. Lett. **120** (2018) 171802 [arXiv:1708.08856] [INSPIRE].

[20] S. Matsuzaki, K. Nishiwaki and R. Watanabe, *Phenomenology of flavorful composite vector bosons in light of B anomalies*, JHEP **08** (2017) 145 [arXiv:1706.01463] [INSPIRE].

[21] I. Doršner, S. Fajfer, A. Greljo, J.F. Kamenik and N. Košnik, *Physics of leptoquarks in precision experiments and at particle colliders*, Phys. Rept. **641** (2016) 1 [arXiv:1603.04993] [INSPIRE].

[22] N. Assad, B. Fornal and B. Grinstein, *Baryon Number and Lepton Universality Violation in Leptoquark and Diquark Models*, Phys. Lett. **B 777** (2018) 324 [arXiv:1708.06350] [INSPIRE].

[23] M. Bando, T. Kugo, S. Uehara, K. Yamawaki and T. Yanagida, *Is rho Meson a Dynamical Gauge Boson of Hidden Local Symmetry?*, Phys. Rev. Lett. **54** (1985) 1215 [INSPIRE].

[24] M. Bando, T. Kugo and K. Yamawaki, *On the Vector Mesons as Dynamical Gauge Bosons of Hidden Local Symmetries*, Nucl. Phys. **B 259** (1985) 493 [INSPIRE].

[25] M. Bando, T. Fujiwara and K. Yamawaki, *Generalized Hidden Local Symmetry and the A1 Meson*, Prog. Theor. Phys. **79** (1988) 1140 [INSPIRE].

[26] M. Bando, T. Kugo and K. Yamawaki, *Nonlinear Realization and Hidden Local Symmetries*, Phys. Rept. **164** (1988) 217 [INSPIRE].

[27] M. Harada and K. Yamawaki, *Hidden local symmetry at loop: A New perspective of composite gauge boson and chiral phase transition*, Phys. Rept. **381** (2003) 1 [hep-ph/0302103] [INSPIRE].

[28] H.S. Fukano, S. Matsuzaki, K. Terashi and K. Yamawaki, *Conformal Barrier and Hidden Local Symmetry Constraints: Walking Technirhos in LHC Diboson Channels*, Nucl. Phys. **B 904** (2016) 400 [arXiv:1510.08184] [INSPIRE].

[29] A.J. Buras, *New physics patterns in ε'/ε and ε_K with implications for rare kaon decays and ΔM_K*, JHEP **04** (2016) 071 [arXiv:1601.00005] [INSPIRE].

[30] A.J. Buras, F. De Fazio and J. Girrbach, *$\Delta I = 1/2$ rule, ε'/ε and $K \to \pi\nu\bar{\nu}$ in $Z'(Z)$ and G' models with FCNC quark couplings*, Eur. Phys. J. **C 74** (2014) 2950 [arXiv:1404.3824] [INSPIRE].

[31] B. Bhattacharya, A. Datta, J.-P. Guévin, D. London and R. Watanabe, *Simultaneous Explanation of the R_K and $R_{D^{(*)}}$ Puzzles: a Model Analysis*, JHEP **01** (2017) 015 [arXiv:1609.09078] [INSPIRE].

[32] M. González-Alonso, J. Martin Camalich and K. Mimouni, *Renormalization-group evolution of new physics contributions to (semi)leptonic meson decays*, Phys. Lett. **B 772** (2017) 777 [arXiv:1706.00410] [INSPIRE].

[33] H. Arason et al., *Renormalization group study of the standard model and its extensions. 1. The Standard model*, Phys. Rev. **D 46** (1992) 3945 [INSPIRE].

[34] C. Ford, I. Jack and D.R.T. Jones, *The Standard model effective potential at two loops*, Nucl. Phys. **B 387** (1992) 373 [*Erratum ibid.* **B 504** (1997) 551] [hep-ph/0111190] [INSPIRE].

[35] Y. Hamada, H. Kawai and K.-y. Oda, *Bare Higgs mass at Planck scale*, Phys. Rev. **D 87** (2013) 053009 [*Erratum ibid.* **D 89** (2014) 059901] [arXiv:1210.2538] [INSPIRE].

[36] G. Degrassi et al., *Higgs mass and vacuum stability in the Standard Model at NNLO*, JHEP **08** (2012) 098 [arXiv:1205.6497] [INSPIRE].

[37] J. Charles et al., *Current status of the Standard Model CKM fit and constraints on $\Delta F = 2$ New Physics*, Phys. Rev. **D 91** (2015) 073007 [arXiv:1501.05013] [INSPIRE].

[38] C. Bobeth, M. Gorbahn, T. Hermann, M. Misiak, E. Stamou and M. Steinhauser, *$B_{s,d} \to l^+l^-$ in the Standard Model with Reduced Theoretical Uncertainty*, Phys. Rev. Lett. **112** (2014) 101801 [arXiv:1311.0903] [INSPIRE].

[39] B. Capdevila, A. Crivellin, S. Descotes-Genon, J. Matias and J. Virto, *Patterns of New Physics in $b \to s\ell^+\ell^-$ transitions in the light of recent data*, JHEP **01** (2018) 093 [arXiv:1704.05340] [INSPIRE].

[40] G. D'Amico et al., *Flavour anomalies after the R_{K^*} measurement*, JHEP **09** (2017) 010 [arXiv:1704.05438] [INSPIRE].

[41] W. Altmannshofer, P. Stangl and D.M. Straub, *Interpreting Hints for Lepton Flavor Universality Violation*, Phys. Rev. **D 96** (2017) 055008 [arXiv:1704.05435] [INSPIRE].

[42] L.-S. Geng, B. Grinstein, S. Jäger, J. Martin Camalich, X.-L. Ren and R.-X. Shi, *Towards the discovery of new physics with lepton-universality ratios of $b \to s\ell\ell$ decays*, Phys. Rev. **D 96** (2017) 093006 [arXiv:1704.05446] [INSPIRE].

[43] M. Ciuchini et al., *On Flavourful Easter eggs for New Physics hunger and Lepton Flavour Universality violation*, Eur. Phys. J. **C 77** (2017) 688 [arXiv:1704.05447] [INSPIRE].

[44] G. Hiller and I. Nisandzic, *R_K and R_{K^*} beyond the standard model*, Phys. Rev. **D 96** (2017) 035003 [arXiv:1704.05444] [INSPIRE].

[45] A. Celis, J. Fuentes-Martin, A. Vicente and J. Virto, *Gauge-invariant implications of the LHCb measurements on lepton-flavor nonuniversality*, Phys. Rev. **D 96** (2017) 035026 [arXiv:1704.05672] [INSPIRE].

[46] D. Ghosh, *Explaining the R_K and R_{K^*} anomalies*, Eur. Phys. J. **C 77** (2017) 694 [arXiv:1704.06240] [INSPIRE].

[47] A.K. Alok, D. Kumar, J. Kumar and R. Sharma, *Lepton flavor non-universality in the B-sector: a global analyses of various new physics models*, arXiv:1704.07347 [INSPIRE].

[48] A.K. Alok, B. Bhattacharya, A. Datta, D. Kumar, J. Kumar and D. London, *New Physics in $b \to s\mu^+\mu^-$ after the Measurement of R_{K^*}*, Phys. Rev. **D 96** (2017) 095009 [arXiv:1704.07397] [INSPIRE].

[49] W. Wang and S. Zhao, *Implications of the R_K and R_{K^*} anomalies*, Chin. Phys. **C 42** (2018) 013105 [arXiv:1704.08168] [INSPIRE].

[50] D. Bardhan, P. Byakti and D. Ghosh, *Role of Tensor operators in R_K and R_{K^*}*, *Phys. Lett.* **B 773** (2017) 505 [arXiv:1705.09305] [INSPIRE].

[51] S. Descotes-Genon, J. Matias, M. Ramon and J. Virto, *Implications from clean observables for the binned analysis of $B \to K^* \mu^+ \mu^-$ at large recoil*, *JHEP* **01** (2013) 048 [arXiv:1207.2753] [INSPIRE].

[52] LHCb collaboration, *Measurement of Form-Factor-Independent Observables in the Decay $B^0 \to K^{*0} \mu^+ \mu^-$*, *Phys. Rev. Lett.* **111** (2013) 191801 [arXiv:1308.1707] [INSPIRE].

[53] LHCb collaboration, *Angular analysis of the $B^0 \to K^{*0} \mu^+ \mu^-$ decay using $3\,fb^{-1}$ of integrated luminosity*, *JHEP* **02** (2016) 104 [arXiv:1512.04442] [INSPIRE].

[54] BELLE collaboration, A. Abdesselam et al., *Angular analysis of $B^0 \to K^*(892)^0 \ell^+ \ell^-$*, in *Proceedings, LHCSki 2016 — A First Discussion of 13 TeV Results*, Obergurgl, Austria, April 10–15, 2016 (2016) [arXiv:1604.04042] [INSPIRE].

[55] BELLE collaboration, S. Wehle et al., *Lepton-Flavor-Dependent Angular Analysis of $B \to K^* \ell^+ \ell^-$*, *Phys. Rev. Lett.* **118** (2017) 111801 [arXiv:1612.05014] [INSPIRE].

[56] ATLAS collaboration, *Angular analysis of $B_d^0 \to K^* \mu^+ \mu^-$ decays in pp collisions at $\sqrt{s} = 8$ TeV with the ATLAS detector*, ATLAS-CONF-2017-023.

[57] CMS collaboration, *Measurement of the P_1 and P_5' angular parameters of the decay $\mathrm{B}^0 \to \mathrm{K}^{*0} \mu^+ \mu^-$ in proton-proton collisions at $\sqrt{s} = 8$ TeV*, CMS-PAS-BPH-15-008 (2015).

[58] W. Altmannshofer and D.M. Straub, *New Physics in $B \to K^* \mu\mu$?*, *Eur. Phys. J.* **C 73** (2013) 2646 [arXiv:1308.1501] [INSPIRE].

[59] R. Gauld, F. Goertz and U. Haisch, *On minimal Z' explanations of the $B \to K^* \mu^+ \mu^-$ anomaly*, *Phys. Rev.* **D 89** (2014) 015005 [arXiv:1308.1959] [INSPIRE].

[60] A.J. Buras and J. Girrbach, *Left-handed Z' and Z FCNC quark couplings facing new $b \to s \mu^+ \mu^-$ data*, *JHEP* **12** (2013) 009 [arXiv:1309.2466] [INSPIRE].

[61] W. Altmannshofer, S. Gori, M. Pospelov and I. Yavin, *Quark flavor transitions in $L_\mu - L_\tau$ models*, *Phys. Rev.* **D 89** (2014) 095033 [arXiv:1403.1269] [INSPIRE].

[62] P. Biancofiore, P. Colangelo and F. De Fazio, *Rare semileptonic $B \to K^* \ell^+ \ell^-$ decays in RS_c model*, *Phys. Rev.* **D 89** (2014) 095018 [arXiv:1403.2944] [INSPIRE].

[63] G. Hiller and M. Schmaltz, *R_K and future $b \to s \ell \ell$ physics beyond the standard model opportunities*, *Phys. Rev.* **D 90** (2014) 054014 [arXiv:1408.1627] [INSPIRE].

[64] A. Crivellin, G. D'Ambrosio and J. Heeck, *Explaining $h \to \mu^\pm \tau^\mp$, $B \to K^* \mu^+ \mu^-$ and $B \to K \mu^+ \mu^- / B \to K e^+ e^-$ in a two-Higgs-doublet model with gauged $L_\mu - L_\tau$*, *Phys. Rev. Lett.* **114** (2015) 151801 [arXiv:1501.00993] [INSPIRE].

[65] A. Crivellin, G. D'Ambrosio and J. Heeck, *Addressing the LHC flavor anomalies with horizontal gauge symmetries*, *Phys. Rev.* **D 91** (2015) 075006 [arXiv:1503.03477] [INSPIRE].

[66] C. Niehoff, P. Stangl and D.M. Straub, *Violation of lepton flavour universality in composite Higgs models*, *Phys. Lett.* **B 747** (2015) 182 [arXiv:1503.03865] [INSPIRE].

[67] A. Celis, J. Fuentes-Martin, M. Jung and H. Serodio, *Family nonuniversal Z' models with protected flavor-changing interactions*, *Phys. Rev.* **D 92** (2015) 015007 [arXiv:1505.03079] [INSPIRE].

[68] A. Greljo, G. Isidori and D. Marzocca, *On the breaking of Lepton Flavor Universality in B decays*, JHEP **07** (2015) 142 [arXiv:1506.01705] [INSPIRE].

[69] C. Niehoff, P. Stangl and D.M. Straub, *Direct and indirect signals of natural composite Higgs models*, JHEP **01** (2016) 119 [arXiv:1508.00569] [INSPIRE].

[70] W. Altmannshofer and I. Yavin, *Predictions for lepton flavor universality violation in rare B decays in models with gauged $L_\mu - L_\tau$*, Phys. Rev. **D 92** (2015) 075022 [arXiv:1508.07009] [INSPIRE].

[71] A. Falkowski, M. Nardecchia and R. Ziegler, *Lepton Flavor Non-Universality in B-meson Decays from a* U(2) *Flavor Model*, JHEP **11** (2015) 173 [arXiv:1509.01249] [INSPIRE].

[72] A. Carmona and F. Goertz, *Lepton Flavor and Nonuniversality from Minimal Composite Higgs Setups*, Phys. Rev. Lett. **116** (2016) 251801 [arXiv:1510.07658] [INSPIRE].

[73] C.-W. Chiang, X.-G. He and G. Valencia, *Z' model for $b \to s\ell$overlineℓ flavor anomalies*, Phys. Rev. **D 93** (2016) 074003 [arXiv:1601.07328] [INSPIRE].

[74] W. Altmannshofer, M. Carena and A. Crivellin, *$L_\mu - L_\tau$ theory of Higgs flavor violation and $(g-2)_\mu$*, Phys. Rev. **D 94** (2016) 095026 [arXiv:1604.08221] [INSPIRE].

[75] S.M. Boucenna, A. Celis, J. Fuentes-Martin, A. Vicente and J. Virto, *Non-abelian gauge extensions for B-decay anomalies*, Phys. Lett. **B 760** (2016) 214 [arXiv:1604.03088] [INSPIRE].

[76] S.M. Boucenna, A. Celis, J. Fuentes-Martin, A. Vicente and J. Virto, *Phenomenology of an* $\mathrm{SU}(2) \times \mathrm{SU}(2) \times \mathrm{U}(1)$ *model with lepton-flavour non-universality*, JHEP **12** (2016) 059 [arXiv:1608.01349] [INSPIRE].

[77] E. Megias, G. Panico, O. Pujolàs and M. Quirós, *A Natural origin for the LHCb anomalies*, JHEP **09** (2016) 118 [arXiv:1608.02362] [INSPIRE].

[78] A. Celis, W.-Z. Feng and M. Vollmann, *Dirac dark matter and $b \to s\ell^+\ell^-$ with* U(1) *gauge symmetry*, Phys. Rev. **D 95** (2017) 035018 [arXiv:1608.03894] [INSPIRE].

[79] W. Altmannshofer, S. Gori, S. Profumo and F.S. Queiroz, *Explaining dark matter and B decay anomalies with an $L_\mu - L_\tau$ model*, JHEP **12** (2016) 106 [arXiv:1609.04026] [INSPIRE].

[80] A. Crivellin, J. Fuentes-Martin, A. Greljo and G. Isidori, *Lepton Flavor Non-Universality in B decays from Dynamical Yukawas*, Phys. Lett. **B 766** (2017) 77 [arXiv:1611.02703] [INSPIRE].

[81] I. Garcia Garcia, *LHCb anomalies from a natural perspective*, JHEP **03** (2017) 040 [arXiv:1611.03507] [INSPIRE].

[82] D. Bhatia, S. Chakraborty and A. Dighe, *Neutrino mixing and R_K anomaly in* $\mathrm{U}(1)_X$ *models: a bottom-up approach*, JHEP **03** (2017) 117 [arXiv:1701.05825] [INSPIRE].

[83] J.M. Cline, J.M. Cornell, D. London and R. Watanabe, *Hidden sector explanation of B-decay and cosmic ray anomalies*, Phys. Rev. **D 95** (2017) 095015 [arXiv:1702.00395] [INSPIRE].

[84] P. Ko, Y. Omura, Y. Shigekami and C. Yu, *LHCb anomaly and B physics in flavored Z' models with flavored Higgs doublets*, Phys. Rev. **D 95** (2017) 115040 [arXiv:1702.08666] [INSPIRE].

[85] E. Megias, M. Quirós and L. Salas, *Lepton-flavor universality violation in R_K and $R_{D^{(*)}}$ from warped space*, JHEP **07** (2017) 102 [arXiv:1703.06019] [INSPIRE].

[86] J.F. Kamenik, Y. Soreq and J. Zupan, *Lepton flavor universality violation without new sources of quark flavor violation*, Phys. Rev. **D 97** (2018) 035002 [arXiv:1704.06005] [INSPIRE].

[87] R. Alonso, P. Cox, C. Han and T.T. Yanagida, *Anomaly-free local horizontal symmetry and anomaly-full rare B-decays*, Phys. Rev. **D 96** (2017) 071701 [arXiv:1704.08158] [INSPIRE].

[88] C. Bonilla, T. Modak, R. Srivastava and J.W.F. Valle, *$U(1)_{B_3-3L_\mu}$ gauge symmetry as a simple description of $b \to s$ anomalies*, Phys. Rev. **D 98** (2018) 095002 [arXiv:1705.00915] [INSPIRE].

[89] J. Ellis, M. Fairbairn and P. Tunney, *Anomaly-Free Models for Flavour Anomalies*, Eur. Phys. J. **C 78** (2018) 238 [arXiv:1705.03447] [INSPIRE].

[90] R. Alonso, P. Cox, C. Han and T.T. Yanagida, *Flavoured $B - L$ local symmetry and anomalous rare B decays*, Phys. Lett. **B 774** (2017) 643 [arXiv:1705.03858] [INSPIRE].

[91] J. Kawamura, S. Okawa and Y. Omura, *Interplay between the $b \to s\ell\ell$ anomalies and dark matter physics*, Phys. Rev. **D 96** (2017) 075041 [arXiv:1706.04344] [INSPIRE].

[92] S.F. King, *Flavourful $Z^{'}$ models for $R_{K^{(*)}}$*, JHEP **08** (2017) 019 [arXiv:1706.06100] [INSPIRE].

[93] C.-H. Chen and T. Nomura, *Penguin $b \to s\ell'^+\ell'^-$ and B-meson anomalies in a gauged $L_\mu - L_\tau$*, Phys. Lett. **B 777** (2018) 420 [arXiv:1707.03249] [INSPIRE].

[94] E. Megias, M. Quirós and L. Salas, *Lepton-flavor universality limits in warped space*, Phys. Rev. **D 96** (2017) 075030 [arXiv:1707.08014] [INSPIRE].

[95] S. Baek, *Dark matter contribution to $b \to s\mu^+\mu^-$ anomaly in local $U(1)_{L_\mu - L_\tau}$ model*, Phys. Lett. **B 781** (2018) 376 [arXiv:1707.04573] [INSPIRE].

[96] L. Bian, S.-M. Choi, Y.-J. Kang and H.M. Lee, *A minimal flavored $U(1)'$ for B-meson anomalies*, Phys. Rev. **D 96** (2017) 075038 [arXiv:1707.04811] [INSPIRE].

[97] H.M. Lee, *Gauged $U(1)$ clockwork theory*, Phys. Lett. **B 778** (2018) 79 [arXiv:1708.03564] [INSPIRE].

[98] K. Fuyuto, H.-L. Li and J.-H. Yu, *Implications of hidden gauged $U(1)$ model for B anomalies*, Phys. Rev. **D 97** (2018) 115003 [arXiv:1712.06736] [INSPIRE].

[99] G. D'Ambrosio and A.M. Iyer, *Flavour issues in warped custodial models: B anomalies and rare K decays*, Eur. Phys. J. **C 78** (2018) 448 [arXiv:1712.08122] [INSPIRE].

[100] S. Dasgupta, U.K. Dey, T. Jha and T.S. Ray, *Status of a flavor-maximal nonminimal universal extra dimension model*, Phys. Rev. **D 98** (2018) 055006 [arXiv:1801.09722] [INSPIRE].

[101] A. Falkowski, S.F. King, E. Perdomo and M. Pierre, *Flavourful Z' portal for vector-like neutrino Dark Matter and $R_{K^{(*)}}$*, JHEP **08** (2018) 061 [arXiv:1803.04430] [INSPIRE].

[102] P. Asadi, M.R. Buckley and D. Shih, *It's all right(-handed neutrinos): a new $W^{'}$ model for the $R_{D^{(*)}}$ anomaly*, JHEP **09** (2018) 010 [arXiv:1804.04135] [INSPIRE].

[103] A. Greljo, D.J. Robinson, B. Shakya and J. Zupan, *$R(D^{(*)})$ from $W^{'}$ and right-handed neutrinos*, JHEP **09** (2018) 169 [arXiv:1804.04642] [INSPIRE].

[104] L. Calibbi, A. Crivellin and T. Ota, *Effective Field Theory Approach to $b \to s\ell\ell^{(\prime)}$, $B \to K^{(*)}\nu\bar{\nu}$ and $B \to D^{(*)}\nu\bar{\nu}$ with Third Generation Couplings*, Phys. Rev. Lett. **115** (2015) 181801 [arXiv:1506.02661] [INSPIRE].

[105] S. Fajfer and N. Košnik, *Vector leptoquark resolution of R_K and $R_{D^{(*)}}$ puzzles*, Phys. Lett. **B 755** (2016) 270 [arXiv:1511.06024] [INSPIRE].

[106] R. Barbieri, G. Isidori, A. Pattori and F. Senia, *Anomalies in B-decays and* U(2) *flavour symmetry*, Eur. Phys. J. **C 76** (2016) 67 [arXiv:1512.01560] [INSPIRE].

[107] S. Sahoo, R. Mohanta and A.K. Giri, *Explaining the R_K and $R_{D^{(*)}}$ anomalies with vector leptoquarks*, Phys. Rev. **D 95** (2017) 035027 [arXiv:1609.04367] [INSPIRE].

[108] G. Hiller, D. Loose and K. Schönwald, *Leptoquark Flavor Patterns & B Decay Anomalies*, JHEP **12** (2016) 027 [arXiv:1609.08895] [INSPIRE].

[109] R. Barbieri, C.W. Murphy and F. Senia, *B-decay Anomalies in a Composite Leptoquark Model*, Eur. Phys. J. **C 77** (2017) 8 [arXiv:1611.04930] [INSPIRE].

[110] D. Buttazzo, A. Greljo, G. Isidori and D. Marzocca, *B-physics anomalies: a guide to combined explanations*, JHEP **11** (2017) 044 [arXiv:1706.07808] [INSPIRE].

[111] L. Di Luzio, A. Greljo and M. Nardecchia, *Gauge leptoquark as the origin of B-physics anomalies*, Phys. Rev. **D 96** (2017) 115011 [arXiv:1708.08450] [INSPIRE].

[112] L. Calibbi, A. Crivellin and T. Li, *A model of vector leptoquarks in view of the B-physics anomalies*, arXiv:1709.00692 [INSPIRE].

[113] J.M. Cline, *B decay anomalies and dark matter from vectorlike confinement*, Phys. Rev. **D 97** (2018) 015013 [arXiv:1710.02140] [INSPIRE].

[114] M. Bordone, C. Cornella, J. Fuentes-Martin and G. Isidori, *A three-site gauge model for flavor hierarchies and flavor anomalies*, Phys. Lett. **B 779** (2018) 317 [arXiv:1712.01368] [INSPIRE].

[115] M. Blanke and A. Crivellin, *B Meson Anomalies in a Pati-Salam Model within the Randall-Sundrum Background*, Phys. Rev. Lett. **121** (2018) 011801 [arXiv:1801.07256] [INSPIRE].

[116] A. Azatov, D. Bardhan, D. Ghosh, F. Sgarlata and E. Venturini, *Anatomy of $b \to c\tau\nu$ anomalies*, arXiv:1805.03209 [INSPIRE].

[117] M. Bordone, C. Cornella, J. Fuentes-Martín and G. Isidori, *Low-energy signatures of the* PS^3 *model: from B-physics anomalies to LFV*, JHEP **10** (2018) 148 [arXiv:1805.09328] [INSPIRE].

[118] S. Sahoo and R. Mohanta, *Impact of vector leptoquark on $\bar{B} \to \bar{K}^* l^+ l^-$ anomalies*, J. Phys. **G 45** (2018) 085003 [arXiv:1806.01048] [INSPIRE].

[119] BaBar collaboration, J.P. Lees et al., *Search for $B \to K^{(*)}\nu\bar{\nu}$ and invisible quarkonium decays*, Phys. Rev. **D 87** (2013) 112005 [arXiv:1303.7465] [INSPIRE].

[120] Belle collaboration, O. Lutz et al., *Search for $B \to h^{(*)}\nu\bar{\nu}$ with the full Belle $\Upsilon(4S)$ data sample*, Phys. Rev. **D 87** (2013) 111103 [arXiv:1303.3719] [INSPIRE].

[121] A.J. Buras, J. Girrbach-Noe, C. Niehoff and D.M. Straub, *$B \to K^{(*)}\nu\bar{\nu}$ decays in the Standard Model and beyond*, JHEP **02** (2015) 184 [arXiv:1409.4557] [INSPIRE].

[122] Belle collaboration, Y. Miyazaki et al., *Search for Lepton-Flavor-Violating tau Decays into a Lepton and a Vector Meson*, Phys. Lett. **B 699** (2011) 251 [arXiv:1101.0755] [INSPIRE].

[123] Y. Kuno and Y. Okada, *Muon decay and physics beyond the standard model*, Rev. Mod. Phys. **73** (2001) 151 [hep-ph/9909265] [INSPIRE].

[124] Z. Calcuttawala, A. Kundu, S. Nandi and S. Kumar Patra, *New physics with the lepton flavor violating decay $\tau \to 3\mu$*, Phys. Rev. **D 97** (2018) 095009 [arXiv:1802.09218] [INSPIRE].

[125] K. Hayasaka et al., *Search for Lepton Flavor Violating Tau Decays into Three Leptons with 719 Million Produced $\tau^+\tau^-$ Pairs*, Phys. Lett. **B 687** (2010) 139 [arXiv:1001.3221] [INSPIRE].

[126] A.K. Alok, B. Bhattacharya, D. Kumar, J. Kumar, D. London and S.U. Sankar, *New physics in $b \to s\mu^+\mu^-$: Distinguishing models through CP-violating effects*, Phys. Rev. **D 96** (2017) 015034 [arXiv:1703.09247] [INSPIRE].

[127] T. Inami and C.S. Lim, *Effects of Superheavy Quarks and Leptons in Low-Energy Weak Processes $K_L \to \mu\bar{\mu}, K^+ \to \pi^+\nu\bar{\nu}$ and $K^0 \leftrightarrow \bar{K}^0$*, Prog. Theor. Phys. **65** (1981) 297 [*Erratum ibid.* **65** (1981) 1772] [INSPIRE].

[128] G. Buchalla, A.J. Buras and M.E. Lautenbacher, *Weak decays beyond leading logarithms*, Rev. Mod. Phys. **68** (1996) 1125 [hep-ph/9512380] [INSPIRE].

[129] S. Alekhin, J. Blümlein and S. Moch, *NLO PDFs from the ABMP16 fit*, Eur. Phys. J. **C 78** (2018) 477 [arXiv:1803.07537] [INSPIRE].

[130] S. Aoki et al., *Review of lattice results concerning low-energy particle physics*, Eur. Phys. J. **C 74** (2014) 2890 [arXiv:1310.8555] [INSPIRE].

[131] S. Aoki et al., *Review of lattice results concerning low-energy particle physics*, Eur. Phys. J. **C 77** (2017) 112 [arXiv:1607.00299] [INSPIRE].

[132] Heavy Flavor Averaging Group (HFAG) collaboration, Y. Amhis et al., *Averages of b-hadron, c-hadron and τ-lepton properties as of summer 2014*, arXiv:1412.7515 [INSPIRE].

[133] A. Hocker, H. Lacker, S. Laplace and F. Le Diberder, *A New approach to a global fit of the CKM matrix*, Eur. Phys. J. **C 21** (2001) 225 [hep-ph/0104062] [INSPIRE].

[134] CKMfitter Group collaboration, J. Charles et al., *CP violation and the CKM matrix: Assessing the impact of the asymmetric B factories*, Eur. Phys. J. **C 41** (2005) 1 [hep-ph/0406184] [INSPIRE].

[135] L. Di Luzio, M. Kirk and A. Lenz, *Updated B_s-mixing constraints on new physics models for $b \to s\ell^+\ell^-$ anomalies*, Phys. Rev. **D 97** (2018) 095035 [arXiv:1712.06572] [INSPIRE].

[136] D. Becirevic et al., *$B_d - \bar{B}_d$ mixing and the $B_d \to J/\psi K_s$ asymmetry in general SUSY models*, Nucl. Phys. **B 634** (2002) 105 [hep-ph/0112303] [INSPIRE].

[137] M. Ciuchini, E. Franco, V. Lubicz, G. Martinelli, I. Scimemi and L. Silvestrini, *Next-to-leading order QCD corrections to $\Delta F = 2$ effective Hamiltonians*, Nucl. Phys. **B 523** (1998) 501 [hep-ph/9711402] [INSPIRE].

[138] A.J. Buras, M. Misiak and J. Urban, *Two loop QCD anomalous dimensions of flavor changing four quark operators within and beyond the standard model*, Nucl. Phys. **B 586** (2000) 397 [hep-ph/0005183] [INSPIRE].

[139] E. Gardi, G. Grunberg and M. Karliner, *Can the QCD running coupling have a causal analyticity structure?*, JHEP **07** (1998) 007 [hep-ph/9806462] [INSPIRE].

[140] A. Deur, S.J. Brodsky and G.F. de Teramond, *The QCD Running Coupling*, *Prog. Part. Nucl. Phys.* **90** (2016) 1 [arXiv:1604.08082] [INSPIRE].

[141] D. Barry, J.-Y. Parlange, L. Li, H. Prommer, C. Cunningham and F. Stagnitti, *Analytical approximations for real values of the lambert w-function*, *Math. Comput. Simul.* **53** (2000) 95.

[142] M. Blanke, A.J. Buras and S. Recksiegel, *Quark flavour observables in the Littlest Higgs model with T-parity after LHC Run 1*, *Eur. Phys. J.* **C 76** (2016) 182 [arXiv:1507.06316] [INSPIRE].

[143] A.J. Buras and F. De Fazio, *ε'/ε in 331 Models*, *JHEP* **03** (2016) 010 [arXiv:1512.02869] [INSPIRE].

[144] M. Tanimoto and K. Yamamoto, *Probing SUSY with 10 TeV stop mass in rare decays and CP-violation of kaon*, *PTEP* **2016** (2016) 123B02 [arXiv:1603.07960] [INSPIRE].

[145] T. Kitahara, U. Nierste and P. Tremper, *Supersymmetric Explanation of CP-violation in $K \to \pi\pi$ Decays*, *Phys. Rev. Lett.* **117** (2016) 091802 [arXiv:1604.07400] [INSPIRE].

[146] M. Endo, S. Mishima, D. Ueda and K. Yamamoto, *Chargino contributions in light of recent ϵ'/ϵ*, *Phys. Lett.* **B 762** (2016) 493 [arXiv:1608.01444] [INSPIRE].

[147] C. Bobeth, A.J. Buras, A. Celis and M. Jung, *Patterns of Flavour Violation in Models with Vector-Like Quarks*, *JHEP* **04** (2017) 079 [arXiv:1609.04783] [INSPIRE].

[148] M. Endo, T. Kitahara, S. Mishima and K. Yamamoto, *Revisiting Kaon Physics in General Z Scenario*, *Phys. Lett.* **B 771** (2017) 37 [arXiv:1612.08839] [INSPIRE].

[149] A. Crivellin, G. D'Ambrosio, T. Kitahara and U. Nierste, *$K \to \pi\nu\bar{\nu}$ in the MSSM in light of the ϵ'_K/ϵ_K anomaly*, *Phys. Rev.* **D 96** (2017) 015023 [arXiv:1703.05786] [INSPIRE].

[150] V. Chobanova et al., *Probing SUSY effects in $K^0_S \to \mu^+\mu^-$*, *JHEP* **05** (2018) 024 [arXiv:1711.11030] [INSPIRE].

[151] M. Endo, T. Goto, T. Kitahara, S. Mishima, D. Ueda and K. Yamamoto, *Gluino-mediated electroweak penguin with flavor-violating trilinear couplings*, *JHEP* **04** (2018) 019 [arXiv:1712.04959] [INSPIRE].

[152] C. Bobeth and A.J. Buras, *Leptoquarks meet ε'/ε and rare Kaon processes*, *JHEP* **02** (2018) 101 [arXiv:1712.01295] [INSPIRE].

[153] N. Haba, H. Umeeda and T. Yamada, *ϵ'/ϵ Anomaly and Neutron EDM in $\mathrm{SU}(2)_L \times \mathrm{SU}(2)_R \times \mathrm{U}(1)_{B-L}$ model with Charge Symmetry*, *JHEP* **05** (2018) 052 [arXiv:1802.09903] [INSPIRE].

[154] C.-H. Chen and T. Nomura, *$Re(\epsilon'_K/\epsilon_K)$ and $K \to \pi\nu\bar{\nu}$ in a two-Higgs doublet model*, *JHEP* **08** (2018) 145 [arXiv:1804.06017] [INSPIRE].

[155] C.-H. Chen and T. Nomura, *ϵ'/ϵ from charged-Higgs-induced gluonic dipole operators*, *Phys. Lett.* **B 787** (2018) 182 [arXiv:1805.07522] [INSPIRE].

[156] A.J. Buras, *The Return of Kaon Flavour Physics*, *Acta Phys. Polon.* **B 49** (2018) 1043 [arXiv:1805.11096] [INSPIRE].

[157] T. Blum et al., *$K \to \pi\pi$ $\Delta I = 3/2$ decay amplitude in the continuum limit*, *Phys. Rev.* **D 91** (2015) 074502 [arXiv:1502.00263] [INSPIRE].

[158] V. Cirigliano, G. Ecker, H. Neufeld and A. Pich, *Isospin breaking in $K \to \pi\pi$ decays*, *Eur. Phys. J.* **C 33** (2004) 369 [hep-ph/0310351] [INSPIRE].

[159] S. Fajfer, N. Košnik and L. Vale Silva, *Footprints of leptoquarks: from $R_{K^{(*)}}$ to $K \to \pi\nu\bar{\nu}$*, Eur. Phys. J. **C 78** (2018) 275 [arXiv:1802.00786] [INSPIRE].

[160] A.J. Buras, F. De Fazio, J. Girrbach and M.V. Carlucci, *The Anatomy of Quark Flavour Observables in 331 Models in the Flavour Precision Era*, JHEP **02** (2013) 023 [arXiv:1211.1237] [INSPIRE].

[161] A.J. Buras and J. Girrbach, *Complete NLO QCD Corrections for Tree Level Delta $F = 2$ FCNC Processes*, JHEP **03** (2012) 052 [arXiv:1201.1302] [INSPIRE].

[162] A. Bazavov et al., *Short-distance matrix elements for D^0-meson mixing for $N_f = 2+1$ lattice QCD*, Phys. Rev. **D 97** (2018) 034513 [arXiv:1706.04622] [INSPIRE].

[163] E. Golowich, J. Hewett, S. Pakvasa and A.A. Petrov, *Relating $D^0 - \bar{D}^0$ Mixing and $D_0 \to \ell^+\ell^-$ with New Physics*, Phys. Rev. **D 79** (2009) 114030 [arXiv:0903.2830] [INSPIRE].

[164] http://www.slac.stanford.edu/xorg/hflav/charm/CHARM18/results_mix_cpv.html.

[165] A.L. Kagan and M.D. Sokoloff, *On Indirect CP-violation and Implications for $D^0 - \bar{D}^0$ and $B_s - \bar{B}_s$ mixing*, Phys. Rev. **D 80** (2009) 076008 [arXiv:0907.3917] [INSPIRE].

[166] Particle Data Group collaboration, M. Tanabashi et al., *Review of Particle Physics*, Phys. Rev. **D 98** (2018) 030001 [INSPIRE].

[167] E. Golowich and A.A. Petrov, *Short distance analysis of $D^0 - \bar{D}^0$ mixing*, Phys. Lett. **B 625** (2005) 53 [hep-ph/0506185] [INSPIRE].

[168] A.F. Falk, Y. Grossman, Z. Ligeti, Y. Nir and A.A. Petrov, *The $D^0 - \bar{D}^0$ mass difference from a dispersion relation*, Phys. Rev. **D 69** (2004) 114021 [hep-ph/0402204] [INSPIRE].

[169] A.F. Falk, Y. Grossman, Z. Ligeti and A.A. Petrov, SU(3) *breaking and $D^0 - \bar{D}^0$ mixing*, Phys. Rev. **D 65** (2002) 054034 [hep-ph/0110317] [INSPIRE].

[170] E. Golowich, J. Hewett, S. Pakvasa and A.A. Petrov, *Implications of $D^0 - \bar{D}^0$ Mixing for New Physics*, Phys. Rev. **D 76** (2007) 095009 [arXiv:0705.3650] [INSPIRE].

[171] E949 collaboration, A.V. Artamonov et al., *New measurement of the $K^+ \to \pi^+\nu\bar{\nu}$ branching ratio*, Phys. Rev. Lett. **101** (2008) 191802 [arXiv:0808.2459] [INSPIRE].

[172] KOTO collaboration, J.K. Ahn et al., *Search for the $K_L \to \pi^0\nu\bar{\nu}$ and $K_L \to \pi^0 X^0$ decays at the J-PARC KOTO experiment*, arXiv:1810.09655 [INSPIRE].

[173] E391a collaboration, J.K. Ahn et al., *Experimental study of the decay $K_L^0 \to \pi^0\nu\bar{\nu}$*, Phys. Rev. **D 81** (2010) 072004 [arXiv:0911.4789] [INSPIRE].

[174] T. Kitahara, private communication.

[175] NA62 collaboration, E. Cortina Gil et al., *The Beam and detector of the NA62 experiment at CERN*, 2017 JINST **12** P05025 [arXiv:1703.08501] [INSPIRE].

[176] KOTO collaboration, J.K. Ahn et al., *A new search for the $K_L \to \pi^0\nu\bar{\nu}$ and $K_L \to \pi^0 X^0$ decays*, PTEP **2017** (2017) 021C01 [arXiv:1609.03637] [INSPIRE].

[177] S. Wehle, S. Yaschenko, C. Niebuhr and A. Ishikawa, private communication, Tech. Rep. (2017).

[178] Y. Nomura, *Status of KOTO experiment: $K_L \to \pi^0\nu\bar{\nu}$ at J-PARC*, talk at *Heavy Quarks and Leptons 2018*, Yamagata Terrsa, Japan, 27 May–1 June 2018.

JHEP11(2018)164

[179] ATLAS collaboration, *Search for new high-mass phenomena in the dilepton final state using* 36.1 *fb*$^{-1}$ *of proton-proton collision data at* $\sqrt{s} = 13$ *TeV with the ATLAS detector*, ATLAS-CONF-2017-027.

[180] J. Pumplin, D.R. Stump, J. Huston, H.L. Lai, P.M. Nadolsky and W.K. Tung, *New generation of parton distributions with uncertainties from global QCD analysis*, JHEP **07** (2002) 012 [hep-ph/0201195] [INSPIRE].

[181] D.B. Clark, E. Godat and F.I. Olness, *ManeParse: A Mathematica reader for Parton Distribution Functions*, Comput. Phys. Commun. **216** (2017) 126 [arXiv:1605.08012] [INSPIRE].

[182] T. Hahn, *CUBA: A Library for multidimensional numerical integration*, Comput. Phys. Commun. **168** (2005) 78 [hep-ph/0404043] [INSPIRE].

[183] F. Feruglio, P. Paradisi and A. Pattori, *Revisiting Lepton Flavor Universality in B Decays*, Phys. Rev. Lett. **118** (2017) 011801 [arXiv:1606.00524] [INSPIRE].

[184] F. Feruglio, P. Paradisi and A. Pattori, *On the Importance of Electroweak Corrections for B Anomalies*, JHEP **09** (2017) 061 [arXiv:1705.00929] [INSPIRE].

[185] A. Falkowski, M. González-Alonso and K. Mimouni, *Compilation of low-energy constraints on 4-fermion operators in the SMEFT*, JHEP **08** (2017) 123 [arXiv:1706.03783] [INSPIRE].

[186] D. Aloni, A. Efrati, Y. Grossman and Y. Nir, *Υ and ψ leptonic decays as probes of solutions to the $R_D^{(*)}$ puzzle*, JHEP **06** (2017) 019 [arXiv:1702.07356] [INSPIRE].

[187] CLEO collaboration, D. Besson et al., *First Observation of $\Upsilon(3S) \to \tau^+\tau^-$ and Tests of Lepton Universality in Υ Decays*, Phys. Rev. Lett. **98** (2007) 052002 [hep-ex/0607019] [INSPIRE].

[188] BaBar collaboration, P. del Amo Sanchez et al., *Test of lepton universality in $\Upsilon(1S)$ decays at BaBar*, Phys. Rev. Lett. **104** (2010) 191801 [arXiv:1002.4358] [INSPIRE].

[189] Z. Bai, N.H. Christ, T. Izubuchi, C.T. Sachrajda, A. Soni and J. Yu, *$K_L - K_S$ Mass Difference from Lattice QCD*, Phys. Rev. Lett. **113** (2014) 112003 [arXiv:1406.0916] [INSPIRE].

[190] B. Dumont, K. Nishiwaki and R. Watanabe, *LHC constraints and prospects for S_1 scalar leptoquark explaining the $\bar{B} \to D^{(*)}\tau\bar{\nu}$ anomaly*, Phys. Rev. **D 94** (2016) 034001 [arXiv:1603.05248] [INSPIRE].

[191] Y. Takahashi, *Leptoquark (LQ) searches in CMS*, talk at *The 53rd Rencontres de Moriond*, La Thuile, 10–17 March 2018.

[192] J. Kumar, D. London and R. Watanabe, *Combined Explanations of the $b \to s\mu^+\mu^-$ and $b \to c\tau^-\bar{\nu}$ Anomalies: a General Model Analysis*, arXiv:1806.07403 [INSPIRE].

[193] BaBar collaboration, J.P. Lees et al., *A search for the decay modes $B^{+-} \to h^{+-}\tau^{+-}l$*, Phys. Rev. **D 86** (2012) 012004 [arXiv:1204.2852] [INSPIRE].

[194] BaBar collaboration, J.P. Lees et al., *Search for Charged Lepton Flavor Violation in Narrow Upsilon Decays*, Phys. Rev. Lett. **104** (2010) 151802 [arXiv:1001.1883] [INSPIRE].

[195] MEG collaboration, A.M. Baldini et al., *Search for the lepton flavour violating decay $\mu^+ \to \mathrm{e}^+\gamma$ with the full dataset of the MEG experiment*, Eur. Phys. J. **C 76** (2016) 434 [arXiv:1605.05081] [INSPIRE].

JHEP11(2018)164

[196] MEG II collaboration, A.M. Baldini et al., *The design of the MEG II experiment*, *Eur. Phys. J.* **C 78** (2018) 380 [arXiv:1801.04688] [INSPIRE].

[197] SINDRUM collaboration, U. Bellgardt et al., *Search for the Decay* $\mu^+ \to e^+e^+e^-$, *Nucl. Phys.* **B 299** (1988) 1 [INSPIRE].

[198] D. Bečirević and O. Sumensari, *A leptoquark model to accommodate* $R_K^{\rm exp} < R_K^{\rm SM}$ *and* $R_{K^*}^{\rm exp} < R_{K^*}^{\rm SM}$, *JHEP* **08** (2017) 104 [arXiv:1704.05835] [INSPIRE].

[199] N. Carrasco et al., *Leptonic decay constants* f_K, f_D, *and* f_{D_s} *with* $N_f = 2+1+1$ *twisted-mass lattice QCD*, *Phys. Rev.* **D 91** (2015) 054507 [arXiv:1411.7908] [INSPIRE].

[200] BNL collaboration, D. Ambrose et al., *New limit on muon and electron lepton number violation from* $K_L^0 \to \mu^\pm e^\mp$ *decay*, *Phys. Rev. Lett.* **81** (1998) 5734 [hep-ex/9811038] [INSPIRE].

[201] A. Pich, *Precision Tau Physics*, *Prog. Part. Nucl. Phys.* **75** (2014) 41 [arXiv:1310.7922] [INSPIRE].

[202] A. Abdesselam et al., *Measurement of the* τ *lepton polarization in the decay* $\bar{B} \to D^*\tau^-\bar{\nu}_\tau$, arXiv:1608.06391 [INSPIRE].

[203] Belle collaboration, A. Abdesselam et al., *Precise determination of the CKM matrix element* $|V_{cb}|$ *with* $\bar{B}^0 \to D^{*\,+}\,\ell^-\,\bar{\nu}_\ell$ *decays with hadronic tagging at Belle*, arXiv:1702.01521 [INSPIRE].

[204] LHCb collaboration, *Measurement of the ratio of branching fractions* $\mathcal{B}(B_c^+ \to J/\psi\tau^+\nu_\tau)/\mathcal{B}(B_c^+ \to J/\psi\mu^+\nu_\mu)$, *Phys. Rev. Lett.* **120** (2018) 121801 [arXiv:1711.05623] [INSPIRE].

[205] BES collaboration, M. Ablikim et al., *Search for the lepton flavor violation processes* $J/\psi \to \mu\tau$ *and* $e\tau$, *Phys. Lett.* **B 598** (2004) 172 [hep-ex/0406018] [INSPIRE].

JHEP11(2018)164